J. Differential Equations 250 (2011) 1967–2023

Contents lists available at ScienceDirect

Journal of Differential Equations

www.elsevier.com/locate/jde

# Generic bifurcations of low codimension of planar Filippov Systems

M. Guardia [a,*], T.M. Seara [a], M.A. Teixeira [b]

[a] Departament de Matemàtica Aplicada I, Universitat Politècnica de Catalunya, Diagonal 647, 08028 Barcelona, Spain
[b] Department of Mathematics, IMECC, Universidade Estadual de Campinas, Rua Sergio Buarque de Holanda 651, Cidade Universitária – Barão Geraldo, 6065, Campinas (SP), Brazil

ARTICLE INFO

*Article history:*
Received 20 October 2009
Revised 2 November 2010
Available online 26 November 2010

*Keywords:*
Singularity
Non-smooth vector field
Structural stability
Bifurcation

ABSTRACT

In this article some qualitative and geometric aspects of non-smooth dynamical systems theory are discussed. The main aim of this article is to develop a systematic method for studying local (and global) bifurcations in non-smooth dynamical systems. Our results deal with the classification and characterization of generic codimension-2 singularities of planar Filippov Systems as well as the presentation of the bifurcation diagrams and some dynamical consequences.



## 1. Introduction

In this article some qualitative and geometric aspects of non-smooth dynamical systems theory are discussed. Non-smooth dynamical systems is a subject that has been developed at a very fast pace in recent years and it has become certainly one of the common frontiers between Mathematics and Physics and Engineering.

The main aim of this article is to use the general approach of bifurcation theory of [19], to study local (and global) bifurcations in non-smooth dynamical systems. More concretely, we focus our attention on Filippov Systems (see [10]), which are systems modeled by ordinary differential equations discontinuous along a hypersurface in the phase space. Non-smooth systems often appear as models for plenty of phenomena such as dry friction in mechanical systems or switches in electronic circuits. Moreover, many of these models (see, for instance, [5]) occur in generic two-parameter families and therefore they typically undergo generic codimension-2 bifurcations, whose study is one of the main goals of this paper.

* Corresponding author.
*E-mail addresses:* marcel.guardia@upc.edu (M. Guardia), tere.m-seara@upc.edu (T.M. Seara), teixeira@ime.unicamp.br (M.A. Teixeira).

0022-0396/$ – see front matter 
doi:10.1016/j.jde.2010.11.016

Many authors have contributed to the study of Filippov Systems (see, for instance, [2,10,15]). See also [28] and references therein. One of the starting points for our approach in the study of bifurcations in these systems was the work of M.A. Teixeira [21] about smooth systems in 2-dimensional manifolds with boundary. This work was generalized in [3] to the study of structurally stable Filippov Systems defined in 2-dimensional manifolds with several discontinuity curves which intersect. The classification of codimension-1 local and some global bifurcations for planar systems was given in [17] (see also [9] for the study of some higher codimension bifurcations). Concerning higher dimensions, see [22–27,12] for the study of local bifurcations in $\mathbb{R}^3$ and [5,4,14] for bifurcations of periodic orbits. Nevertheless, in dimension higher than 2 even the codimension-1 local bifurcations are not completely well understood (see [24]).

In this paper we give a complete classification of the codimension-2 local bifurcations of planar Filippov Systems and we exhibit their intrinsic characterizations. For some of them, we study their generic unfoldings and we present their bifurcation diagrams. Let us point out that, since we are considering Filippov vector fields in $\mathbb{R}^2$, the discontinuity set is given by a smooth curve $\Sigma$.

Due to the discontinuities of the vector field, the usual concepts of orbit, singularity and topological equivalence cannot be straightforwardly generalized to Filippov Systems. Thus, when one wants to study some features of these systems, one has to decide first how to generalize these definitions from the classical smooth ones. In fact, in the literature of Filippov Systems one finds several definitions of orbit. The authors choose it adapted to their purposes, but some of them fail to be consistent for general Filippov Systems (see for instance [10,3]). In this paper, we present definitions (based on [3]) which seem to be a consistent and natural generalization of the concept of trajectory, orbit, singularity and topological equivalence to planar Filippov Systems. In particular, the definition of orbit preserves the existence and uniqueness property. Thus, in Section 2 we make an introduction to planar Filippov Systems from a rigorous point of view, showing examples to justify our choices in the definition of trajectory, orbit and singularity.

One of our concerns is the problem of structural stability, the most comprehensive of many different notions of stability. This problem is of obvious importance, since in practice one obtains a lot of qualitative information not only on a concrete system but also on its nearby ones. In Section 2.3, we consider both the classical notion of topological equivalence and also the notion of $\Sigma$-equivalence, which has been widely used in the setting of Filippov Systems (see [17,3]). This last definition is more restrictive than the classical one but it is important in applications, where the preservation of the discontinuity surface is a natural constraint. In Section 9, a comparative analysis between both concepts of topological equivalence and $\Sigma$-equivalence based in some models is provided.

Even if the definition of bifurcation is based on breaking structural stability, as far as the authors know, none of the papers studying bifurcations in Filippov Systems show how to construct the homeomorphisms which lead to equivalences. Thus, even if the regular points and codimension-0 singularities had already been classified (see [3]), in Section 3, we provide their normal forms and we rigorously prove that any vector field is structurally stable around these points constructing the homeomorphism which gives the equivalence between it and its normal form. We use the concept of normal form in the usual $\mathcal{C}^0$ sense. That is, the simplest Filippov vector field in any equivalence class given either by topological or $\Sigma$-equivalence.

The codimension-1 local and global bifurcations were studied in [10,17]. Thus, we use these works as a basis from which our study on codimension-2 local bifurcations is developed. Nevertheless, in Section 4, we give some remarks on these previous works. First, concerning local bifurcations, we give the necessary generic non-degeneracy conditions needed to define the bifurcations and their codimension intrinsically. The results concerning the behavior of the generic unfoldings of codimension-1 local bifurcations given in [17], were achieved mainly from studying such behavior for certain normal forms. However, some of the non-degeneracy conditions needed for this study were not explicitly stated there even though such normal forms satisfied them. Regarding the codimension-1 global bifurcations, we propose a systematic approach from the point of view of separatrix connections following the ideas in [21]. The authors think that this new approach, being more systematic, helps more to understand the full classification of global bifurcations and sharpens some results obtained in [17].

Section 5 is devoted to establish a preliminary classification of the codimension-2 singularities. In Sections 6–14, we study some of these singularities and we obtain their bifurcation diagrams. All the local and global codimension-1 bifurcations which appear in their unfoldings are also described. In this study we detect several rich phenomena which are not present in any codimension-1 singularity and are genuinely non-smooth.

For instance, in Section 9 we show a singularity whose bifurcation diagram differs whether one considers topological or $\Sigma$-equivalence, and, in Section 10 we encounter a codimension-2 singularity whose unfolding presents some of the classical sliding bifurcations of periodic orbits (see [5]).

Finally, in Sections 11 and 12, we detect codimension-2 singularities whose unfoldings present infinitely many branches of codimension-1 global bifurcations emerging from the codimension-2 singularities.

It is not the purpose of this paper to give a complete study of all the codimension-2 singularities. After listing its whole set, we only study those which present rich dynamics in their unfolding. Moreover, to rigorously complete this study, one would need to see that any generic unfolding of the chosen singularities presents the same behavior as the studied normal form. Nevertheless, since we give the intrinsic conditions which define the codimension-2 singularities and we state the generic non-degeneracy conditions which their generic unfoldings need to satisfy, we expect that any generic unfolding satisfying these conditions presents the same behavior as the normal forms studied in this paper.

## 2. Preliminaries on Filippov Systems

### 2.1. Orbits and singularities

The basic notions of dynamical systems cannot be translated directly to Filippov Systems due to the presence of discontinuities, but they have to be reformulated. The first step in order to clarify the study of this kind of systems is to establish the notion of trajectory, orbit and singularity.

In this section, we state these basic notions. Basically, we follow in spirit the approach done in [3]. Nevertheless, since we do not consider Filippov vector fields with several discontinuity curves which intersect in vertices as was done in that paper, we do not need to consider their approach in its full generality.

Moreover, in [3], the authors only study generic Filippov vector fields, in such a way that they avoid some *particular* behaviors which have positive codimension. For this reason, their definitions turn out to be simpler but cannot be directly generalized to a wider class of systems. Throughout this section, some of these non-generic examples will be shown in order to justify our choices in the definitions of trajectory, orbit and singularity.

First, we state here some general assumptions and we fix some notation. Since we study Filippov Systems locally, we deal with germs of vector fields and functions and we do not distinguish them from any of their representatives.

We also assume that discontinuities only appear in a differentiable submanifold $\Sigma$, which can be given as $\Sigma = f^{-1}(0) \cap U$ where $f$ is a germ of a $\mathcal{C}^r$ function with $r > 1$ ($\mathcal{C}^r$ denotes the set of functions continuously differentiable up to order $r$) which has 0 as a regular value and $U$ is an open neighborhood of 0. Then, the curve $\Sigma$ splits the open set $U$ in two open sets

$$\Sigma^+ = \left\{(x, y) \in U\colon\ f(x, y) > 0\right\} \quad \text{and} \quad \Sigma^- = \left\{(x, y) \in U\colon\ f(x, y) < 0\right\}.$$

In this paper, we consider the germs of discontinuous vector fields, which are of the form

$$Z(x, y) = \begin{cases} X(x, y), & (x, y) \in \Sigma^+, \\ Y(x, y), & (x, y) \in \Sigma^-. \end{cases} \tag{1}$$

For simplicity, we only consider germs of vector fields in a neighborhood of $(0, 0)$.

We denote $Z = (X, Y)$ in order to clarify which are the components of the vector field. Furthermore we assume that $X$ and $Y$ are $\mathcal{C}^r$ for $r > 1$ in $\overline{\Sigma^+}$ and $\overline{\Sigma^-}$ respectively, where $\overline{\Sigma^\pm}$ denotes the closure of $\Sigma^{\pm}$. In this assumption we are using the standard convention that for a function defined in a non-open domain $D$, being class $\mathcal{C}^r$ means that it can be extended to a $\mathcal{C}^r$ function defined on an open set containing $D$, and the same applies to vector fields.

We call $\mathcal{Z}^r$ to the space of vector fields of this type. It can be taken as $\mathcal{Z}^r = \mathfrak{X}^r \times \mathfrak{X}^r$, where we abuse notation and denote by $\mathfrak{X}^r$ both the sets of $\mathcal{C}^r$ vector fields in $\overline{\Sigma^+}$ and $\overline{\Sigma^-}$. We consider $\mathcal{Z}^r$ with the product $\mathcal{C}^r$ topology.

The first step is to define rigorously the flow $\varphi_Z(t,p)$, that is the solution of the vector field (1) through a point $p \in U$. In other words, in order to establish the dynamics given by the Filippov vector field $Z = (X,Y)$ in $U$, the first step is to define the local trajectory through a point $p \in U$. To this end, we need to distinguish whether this point belongs to $\Sigma^+$, $\Sigma^-$ or $\Sigma$.

For the first two regions, the local trajectory is defined by the vector fields $X$ and $Y$ as usual. In order to extend the definition of a trajectory to $\Sigma$, we split $\Sigma$ into three parts depending on whether or not the vector field points towards it:

1. crossing region: $\Sigma^c = \{p \in \Sigma\colon\ Xf(p) \cdot Yf(p) > 0\}$,
2. sliding region: $\Sigma^s = \{p \in \Sigma\colon\ Xf(p) < 0,\ Yf(p) > 0\}$,
3. escaping region: $\Sigma^e = \{p \in \Sigma\colon\ Xf(p) > 0,\ Yf(p) < 0\}$,

where $Xf(p) = X(p) \cdot \operatorname{grad} f(p)$ is the Lie derivative of $f$ with respect to the vector field $X$ at $p$.

These three regions are relatively open in $\Sigma$ and can have several connected components. Therefore, their definitions exclude the so-called *tangency points*, that is, points where one of the two vector fields is tangent to $\Sigma$, which can be characterized by $p \in \Sigma$ such that $Xf(p) = 0$ or $Yf(p) = 0$. These points are on the boundary of the regions $\Sigma^c$, $\Sigma^s$ and $\Sigma^e$, which we denote by $\partial\Sigma^c$, $\partial\Sigma^s$ and $\partial\Sigma^e$ respectively, and will be carefully studied later. Tangency points include the case $X(p) = 0$ or $Y(p) = 0$, that is, when one of the two vector fields has a critical point at $\Sigma$.

We define two types of tangencies between a smooth vector field and a manifold, which will be used in all the paper.

**Definition 2.1.** A smooth vector field $X$ has a fold or quadratic tangency with $\Sigma = \{(x,y) \in U\colon f(x,y) = 0\}$ at a point $p \in \Sigma$ provided $Xf(p) = 0$ and $X^2 f(p) \neq 0$.

**Definition 2.2.** A smooth vector field $X$ has a cusp or cubic tangency with $\Sigma = \{(x,y) \in U\colon f(x,y) = 0\}$ at a point $p \in \Sigma$ provided $Xf(p) = X^2 f(p) = 0$ and $X^3 f(p) \neq 0$.

**Remark 2.3.** Throughout this article we assume that the tangency points are isolated in $\Sigma$. This happens when one studies low codimension bifurcations in planar Filippov Systems, but in more degenerate systems (of infinite codimension) there could exist a continuum of tangency points.

For the sake of simplicity, the definition of orbit that is stated in this section only applies to Filippov Systems with isolated singularities.

We will define the trajectory through a point $p$ in $\Sigma^c$, $\Sigma^s$ and $\Sigma^e$. In $\Sigma^c$, since both vector fields point either towards $\Sigma^+$ or $\Sigma^-$, it is enough to match the trajectories of $X$ and $Y$ through that point.

In $\Sigma^s$ and $\Sigma^e$, the definition of the local orbit is given by the Filippov convention [10]. We consider the vector field $Z^s$ which is the linear convex combination of $X$ and $Y$ tangent to $\Sigma$, that is

$$Z^s(p) = \frac{1}{Yf(p) - Xf(p)} F_Z(p) = \frac{1}{Yf(p) - Xf(p)} \big(Yf(p)X(p) - Xf(p)Y(p)\big). \tag{2}$$

This vector field is called the *sliding vector field* independently whether it is defined in the sliding or escaping region, and for $p \in \Sigma^s \cup \Sigma^e$ the local trajectory of $p$ is given by this vector field (and therefore is contained in $\Sigma^s$ or $\Sigma^e$). The definitions of trajectory and orbit are given in Definitions 2.5 and 2.6. First we establish some notation.

**Notation 2.4.** Let us consider a smooth autonomous vector field $X$ defined in an open set $U$. Then, we denote its flow as $\varphi_X(t,p)$, that is

$$\begin{cases} \dfrac{d}{dt}\varphi_X(t,p) = X\big(\varphi_X(t,p)\big), \\ \varphi_X(0,p) = p. \end{cases}$$

The flow $\varphi_X(t,p)$ is defined in time for $t \in I \subset \mathbb{R}$, where $I = I(p,X)$ is a real interval which depends on the point $p \in U$ and the vector field $X$. To simplify notation through the paper we will not write this dependence explicitly. Let us point out that, since we are dealing with autonomous vector fields, we can choose the origin of time at $t = 0$.

**Definition 2.5.** The local trajectory (or orbital solution) of a Filippov vector field of the form (1) through a point $p$ is defined as follows:

- For $p \in \Sigma^+$ and $p \in \Sigma^-$ such that $X(p) \neq 0$ and $Y(p) \neq 0$ respectively, the trajectory is given by $\varphi_Z(t,p) = \varphi_X(t,p)$ and $\varphi_Z(t,p) = \varphi_Y(t,p)$ respectively, for $t \in I \subset \mathbb{R}$.
- For $p \in \Sigma^c$ such that $Xf(p), Yf(p) > 0$ and taking the origin of time at $p$, the trajectory is defined as $\varphi_Z(t,p) = \varphi_Y(t,p)$ for $t \in I \cap \{t \leqslant 0\}$ and $\varphi_Z(t,p) = \varphi_X(t,p)$ for $t \in I \cap \{t \geqslant 0\}$. For the case $Xf(p), Yf(p) < 0$ the definition is the same reversing time.
- For $p \in \Sigma^e \cup \Sigma^s$ such that $Z^s(p) \neq 0$, $\varphi_Z(t,p) = \varphi_{Z^s}(t,p)$ for $t \in I \subset \mathbb{R}$, where $Z^s$ is the sliding vector field given in (2).
- For $p \in \partial\Sigma^c \cup \partial\Sigma^s \cup \partial\Sigma^e$ such that the definitions of trajectories for points in $\Sigma$ in both sides of $p$ can be extended to $p$ and coincide, the trajectory through $p$ is this trajectory. We will call these points *regular tangency points*.
- For any other point $\varphi_Z(t,p) = p$ for all $t \in \mathbb{R}$. This is the case of the tangency points in $\Sigma$ which are not regular and which will be called *singular tangency points* and the critical points of $X$ in $\Sigma^+$, $Y$ in $\Sigma^-$ and $Z^s$ in $\Sigma^s \cup \Sigma^e$.

As usual, from the definition of trajectory, we can define orbit.

**Definition 2.6.** The local orbit of a point $p \in U$, is the set

$$\gamma(p) = \big\{\varphi_Z(t,p):\ t \in I\big\}.$$

Since we are dealing with autonomous systems, from now on we will use trajectory and orbit indistinctly when there is no danger of confusion.

**Remark 2.7.** In the case of $p \in \Sigma^s \cup \Sigma^e$, there have been stated different definitions of $\varphi_Z(t,p)$ in the literature (see for instance [17]), since besides the trajectory given by $Z^s$, there are two trajectories (of $X$ and $Y$) which arrive to $p$ in finite (positive or negative) time. Defining the trajectory through these points as $\varphi_{Z^s}(t,p)$ we have followed the approach in [3], since two main features of classical smooth dynamical systems persist: every point belongs to a unique orbit and the phase space is the disjoint union of all the orbits. We consider that the trajectory $\varphi_Z(t,p)$ for $p \in \Sigma^s \cup \Sigma^e$ is the trajectory given by the sliding vector field, and we will consider that the orbits of $X$ and $Y$ arrive at this point relatively open. With this choice $\Sigma^s$ and $\Sigma^e$ are locally invariant curves of $Z$.

**Definition 2.8.** (See [17].) The points $p \in \Sigma^s \cup \Sigma^e$ which satisfy $Z^s(p) = 0$, that is, the critical points of the sliding vector field, will be called *pseudo-equilibria* of $Z$ following [17] (called singular equilibria in [3]). Observe that in these points the vector fields $X$ and $Y$ must be collinear.

Moreover, we will call stable pseudonode to any point $p \in \Sigma^s$ such that $Z^s(p) = 0$ and $(Z^s)'(p) < 0$, unstable pseudonode to any point $p \in \Sigma^e$ such that $Z^s(p) = 0$ and $(Z^s)'(p) > 0$ and pseudosaddle to any point $p \in \Sigma^s$ such that $Z^s(p) = 0$ and $(Z^s)'(p) > 0$ or $p \in \Sigma^e$ such that $Z^s(p) = 0$ and $(Z^s)'(p) < 0$.

The next definition is a generalization of the definition of singularity stated in [3]. Roughly speaking, a singularity can be characterized by being the zero of a suitable function.

**Definition 2.9.** (See [3].) The singularities of a Filippov vector field (1) are:

- $p \in \Sigma^{\pm}$ such that $p$ is an equilibrium of $X$ or $Y$, that is, $X(p) = 0$ or $Y(p) = 0$ respectively.
- $p \in \Sigma^s \cup \Sigma^e$ such that $p$ is a pseudoequilibrium, that is, $Z^s(p) = 0$.
- $p \in \partial\Sigma^c \cup \partial\Sigma^s \cup \partial\Sigma^e$, that is, the (regular and singular) tangency points ($Xf(p) = 0$ or $Yf(p) = 0$).

Any other point will be called regular point.

In smooth dynamical systems, singularities, being zeros of the vector field, correspond to critical points and, as a consequence, the trajectory, and thus the orbit, through these points is just the point itself. Nevertheless, in Filippov Systems there exist singularities (regular tangency points) which have an orbit such that $\gamma(p) \neq \{p\}$ (see Definition 2.6). For this reason (see Definition 2.10), we will classify the singularities as:

- Distinguished singularities: points $p$ such that $\gamma(p) = \{p\}$. They play the role of critical points in smooth vector fields.
- Non-distinguished singularities: points $p \in \Sigma$ which are regular tangency points and then, even if they are not regular points, their local orbit is homeomorphic to $\mathbb{R}$. As we will see in Section 3, these singularities are always non-generic.

**Definition 2.10.** A distinguished singularity is a point $p$ such that $\gamma(p) = \{p\}$. They can be classified as:

- $p \in \Sigma^{\pm}$ such that $p$ is an equilibrium of $X$ or $Y$, that is, $X(p) = 0$ or $Y(p) = 0$ respectively.
- $p \in \Sigma^s \cup \Sigma^e$ such that $p$ is a pseudoequilibrium, that is, $Z^s(p) = 0$.
- $p \in \partial\Sigma^c \cup \partial\Sigma^s \cup \partial\Sigma^e$ such that it is a singular tangency point.

**Remark 2.11.** The components $X$ and $Y$ of a Filippov vector field $Z = (X, Y)$ are defined in open neighborhoods of $\overline{\Sigma}^+$ and $\overline{\Sigma}^-$ respectively. Then, as smooth vector fields, $X$ and $Y$ can have critical points which do not belong to $\overline{\Sigma}^+$ and $\overline{\Sigma}^-$ respectively. We refer to these critical points as *non-admissible critical points*, in contraposition to the *admissible* ones, which are true critical points of the Filippov vector field $Z = (X, Y)$.

Analogously, invariant objects (stable and unstable manifolds, periodic orbits) of the smooth vector fields $X$ and $Y$ not belonging to $\overline{\Sigma}^+$ and $\overline{\Sigma}^-$ respectively, are also referred to as non-admissible.

Even if the chosen definition of orbit leads to the uniqueness property, a point $p \in \Sigma$ may belong to the closure of several other orbits. To take into account this fact, we use the following definition from [3] which will be also used throughout the paper.

**Definition 2.12.** (See [3].) Given a trajectory $\varphi_Z(t, q) \in \Sigma^+ \cup \Sigma^-$ and a point $p \in \Sigma$, we say that $p$ is a departing point of $\varphi_Z(t, q)$ if there exists $t_0 < 0$ such that $\lim_{t \to t_0^+} \varphi_Z(t, q) = p$ and that it is an arrival point of $\varphi_Z(t, q)$ if there exists $t_0 > 0$ such that $\lim_{t \to t_0^-} \varphi_Z(t, q) = p$.

According to Definition 2.5, if $p \in \Sigma^c$, $p$ is a departing point of $\varphi_Z(t, q)$ for any $q$ belonging to the forward orbit

$$\gamma^+(p) = \{\varphi_Z(t, p)\colon t \in I \cap \{t \geqslant 0\}\}$$

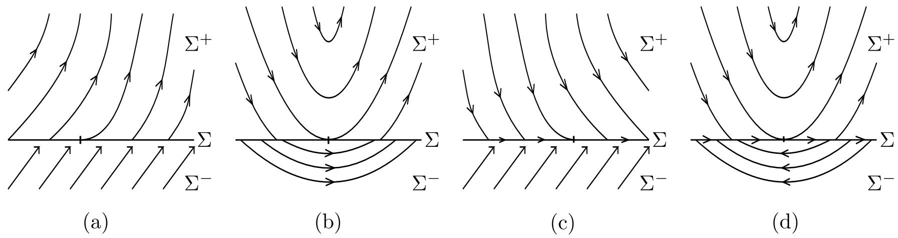


**Fig. 1.** From left to right, phase portraits of the Filippov vector fields $Z_1$, $Z_2$, $Z_3$ and $Z_4$ defined in (3), (4), (5) and (6) respectively. These four Filippov vector fields have a regular tangency point (see Definition 2.5).

and is an arrival point of $\varphi_Z(t,q)$ for any $q$ belonging to the backward orbit

$$\gamma^-(p) = \{\varphi_Z(t,p)\colon\ t \in I \cap \{t \leqslant 0\}\}.$$

Namely, the orbit through a point $p \in \Sigma^c$ is the union of the point and its departing and arrival orbits.

In the rest of this section, we will give some examples of tangency points, which in most of the cases were not considered in [3], to show how Definitions 2.5, 2.9 and 2.10 apply to them.

The first example of a regular tangency point is a cusp point $p \in \partial\Sigma^c$ of $X$ (see Definition 2.2). For instance, we take $p = (0,0)$, $\Sigma = \{(x,y)\colon\ y = 0\}$ and

$$Z_1 = \begin{cases} X_1 = \binom{1}{x^2} & \text{for } y > 0, \\ Y_1 = \binom{1}{1} & \text{for } y < 0 \end{cases} \tag{3}$$

(see Fig. 1(a)). Following Definition 2.5, the orbit through $p$ is the union of its departing and arrival orbits as happens for points in $\Sigma^c$.

The second example of a regular tangency point is illustrated in the following model (4). Take $p = (0,0) \in \partial\Sigma^c \subset \Sigma = \{(x,y)\colon\ y = 0\}$ and

$$Z_2 = \begin{cases} X_2 = \binom{1}{2x} & \text{for } y > 0, \\ Y_2 = \binom{2}{7x} & \text{for } y < 0 \end{cases} \tag{4}$$

(see Fig. 1(b)). In this case, following Definition 2.5, the trajectory through $p$ is $\varphi_Z(t,p) = \varphi_X(t,p)$.

The third example is a tangency point belonging to $\partial\Sigma^s$. Take $p = (0,0) \in \Sigma = \{(x,y)\colon\ y = 0\}$ and

$$Z_3 = \begin{cases} X_3 = \binom{1}{-x^2} & \text{for } y > 0, \\ Y_3 = \binom{1}{1} & \text{for } y < 0 \end{cases} \tag{5}$$

(see Fig. 1(c)). Following Definition 2.5, we consider as its trajectory the trajectory of the sliding vector field, which for $Z_3$ is given by $Z^s(x) = 1$, so that $\varphi_Z(t,p) = (t,0)^T$.

The fourth example is a regular tangency point $p \in \partial\Sigma^s \cup \partial\Sigma^e$, is $p = (0,0) \in \Sigma = \{(x,y)\colon\ y = 0\}$ for the Filippov vector field

$$Z_4 = \begin{cases} X_4 = \binom{1}{2x} & \text{for } y > 0, \\ Y_4 = \binom{-2}{-7x} & \text{for } y < 0 \end{cases} \tag{6}$$

(see Fig. 1(d)). In that case we have $\Sigma^s = \{(x,y)\colon\ y = 0,\ x < 0\}$ and $\Sigma^e = \{(x,y)\colon\ y = 0,\ x > 0\}$. In both sides of $p$ the orbit is given by the sliding vector field $Z^s(x) = x/3x$, which can be extended to $p$ as $Z^s(0) = 1/3$, therefore for $p$ we have that $\varphi_Z(t,p) = \varphi_{Z^s}(t,p) = (t/3,0)^T$.

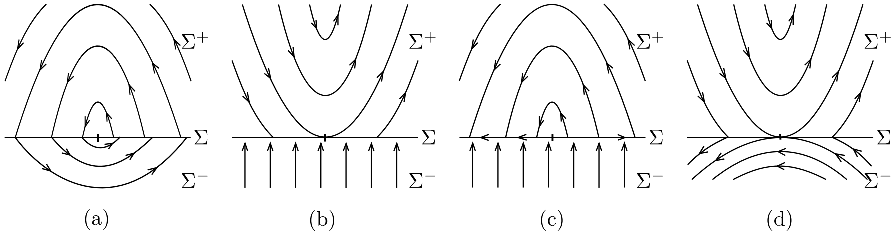


**Fig. 2.** From left to right, phase portraits of the Filippov vector fields $Z_5$, $Z_6^+$, $Z_6^-$ and $Z_7$ defined in (7), (8) and (9). These four Filippov vector fields have a singular tangency point.

Thus, considering Definition 2.5 of trajectory and regarding the local dynamics, one concludes that the regular tangency points, even if they are singularities following Definition 2.9, can be tackled as regular points in $\Sigma$.

The rest of the tangency points are distinguished singularities and then their orbit is just themselves (see Definition 2.10). This definition matches with the one that is done in [3], since all the generic tangencies that are studied in that work are distinguished singularities.

In the set of singular tangency points, which are distinguished singularities, several different behaviors appear, but basically they can be classified in four groups.

The first group of singular tangency points is formed by points in $\partial\Sigma^c$ which are neither arrival or departing points (see Definition 2.12) of any trajectory in such a way that the orbits around them behave analogously to the orbits around a classical focus. As a model we can consider $\Sigma = \{(x, y)\colon\ y = 0\}$ and

$$Z_5 = \begin{cases} X_5 = \left(\begin{smallmatrix} 1 \\ -2x \end{smallmatrix}\right) & \text{for } y > 0, \\ Y_5 = \left(\begin{smallmatrix} -1 \\ -x+x^2 \end{smallmatrix}\right) & \text{for } y < 0 \end{cases} \tag{7}$$

(see Fig. 2(a)), whose trajectories spiral around $p = (0, 0)$ as it happens around a focus for smooth systems.

The second group of singular tangency points is formed by points which belong to $\partial\Sigma^c \cap \partial\Sigma^s$ or $\partial\Sigma^c \cap \partial\Sigma^e$. A model for this case is, for instance, $p = (0, 0) \in \Sigma = \{(x, y)\colon\ y = 0\}$ for

$$Z_6^\pm = \begin{cases} X_6^\pm = \left(\begin{smallmatrix} \pm 1 \\ x \end{smallmatrix}\right) & \text{for } y > 0, \\ Y_6 = \left(\begin{smallmatrix} 0 \\ 1 \end{smallmatrix}\right) & \text{for } y < 0 \end{cases} \tag{8}$$

(see Fig. 2(b) and (c)). For $Z_6^\pm$, since $p \in \partial\Sigma^s \cap \partial\Sigma^c$, for points in $\Sigma$ on one side (left) of $p$ their orbit is given by $Z^s$, whereas for points on the other side (right) of $p$ the orbit is given by the arrival and departing orbits of the point, which are trajectories of $X$ and $Y$, since these points belong to $\Sigma^c$. Therefore, the definition of orbit on both sides do not coincide at $p$ and then this point is a singular tangency point for both $Z_6^+$ and $Z_6^-$. As it is seen in [3] and it will be recalled in Section 3, generic tangency points belong to this set.

The third group is formed by singular tangency points in $\partial\Sigma^c$ which are departing or arrival points of two different trajectories of $X$ and $Y$. Since different trajectories of $X$ and $Y$ depart (or arrive) from this point, we do not have uniqueness of solutions, and therefore the only choice which can be done in order to preserve uniqueness of solutions is to consider the single point as a whole orbit. Examples of this kind of systems are $p = (0, 0) \in \Sigma = \{(x, y)\colon\ y = 0\}$ for

$$Z_7 = \begin{cases} X_7 = \left(\begin{smallmatrix} 1 \\ x \end{smallmatrix}\right) & \text{for } y > 0, \\ Y_7 = \left(\begin{smallmatrix} -1 \\ x \end{smallmatrix}\right) & \text{for } y < 0 \end{cases} \tag{9}$$

(see Fig. 2(d)).

The last group of singular tangency points corresponds to points $p \in \Sigma$ such that $X(p) = 0$ or $Y(p) = 0$.

Once we have defined the local trajectory and local orbit through a point, we can state rigorously the definition of (maximal) orbit. Depending on the point it can be a regular orbit, a sliding orbit or a distinguished singularity.

**Definition 2.13.** A (maximal) regular orbit of $Z$ is a piecewise smooth curve $\gamma$ such that:

1. $\gamma \cap \Sigma^+$ and $\gamma \cap \Sigma^-$ are a union of orbits of the smooth vector fields $X$ and $Y$ respectively.
2. The intersection $\gamma \cap \Sigma$ consists only of crossing points and regular tangency points in $\partial \Sigma^c$.
3. $\gamma$ is maximal with respect to these conditions.

Let us observe that a regular orbit never hits $\Sigma^s$ nor $\Sigma^e$.

**Definition 2.14.** A (maximal) sliding orbit of $Z$ is a smooth curve $\gamma \subset \overline{\Sigma^s} \cup \overline{\Sigma^e}$ such that it is a maximal orbit of the smooth vector field $Z^s$.

In [3], the sliding orbit is called singular orbit.

As we have said, these definitions lead to two features (already present in [3]) that make this approach suitable in the study of the structural stability and generic bifurcations: first, uniqueness of solutions, that is, any $p \in U$ belongs to only one orbit, and second, any neighborhood $U$ of $p$ is decomposed into a disjoint union of orbits.

*2.2. Separatrices, periodic orbits and cycles*

In this section, we generalize the concepts of separatrix and periodic orbit for planar Filippov Systems. For the case of separatrices we follow closely [3,21].

**Definition 2.15.** (See [3].) An unstable separatrix is either:

- A regular orbit $\Gamma$ which is the unstable invariant manifold of a regular saddle point $p \in \overline{\Sigma^+}$ of $X$ or $p \in \overline{\Sigma^-}$ of $Y$, that is,

$$\Gamma = \Big\{ q \in U \text{ such that } \varphi_Z(t, q) \text{ is defined for } t \in (-\infty, 0) \text{ and } \lim_{t \to -\infty} \varphi_Z(t, q) = p \Big\}.$$

  We denote it by $W^u(p)$.
- A regular orbit which has a distinguished singularity $p \in \Sigma$ as a departing point. We denote it by $W^u_\pm(p)$, where the subscript $\pm$ means that it leaves $p$ from $\Sigma^\pm$.

In the first case, as it is well known in smooth systems, the trajectory lying in the separatrix reaches $p$ in infinite time whereas in the second case, it may reach the singularity in finite time.

Stable separatrices $W^s(p)$ and $W^s_\pm(p)$ are defined analogously. If a separatrix is simultaneously stable and unstable it is a *separatrix connection*.

**Remark 2.16.** A pseudonode $p \in \Sigma^s$ does have separatrices which are given by the two regular orbits in $\Sigma^+$ and $\Sigma^-$ which have $p$ as an arrival point. Recall that the points in these separatrices hit the pseudonode in finite time.

Regarding the generalization of the concept of periodic orbit in Filippov Systems we have to deal with different cases. The first one is the *regular periodic orbit*.

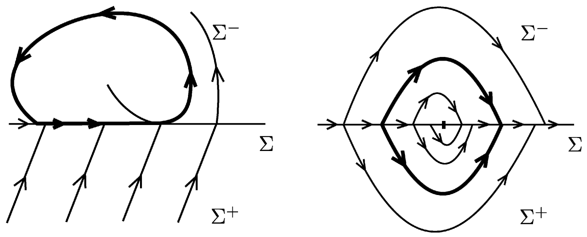


**Fig. 3.** Examples of a cycle (left) and a pseudocycle (right).

**Definition 2.17.** A regular periodic orbit is a regular orbit $\gamma = \{\varphi_Z(t, p)\colon\ t \in \mathbb{R}\}$, which therefore belongs to $\Sigma^+ \cup \Sigma^- \cup \overline{\Sigma^c}$ and satisfies $\varphi_Z(t + T, p) = \varphi_Z(t, p)$ for some $T > 0$.

The second case is the sliding periodic orbit. This case appears when $\Sigma$ is homeomorphic to $\mathbb{T}^1 = \mathbb{R}/\mathbb{Z}$ and $\Sigma = \Sigma^s$ or $\Sigma = \Sigma^e$ in such a way that the sliding vector field does not have critical points. In that case, the whole $\Sigma$ is a periodic orbit. This case does not appear in this article since in it we only study planar Filippov Systems locally and then $\Sigma$ is always homeomorphic to an open segment.

From Definitions 2.13 and 2.14, it is clear that there cannot exist periodic orbits which involve at the same time points in $\Sigma^+ \cup \Sigma^-$ and points in $\Sigma^s \cup \Sigma^e$ (that is, periodic orbits which are a combination of *regular motion* and *sliding motion*) since an orbit cannot intersect both sets. Thus, we will define cycles to deal with *periodic motion* which involves at the same time sliding and regular motion (see left picture of Fig. 3).

**Definition 2.18.** A periodic cycle is the closure of a finite set of pieces of orbits $\gamma_1, \dots, \gamma_n$ such that $\gamma_{2k}$ is a piece of sliding orbit, $\gamma_{2k+1}$ is a maximal regular orbit and the departing and arrival points of $\gamma_{2k+1}$ belong to $\overline{\gamma_{2k}}$ and $\overline{\gamma_{2k+2}}$ respectively.

We define the period of the cycle as the sum of the times that are spent in each of the pieces of orbit $\gamma_i$, $i = 1, \dots, n$.

In [17] the regular periodic orbits are called *standard periodic orbits* if they stay in $\Sigma^+ \cup \Sigma^-$ and *crossing periodic orbits* if they intersect $\overline{\Sigma^c}$. Moreover, they refer to cycles as *sliding periodic orbits*.

Besides cycles and periodic orbits, there exists another distinguished geometric object which is important when one studies topological equivalences and bifurcations in Filippov Systems.

**Definition 2.19.** We define *pseudocycle* as the closure of a set of regular orbits $\gamma_1, \dots, \gamma_n$ such that their edges, that is the arrival and departing points, of any $\gamma_i$ coincide with one of the edges of $\gamma_{i-1}$ and one of the edges of $\gamma_{i+1}$ (and also between $\gamma_1$ and $\gamma_n$) forming a curve homeomorphic to $\mathbb{T}^1 = \mathbb{R}/\mathbb{Z}$, in such a way that in some point coincide two departing or two arrival points (see right picture of Fig. 3).

In Section 2.3 we will define topological equivalence and $\Sigma$-equivalence. We will see that all the objects defined in this section must be preserved by both topological and $\Sigma$-equivalence. In particular, the pseudocycles given in Definition 2.19 must be preserved and therefore, even if this objects do not have any interest in applications, they must be taken into account when one studies bifurcations of planar Filippov Systems. However, in the study of the codimension-2 local singularities we will focus our attention to the cases with more interesting dynamics, and therefore there will not appear any pseudocycle.

## *2.3. Topological equivalence of Filippov Systems*

In this section two different notions of topological equivalence of vector fields of $\mathcal{Z}^r$ are presented. These definitions will lead to the study of the generic local behaviors and codimension-1 and 2 bifurcations. To state them we consider two Filippov vector fields $Z$ and $\tilde{Z}$ defined in open sets $U$ and $\tilde{U}$ of $\mathbb{R}^2$, which intersect discontinuity curves $\Sigma$ and $\tilde{\Sigma}$ respectively.

The first of these concepts is what we call $\Sigma$-equivalence and is the one usually considered in the literature of Filippov Systems (see the definition of orbit equivalence in [3], and also [17]).

**Definition 2.20.** Two Filippov vector fields $Z$ and $\tilde{Z}$ of $\mathcal{Z}^r$ defined in open sets $U$ and $\tilde{U}$ and with discontinuity curves $\Sigma \subset U$ and $\tilde{\Sigma} \subset \tilde{U}$ respectively are $\Sigma$-equivalent if there exists an orientation preserving homeomorphism $h : U \to \tilde{U}$ which sends $\Sigma$ to $\tilde{\Sigma}$ and sends orbits of $Z$ to orbits of $\tilde{Z}$.

It can be easily seen that any $\Sigma$-equivalence sends regular orbits to regular orbits and distinguished singularities to distinguished singularities. Moreover, as it sends arrival and departing points to arrival and departing points, $\overline{\Sigma^c}$, $\overline{\Sigma^s}$ and $\overline{\Sigma^e}$ are preserved, and thus it also sends sliding orbits to sliding orbits and preserves separatrices, separatrix connections, periodic orbits, cycles and pseudocycles.

The definition of $\Sigma$-equivalence is natural because in applications sometimes it is important to preserve the switching manifold. Nevertheless, from the point of view of abstract bifurcation theory, it seems to be too strict. In fact, in order for $Z$ and $\tilde{Z}$ to have similar qualitative behavior from a topological point of view, it is not needed that the crossing region $\overline{\Sigma^c}$ is preserved. From a topological point of view the behavior of the flow is *the same* around a point belonging to the crossing region and around a regular point in $\Sigma^+$ or $\Sigma^-$ where the vector field is smooth. Thus, in this work, besides considering $\Sigma$-equivalence, we will consider also the classical concept of topological equivalence, which, as far as we know, had not been applied to Filippov Systems before.

**Definition 2.21.** Two Filippov vector fields $Z$ and $\tilde{Z}$ of $\mathcal{Z}^r$ defined in open sets $U$ and $\tilde{U}$ and with discontinuity curves $\Sigma \subset U$ and $\tilde{\Sigma} \subset \tilde{U}$ respectively are topologically equivalent if there exists an orientation preserving homeomorphism $h : U \to \tilde{U}$ which sends orbits of $Z$ to orbits of $\tilde{Z}$.

From these definitions it is obvious that if two vector fields are $\Sigma$-equivalent, they are also topologically equivalent but the reciprocal is not true (see Section 9). Analogously to $\Sigma$-equivalences, topological equivalences preserve $\overline{\Sigma^s}$ and $\overline{\Sigma^e}$. Consequently they also preserve $\Sigma^+ \cup \Sigma^- \cup \overline{\Sigma^c}$ and therefore send regular orbits to regular orbits, sliding orbits to sliding orbits and distinguished singularities to distinguished singularities. Moreover, they also preserve separatrices, separatrix connections, periodic orbits, cycles and pseudocycles.

Even if in the literature it has been used the concept of $\Sigma$-equivalence (see [17,3], ...), in most of these works, it is not explained how the homeomorphisms $h$ leading to such equivalences are constructed. So, as a far as the authors know, there is not any rigorous proof of $\Sigma$-equivalence or topological equivalence between two Filippov vector fields.

In Section 3 we will construct some of these homeomorphisms in the case of regular points and generic singularities. Later, in Section 9, we will show how to construct them for a codimension-2 singularity, which has more involved dynamics.

Thus, it will be necessary to obtain tools to construct these homeomorphisms. One of them will be based on the notion of $\mathcal{C}^r$-conjugation of smooth vector fields. In fact, if we have two smooth vector fields $X$ and $\tilde{X}$ with their corresponding flows $\varphi_X(t,x)$ and $\varphi_{\tilde{X}}(t,x)$, they are $\mathcal{C}^r$-conjugated if there exists a $\mathcal{C}^r$ homeomorphism $h$ such that $h(\varphi_X(t,x)) = \varphi_{\tilde{X}}(t,h(x))$. In this case, it can be seen that $h_*X = \tilde{X}$ where

$$(h_*X)(p) = Dh\big(h^{-1}(p)\big)X\big(h^{-1}(p)\big) \tag{10}$$

and $Dh$ denotes the differential of $h$. So, $h$ is just a change of variables. In this work, we will not use an analogous non-smooth concept but we will use conjugations applied to the smooth components $X$ and $Y$ of Filippov vector fields $Z = (X, Y)$.

**Proposition 2.22.** *Let us consider any diffeomorphism $h : U \to \tilde{U}$ which conjugates on one hand, $X$ in $\Sigma^+ \subset U$ and $\tilde{X}$ in $\tilde{\Sigma}^+ \subset \tilde{U}$ and, in the other hand, $Y$ in $\Sigma^- \subset U$ and $\tilde{Y}$ in $\tilde{\Sigma}^- \subset \tilde{U}$. Then, it also conjugates the sliding vector fields $Z^s$ and $\tilde{Z}^s$, and therefore $h$ gives a topological equivalence between $Z = (X, Y)$ and $\tilde{Z} = (\tilde{X}, \tilde{Y})$.*

**Proof.** Since $h$ is $\mathcal{C}^r$, we have $h_* X = \tilde{X}$ and $h_* Y = \tilde{Y}$. Moreover, we have that $\Sigma = \{p \in U\colon\ f(p) = 0\}$ and $\tilde{\Sigma} = \{\tilde{p} \in \tilde{U}\colon\ \tilde{f}(\tilde{p}) = f(h^{-1}(\tilde{p})) = 0\}$ and a standard computation shows that

$$h_*(Xf)(\tilde{p}) = h_* X h_* f(\tilde{p}) = \tilde{X}\tilde{f}(\tilde{p})$$

where $\tilde{p} = h(p)$ and we recall that given a function $F : U \subset \mathbb{R}^2 \to \mathbb{R}$, $h_* F = F \circ h^{-1}$.

Now, an easy computation shows that

$$\big(h_* Z^s\big)(\tilde{p}) = Dh\big(h^{-1}(\tilde{p})\big) Z^s\big(h^{-1}(\tilde{p})\big) = \tilde{Z}^s(\tilde{p}).$$

Then $h$ sends orbits to orbits. $\square$

**Remark 2.23.** All the topological equivalences defined using this proposition preserve $\Sigma$ and therefore are also $\Sigma$-equivalences. Thus, in order to construct topological equivalences not preserving $\Sigma$ other techniques will be needed (see Section 9).

**Remark 2.24.** If we remove the hypothesis of differentiability in Proposition 2.22, that is, if we consider that $h$ is only a homeomorphism, this proposition is no more true. As a counterexample we consider the following two vector fields defined in a neighborhood $U$ of the origin and taking as discontinuity curve $\Sigma = \{(x, y)\colon\ y = 0\}$:

$$\tilde{Z}(x, y) = \begin{cases} \tilde{X} = \binom{-1}{-1} & \text{if } y > 0, \\ \tilde{Y} = \binom{-1}{1} & \text{if } y < 0 \end{cases} \quad \text{and} \quad Z(x, y) = \begin{cases} X = \binom{0}{-1} & \text{if } y > 0, \\ Y = \binom{0}{1} & \text{if } y < 0. \end{cases}$$

In this case $\Sigma = \Sigma^s = \tilde{\Sigma} = \tilde{\Sigma}^s$ and the homeomorphism

$$h(x, y) = \begin{cases} (x - y, y) & \text{if } y > 0, \\ (x, y) & \text{if } y = 0, \\ (x + y, y) & \text{if } y < 0, \end{cases}$$

which is $\mathcal{C}^0$ but not $\mathcal{C}^1$, conjugates $\tilde{X}$ with $X$ for $y > 0$ and $\tilde{Y}$ and $Y$ for $y < 0$ but is not a topological equivalence of $Z$ and $\tilde{Z}$, since the corresponding sliding vector fields are $\tilde{Z}^s(x) = -1$ and $Z^s(x) = 0$ which cannot be topologically equivalent.

The definitions of $\Sigma$-equivalence and equivalence give rise to the concepts of $\Sigma$-structural stability and structural stability.

## 3. Generic local behavior

In this section we study the generic local behavior of planar Filippov Systems. In each case, we show the local $\mathcal{C}^0$ normal form and we construct the homeomorphism which gives the topological equivalence. In this work when we consider normal forms we are referring to $\mathcal{C}^0$ normal forms. That is, the equivalence relations of being topologically equivalent or $\Sigma$-equivalent divide $\mathcal{Z}^r$ in equivalence classes and a normal form of any of these classes is just a representative taken as simple as possible.

First we consider the regular points, namely points which are not singularities, so that they belong to either regular or sliding orbits. It is clear that around regular points which do not belong to $\Sigma$ applies the Flow-Box Theorem (see [1,20]), so that, in this study we only have to deal with points belonging to the discontinuity curve. Next proposition gives the normal form for regular points belonging to $\Sigma^c \cup \Sigma^s \cup \Sigma^e$. First we give some notation.

**Notation 3.1.** Let us consider two smooth vector fields $X$ and $Y$. Then, we denote by $X(p) \parallel Y(p)$ the fact that $X$ and $Y$ are parallel at $p$ and by $X(p) \nparallel Y(p)$ the fact that $X$ and $Y$ are non-parallel at $p$.

**Proposition 3.2.** *Given a Filippov vector field $Z = (X, Y)$ with discontinuity surface $\Sigma$ and $(0,0) \in \Sigma$, then:*

1. *If $(0,0) \in \Sigma^c$, then in a neighborhood $(0,0) \in U$, $Z$ is $\Sigma$-equivalent to the normal form*

$$\tilde{Z}(x,y) = \begin{cases} \tilde{X} = \binom{0}{1} & \text{for } y > 0, \\ \tilde{Y} = \binom{0}{1} & \text{for } y < 0 \end{cases}$$

*in a neighborhood $(0,0) \in \tilde{U}$, and is equivalent to the normal form*

$$\bar{Z}(x,y) = \begin{pmatrix} 0 \\ 1 \end{pmatrix} \quad \text{for } (x,y) \in \mathbb{R}^2,$$

*which is a smooth vector field*

2. *If $(0,0) \in \Sigma^s$ and satisfies $X(0,0) \nparallel Y(0,0)$, then in a neighborhood $(0,0) \in U$, $Z$ is $\Sigma$-equivalent to the normal form*

$$\tilde{Z}(x,y) = \begin{cases} \tilde{X} = \binom{1}{-1} & \text{for } y > 0, \\ \tilde{Y} = \binom{1}{1} & \text{for } y < 0 \end{cases} \tag{11}$$

*in a neighborhood $(0,0) \in \tilde{U}$.*

3. *If $(0,0) \in \Sigma^e$ and satisfies $X(0,0) \nparallel Y(0,0)$, then in a neighborhood $(0,0) \in U$ $Z$ is $\Sigma$-equivalent to the normal form*

$$\tilde{Z}(x,y) = \begin{cases} \tilde{X} = \binom{1}{1} & \text{for } y > 0, \\ \tilde{Y} = \binom{1}{-1} & \text{for } y < 0 \end{cases}$$

*in a neighborhood $(0,0) \in \tilde{U}$.*

**Proof.** In the first case, the construction of the $\Sigma$-equivalence is achieved considering $\varphi_X$, $\varphi_Y$, $\varphi_{\tilde{X}}$ and $\varphi_{\tilde{Y}}$ the flows of the smooth components of both vector fields. Since $(0,0) \in \Sigma^c$ these vector fields are transversal to $\Sigma \cap U$ and $\tilde{\Sigma} \cap \tilde{U}$ respectively. Thus, for any point $p \in \Sigma^+ \cap U$, using the Implicit Function Theorem there exists a time $t(p) \in \mathbb{R}$ depending on $p$ such that $\varphi_X(t(p), p) \in \Sigma$, and analogously for $\Sigma^- \cap U$ and $\varphi_Y$. Thus, imposing that the $\Sigma$-equivalence is the identity restricted to $\Sigma$, it can be given by

$$h(p) = \begin{cases} \varphi_{\tilde{X}}(-t(p), \varphi_X(t(p), p)) & \text{if } p \in \Sigma^+, \\ p & \text{if } p \in \Sigma, \\ \varphi_{\tilde{Y}}(-t(p), \varphi_Y(t(p), p)) & \text{if } p \in \Sigma^- \end{cases} \tag{12}$$

which it can be seen that is $C^0$, and satisfies $\varphi_{\tilde{Z}}(t, h(p)) = h(\varphi_Z(t, p))$.

Finally, in this first case, only remains to point out that in fact $\tilde{Z}$ is a smooth vector field since $\tilde{X} \equiv \tilde{Y}$. Then, $Z$ is equivalent to the smooth vector field $\tilde{Z} = (0, 1)$.

In the second case, in order to construct the homeomorphism, we start with the points in $\Sigma$. Since $X(0,0) \nparallel Y(0,0)$ and $\tilde{X}(0,0) \nparallel \tilde{Y}(0,0)$, $(0,0)$ is a regular point of both sliding vector fields $Z^s$ and $\tilde{Z}^s$. Then, the Flow-Box Theorem assures us that there exists a homeomorphism $\bar{h}$ which locally conjugates them (see [1,20]). For points away from $\Sigma$, the homeomorphism can be extended as in the previous cases by the flow since for any point $p \in \Sigma^+ \cap U$ there exists a time $t(p)$ such that $\varphi_X(t(p), p) \in \Sigma$ (and analogously for $p \in \Sigma^- \cap U$). Thus, the homeomorphism which gives the $\Sigma$-equivalence can be given by

$$h(p) = \begin{cases} \varphi_{\tilde{X}}(-t(p), \bar{h}(\varphi_X(t(p), p))) & \text{if } p \in \Sigma^+ \cap U, \\ \bar{h}(p) & \text{if } p \in \Sigma \cap U, \\ \varphi_{\tilde{Y}}(-t(p), \bar{h}(\varphi_Y(t(p), p))) & \text{if } p \in \Sigma^- \cap U. \end{cases} \tag{13}$$

The third case, can be studied analogously to the second. $\square$

Once we have classified the behavior around regular points of Filippov vector fields, we begin the study of generic singularities. The first type of generic singularities are the hyperbolic critical points of $X$ and $Y$ in $\Sigma^+$ and $\Sigma^-$ respectively. It is clear that around these points one can apply Hartmann–Grobman Theorem (see [20,11]). For this reason, in this study we only have to deal with generic singularities on $\Sigma$. Let us first define the Fold–Regular points.

**Definition 3.3.** A Fold–Regular point is a point $p \in \Sigma$ such that $Xf(p) = 0$ and $X^2 f(p) \neq 0$ and $Yf(p) \neq 0$ or points such that $Yf(p) = 0$ and $Y^2 f(p) \neq 0$ and $Xf(p) \neq 0$. Moreover:

- In the first case, we say that the Fold–Regular point is visible if $X^2 f(p) > 0$ and invisible if $X^2 f(p) < 0$. Furthermore, if $Yf(p) > 0$, the fold $p$ belongs to $\partial\Sigma^s$ and then we refer to it as a sliding fold whereas if $Yf(p) < 0$, the fold $p$ belongs to $\partial\Sigma^e$ and then we refer to it as an escaping fold.
- In the second case, it is visible provided $Y^2 f(p) < 0$ and invisible provided $Y^2 f(p) < 0$, and one can define analogously sliding and escaping folds.

For planar Filippov vector fields, there exist the following generic singularities in $\Sigma$, which are all distinguished singularities (see Definitions 2.9 and 2.10):

1. Fold–Regular points.
2. Hyperbolic critical points of the sliding vector field: points $p \in \Sigma^s \cup \Sigma^e$ such that $X(p) \parallel Y(p)$ and hence $Z^s(p) = 0$, and moreover

$$\left(Z^s\right)'(p) \neq 0. \tag{14}$$

Next proposition deals with the normal forms of these generic singularities.

**Proposition 3.4.** *The following $\Sigma$-equivalences hold*:

1. *If $(0,0) \in \Sigma$ is a Fold–Regular point of the vector field $Z = (X, Y) \in \mathcal{Z}^r$ defined in a neighborhood $U$ of $p$, then $Z$ is $\Sigma$-equivalent in a neighborhood $V$ of $(0,0)$ to its normal form*

$$Z_{a,b} = \begin{cases} X_a = \binom{1}{ax} & \text{for } y > 0, \\ Y_b = \binom{0}{b} & \text{for } y < 0 \end{cases} \tag{15}$$

*where $a = \operatorname{sgn}(X^2 f(p))$ and $b = \operatorname{sgn}(Yf(p))$.*

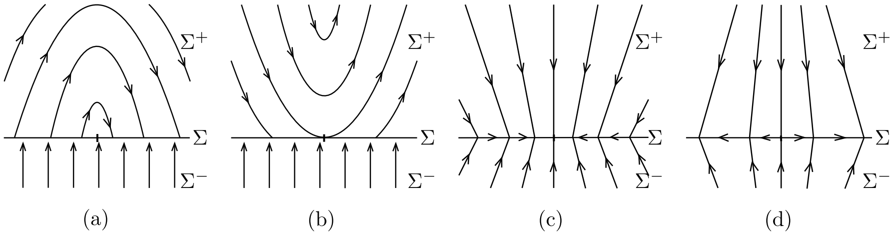


**Fig. 4.** Four examples of codimension 0 singularities. From left to right, the first two are the phase portraits of the Filippov vector field $Z_{a,b}$ in (15) with $a < 0$, $b > 0$ and $a > 0$, $b > 0$ respectively. The third and fourth represent the phase portrait of the Filippov vector field $Z_{a,b}$ in (16) with $a < 0$, $b > 0$ and $a > 0$, $b > 0$ respectively.

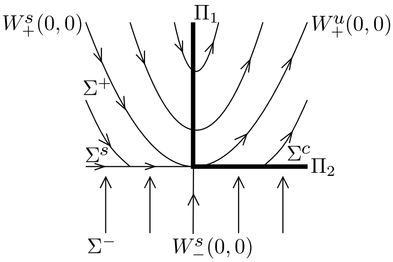


**Fig. 5.** Phase portrait around a generic visible Fold–Regular point. In order to define a homeomorphism between to generic visible Fold–Regular points, one has to define the transversal sections $\Pi_1$ and $\Pi_2$.

2. *If* $(0,0) \in \Sigma^s \cup \Sigma^e$ *is a hyperbolic critical point of the sliding vector field* $Z^s$ *of* $Z = (X, Y) \in \mathcal{Z}^r$ *defined in a neighborhood* $U$ *of* $(0,0)$*, then* $Z$ *is* $\Sigma$*-equivalent in a neighborhood* $V$ *of* $(0,0)$ *to its normal form*

$$Z_{a,b} = \begin{cases} X_{a,b} = \binom{ax}{b} & \textit{for } y > 0, \\ Y_{a,b} = \binom{ax}{-b} & \textit{for } y < 0 \end{cases} \tag{16}$$

*where* $b = \operatorname{sgn}(Xf(p))$ *and* $a = \operatorname{sgn}(Z^s)'(p)$.

**Proof.** We have to construct a homeomorphism that gives the equivalence. Since some of the cases for different $a$ and $b$ are analogous, we only deal with some of them.

For the Fold–Regular point, $a > 0$ and $a < 0$ correspond to tangencies of $X$ which are visible (see Fig. 4(b)) and invisible (see Fig. 4(a)) respectively. We consider only the case $b > 0$. We can construct, by Flow-Box Theorem [20], the homeomorphism which conjugates the sliding vector field sending the Fold–Regular point to itself. In order to extend this homeomorphism to the rest of the neighborhood of the Fold–Regular point it has to be done in different ways depending on the sign of $a$.

In the case of the invisible tangency ($a < 0$), since $\Sigma^s$ acts as an attractor in $U$, the homeomorphism can be extended through the flow of $Z$ as it has been done in the proof of Proposition 3.4. Nevertheless, in order to obtain a $\Sigma$-equivalence time has to be reparameterized by arc-length to ensure that $\Sigma^c$ is preserved.

In the case $a > 0$ by this procedure we can only define the equivalence in a part of the neighborhood delimited by the separatrices of the fold $W^s_+(0,0)$ and $W^s_-(0,0)$, since the orbits which do not belong to this region, do not hit $\Sigma^s$ (see Fig. 5). Hence, for the points lying on the right of $W^s_+(0,0) \cup W^s_-(0,0)$, we define the homeomorphism in different ways depending whether the point belongs to the region delimited by $W^s_+(0,0) \cup W^u_+(0,0)$ or by $W^u_+(0,0) \cup W^s_-(0,0)$. In each region we define sections which are topologically transversal to the corresponding flows. For instance, we can take $\Pi_1$ and $\Pi_2$ as can be seen in Fig. 5. Notice that $\overline{\Sigma^s}$, $\Pi_1$ and $\Pi_2$ only intersect in the Fold–Regular point $(0,0)$.

In the sections $\Pi_1$ and $\Pi_2$, we can define a homeomorphism which sends the Fold–Regular point to itself. Finally, the homeomorphism can be extended to the other points by the flow. Finally, it can be checked *a posteriori* that the homeomorphism is indeed continuous since the homeomorphisms defined in each region coincide in the separatrices.

For the hyperbolic critical points of the sliding vector field $Z^s$ we consider only the case $a<0$ and $b<0$ (see Fig. 4(c)) and the other ones are analogous. We proceed as follows. First, since the sliding vector fields $Z^s$ and $Z^s_{a,b}$ have both an attracting critical point at 0, by Hartmann–Grobman Theorem (see [20,11]), there exists a homeomorphism $\bar{h}$ defined in a neighborhood of $(0,0)$ in $\Sigma$ which conjugates them. For the points which do not belong to $\Sigma$ the homeomorphism can be defined as in (12) since the vector field is transversal to $\Sigma$ in all $p \in \Sigma \cap U$, that is

$$h(p)=\begin{cases}\varphi_{\tilde{X}}(-t(p),\bar{h}(\varphi_X(t(p),p))) & \text{if } p\in\Sigma^+,\\ \bar{h}(p) & \text{if } p\in\Sigma,\\ \varphi_{\tilde{Y}}(-t(p),\bar{h}(\varphi_Y(t(p),p))) & \text{if } p\in\Sigma^-.\end{cases}$$

Since all the equivalences considered in the proof send $\Sigma$ to $\tilde{\Sigma}=\{(x,y)\colon\ y=0\}$, it is clear that all the equivalences stated in Proposition 3.4 are also $\Sigma$-equivalences. $\square$

**Theorem 3.5.** *Let us consider a vector field $Z=(X,Y)\in\mathcal{Z}^r$ in a neighborhood $U$ of $(0,0)$. Then, if $(0,0)$ is a regular point or a generic singularity, then $Z$ is locally structurally stable and locally $\Sigma$-structurally stable.*

**Proof.** When $(0,0)$ is a regular point, it belongs to a regular or sliding orbit. The conditions which define the regular points are open, and thus are robust under perturbation. Therefore, by Proposition 3.2, the perturbed vector field is topologically equivalent to the same normal form as the unperturbed one. When it is a singularity, it is enough to see that the Fold–Regular points and the hyperbolic critical points of the sliding vector field $Z^s$ are the only ones which are generic. In fact, considering for instance the Fold–Regular case, one has to use the Implicit Function Theorem and the generic conditions $Yf(0,0)\neq 0$ and $X^2f(0,0)\neq 0$, in order to see that if $Z_0\in\mathcal{Z}^r$ has a fold at $(0,0)$, then any vector field $Z\in\mathcal{U}\subset\mathcal{Z}^r$ where $\mathcal{U}$ is neighborhood of $Z_0$, has also a fold in a point close to $(0,0)$ with the same signs for $X^2f(p)$ and $Yf(p)$. Thus, since by Proposition 3.4 both $Z_0$ and $Z$ are topologically equivalent to the normal form (15) with the same signs $a$ and $b$, they are topologically equivalent also to each other and therefore $Z_0$ is locally structurally stable.

Proceeding in the same way, it can also be seen that the hyperbolic critical points of $Z^s$ are generic and then Proposition 3.4 can be applied. Finally, since all the topological equivalences that we have considered are also $\Sigma$-equivalences, any vector field of $\mathcal{Z}^r$ such that $(0,0)$ is a regular point or a generic singularity, it is locally $\Sigma$-structurally stable. $\square$

### *3.1. A systematic approach to the study of local bifurcations of planar Filippov Systems*

In this section we present the program used in this paper to exhibit the diagram bifurcation of a singularity of a planar Filippov System, following the approach in [19]. We consider $\Omega=\mathcal{Z}^r$ the space of all vector fields $Z$ defined in some neighborhood of $p\in\mathbb{R}^2$.

1. By Theorem 3.5, we already know the characterization of the set $\Xi_0$ consisting on locally structurally stable Filippov vector fields in $\Omega$, which is open and dense in $\Omega$. The set $\Omega_1=\Omega\setminus\Xi_0$ is the bifurcation set, which is the set that we want to analyze.
2. We consider $\Xi_1\subset\Omega_1$ such that if we select $Z_0\in\Xi_1$, it is locally structurally stable relative to $\Omega_1$. The set $\Xi_1$ is the codimension-1 local bifurcation set. Given $Z_0\in\Xi_1$, we consider $\mathcal{U}$ a small neighborhood of it in $\Omega$ such that:
   (a) There exists a smooth function $L\colon\mathcal{U}\to\mathbb{R}$, such that $DL_{Z_0}$, the differential of $L$ at $Z_0$, is surjective and which vanishes at $\Xi_1\cap\mathcal{U}$.

(b) We consider now all the embeddings $\xi:\mathbb{R}\to\mathcal{U}\subset\Omega$ transversal to $\Xi_1$ at some $Z\in\Xi_1$ and such that $\xi(0)=Z$. We refer to such $\xi$ as an unfolding of $Z$. We select those $Z$ such that any $\xi$ is $C^0$-structurally stable. In this way we are able to exhibit the bifurcation diagram of $Z$. To describe it we choose the simplest possible $Z_0\in\mathcal{U}\subset\Xi_1$ and $\xi_0$ such that $\xi_0(0)=Z_0$ and we refer to $\xi_0$ as a normal form.
(c) We consider now the set $\Omega_2=\Omega_1\setminus\Xi_1$ and similar objects $\Xi_2$ (the set of codimension-2 singularities) and families of objects: $L:\mathcal{U}\to\mathbb{R}^2$, with surjective derivative at $Z_0$ and embeddings $\xi:\mathbb{R}^2\to\Omega$.
(d) In this way we get sequences of sets in $\Omega$, $\Omega_k$ and $\Xi_k$ that allow us to characterize all codimension $k$ singularities.

Even if in this work we follow this approach, we only give the proofs for the regular points and the codimension-0 singularities. In Sections 4.1 and 5 we define intrinsically the sets $\Xi_1$ and $\Xi_2$ as zeros of suitable functionals $L$, which we do not construct explicitly. To describe the codimension-1 and 2 singularities belonging to these sets, we use as normal forms the simplest families of vector fields which intersect these manifolds transversally. We leave as a future work, which would require a more detailed analysis, the rigorous proof that any generic unfolding exhibits the same behavior as the normal forms rigorously studied in this paper.

## 4. Codimension-1 bifurcations revisited

### 4.1. Codimension-1 local bifurcations

Once we have established in Theorem 3.5 which are the locally structurally stable planar Filippov vector fields, in this section we make a review of the codimension-1 local bifurcations. We pay special attention to the ones which appear in the unfoldings of the codimension-2 local bifurcations that are studied in Sections 6–14. The classification of codimension-1 local bifurcations was achieved by Y. Kuznetsov et al. in [17]. Nevertheless, in that paper, the authors did not mention explicitly all the generic non-degeneracy conditions which had to be satisfied in each singularity to be a codimension-1 bifurcation. However, they exhibited as normal forms of each singularity some models of Filippov vector fields which satisfy these conditions. In this section, we explicitly state these lacking non-degeneracy conditions which will be used in Sections 6–14 to derive codimension-2 singularities when one of these conditions fails.

In [17], the authors saw that the codimension-1 local bifurcations of a Filippov vector field $Z=(X,Y)$ with discontinuity surface $\Sigma=\{(x,y)\colon\ f(x,y)=0\}$ can be classified as:

1. Fold–Fold singularity: Both vector fields have a fold or quadratic tangency at the same point $p\in\Sigma$ (see Definition 2.1). That is $Xf(p)=0$, $Yf(p)=0$, $X^2f(p)\neq0$ and $Y^2f(p)\neq0$.
2. Cusp–Regular singularity, called double tangency bifurcation in [17]: $X$ has a cusp in $p\in\Sigma$ (see Definition 2.2) while $Y$ is transversal to $\Sigma$. That is, $Xf(p)=0$, $X^2f(p)=0$, $X^3f(p)\neq0$ and $Yf(p)\neq0$.
3. $Z^s$ has a Saddle–Node singularity in $p\in\Sigma^s\cup\Sigma^e$. That is, $Z^s(p)=0$, $(Z^s)'(p)=0$ and $(Z^s)''(p)\neq0$.
4. $X$ has a hyperbolic non-degenerate critical point $p\in\Sigma$ while $Y$ is transversal to $\Sigma$. That is, $X(p)=0$, the eigenvalues of $DX(p)$ have real part different from zero and $Yf(p)\neq0$. In [17] these bifurcations are classified as *Boundary–Focus*, *Boundary–Node* and *Boundary–Saddle*, and are called *boundary-equilibrium* in [4].

If one would like to study these singularities following rigorously the approach presented in Section 3.1, one should define for each case the surjective function $L$, which has been explained in that section. For instance, for the Fold–Fold singularity, the corresponding function $L$ would be given by the distance in $\Sigma$ between the two folds. Then, $L$ would be surjective and it would vanish in the codimension-1 manifold to which the Fold–Fold singularities belong. An analogous construction of suitable functionals $L$ can be done in the other cases.

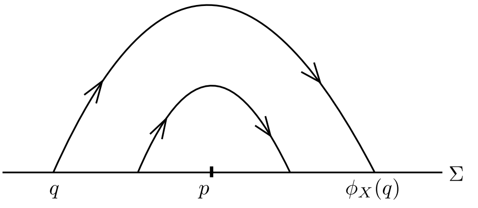


**Fig. 6.** Involution $\phi_X$ associated to an invisible fold $p \in \Sigma$ of the vector field $X$.

We want to remark that the classification of the codimension-1 local bifurcations and their generic unfoldings remain the same with the new definitions of orbit and topological equivalence. This fact will be no longer true in the codimension-2 case as it will be seen in Section 9, where we will find a codimension-2 singularity which has different unfolding whether one considers topological equivalence or $\Sigma$-equivalence.

The first and fourth type of singularities need some additional non-degeneracy conditions to be codimension-1 local bifurcations that will be stated in Sections 4.1.1, 4.1.2, 4.1.3 and 4.1.4.

#### *4.1.1. Generic Fold–Fold bifurcation*

The generic Fold–Fold singularity takes place when at a point $p \in \Sigma$ both vector fields $X$ and $Y$ have a quadratic tangency with $\Sigma$ or fold. Depending on the visibility or invisibility of both folds, the singularity presents different behavior. In this section we focus our attention on two of these cases which need additional generic non-degeneracy conditions.

The first case in which an additional condition is needed are Filippov vector fields $Z = (X, Y)$ such that at $p \in \Sigma$ the vector fields $X$ and $Y$ have a visible and an invisible fold respectively and satisfy that $X(p)$ and $Y(p)$, which are parallel, point oppositely. Then $p \in \partial\Sigma^s \cap \partial\Sigma^e$, and thus the sliding vector field is defined on both sides of $p \in \Sigma$. Moreover, in this point it has a removable singularity and, taking $x$ as a local chart of $\Sigma$, it is equivalent to

$$Z^s(x) = \beta + \mathcal{O}(x)$$

for certain constant $\beta \in \mathbb{R}$. Thus, one has to assume the generic non-degeneracy condition $\beta \neq 0$. Depending on the sign of $\beta$, one has two different local bifurcations which are called $VI_2$ and $VI_3$ in [17].

The second case is when both folds are invisible and $p \in \partial\Sigma^c$. This singularity is called both Fused–Focus and $II_2$ in [17].

To both folds of $X$ and $Y$, one can associate involutions $\phi_X$ and $\phi_Y$ which are defined from $\Sigma$ to itself (see for instance [23,10,17]). They send a point $q \in \Sigma$ to the point in $\Sigma$ which is the intersection between the orbit of $q$ and $\Sigma$ either in forward or backward time, as can be seen in Fig. 6.

Then, taking $x$ as a local chart of $\Sigma$ such that $x = 0$ corresponds to the Fold–Fold point $p$, one can see that, since $\phi_X^2 = \mathrm{Id}$, this involution must be of the form

$$\phi_X(x) = -x + \alpha_X x^2 - \alpha_X^2 x^3 + \mathcal{O}(x^4) \tag{17}$$

for certain constant $\alpha_X \in \mathbb{R}$, and analogously for $\phi_Y$.

Using both involutions, one can define a return map from $\Pi = \{(x, y) \in \Sigma\colon\ x < 0\}$ to itself around the singularity, by composing them: $\phi = \phi_Y \circ \phi_X$. Then, this return map is of the form

$$\phi(x) = x + (\alpha_Y - \alpha_X)x^2 + (\alpha_Y - \alpha_X)^2 x^3 + \mathcal{O}(x^4). \tag{18}$$

Therefore, in order to have a generic Fold–Fold singularity one has to impose that $\alpha_Y - \alpha_X \neq 0$. We call this bifurcation *generic attractor Fold–Fold bifurcation* provided $\alpha_Y - \alpha_X > 0$ and *generic repellor Fold–Fold bifurcation* provided $\alpha_Y - \alpha_X < 0$.

In Section 7 we will study the codimension-2 singularity when $\alpha_Y - \alpha_X = 0$.

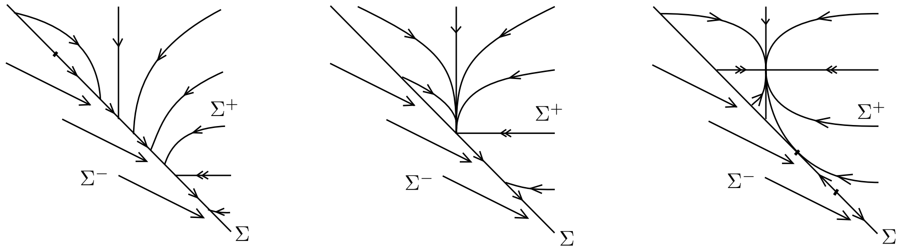


**Fig. 7.** Bifurcation diagram of a generic unfolding of (20).

**Remark 4.1.** In the case in which both $X$ and $Y$ have an invisible fold at $p \in \Sigma$ in such a way that both $X(p)$ and $Y(p)$ point toward the same direction, one has also an involution of the form (17) associated to each fold. Then, even if the return map $\phi = \phi_Y \circ \phi_X$ does not have any dynamical sense, to have a codimension-1 singularity one has to impose $\alpha_X - \alpha_Y \neq 0$. In particular, this condition avoids the appearance of pseudocycles in a generic unfolding (see Definition 2.19).

*4.1.2. Generic Boundary–Saddle bifurcation*

In order to have a generic Boundary–Saddle local bifurcation, that is $X$ has a saddle $p \in \Sigma$ whereas $Y$ is transversal to $\Sigma$ at $p$, one has to impose two generic non-degeneracy conditions.

First, the eigenspaces of the saddle as a critical point of $X$ have to be transversal to $\Sigma$. The failure of this condition leads to higher codimension local bifurcations, which will be studied in Section 8.

Second, it can be seen that the singularity $p = (0, 0) \in \Sigma$ belongs either to $\partial\Sigma^s \cap \partial\Sigma^c$ or $\partial\Sigma^e \cap \partial\Sigma^c$, and thus the sliding vector field is defined in one side of the critical point. As we will see in Sections 4.1.3 and 4.1.4, the same happens if $p$ is a focus or a node of $X$. Taking $x$ as a local chart on $\Sigma$, a straightforward computation shows that

$$Z^s(x) = \alpha x + \mathcal{O}\big(x^2\big), \tag{19}$$

for certain constant $\alpha \in \mathbb{R}$. Namely, the critical point of $X$ creates a critical point of the sliding vector field at the same point $p$, which is in the boundary of $\Sigma^s$ or $\Sigma^e$. Thus, the second non-degeneracy condition requires this critical point of $Z^s$ to be hyperbolic, namely that $\alpha \neq 0$. Depending on the sign of $\alpha$, one has different local singularities. The failure of this condition, that is, a Boundary–Saddle bifurcation which encounters a Saddle–Node bifurcation of the sliding vector field leads to a codimension-2 local bifurcation. In Section 6, this local codimension-2 bifurcation will be studied for the Boundary–Node case, which is analogous and it is explained in Section 4.1.3.

The third generic non-degeneracy condition is that at $p \in \Sigma$, the vector field $Y$ and the eigenspaces of the saddle are transversal. In [17], the authors see that there are three different Boundary–Saddle local bifurcations, which they call $BS_1$, $BS_2$ and $BS_3$. In the first two cases, on one side of the bifurcation value the saddle coexists with a pseudonode in $\Sigma^s$ and $\Sigma^e$. Then, this generic condition avoids the existence of separatrix connections between these two singularities in the unfolding.

Therefore, imposing these three conditions we will obtain a generic codimension-1 Boundary–Saddle bifurcation.

*4.1.3. Generic Boundary–Node bifurcation*

In order to have a Boundary–Node bifurcation, that is $X$ has a node in $p \in \Sigma$ whereas $Y(p)$ is transversal to $\Sigma$, one has to impose also three non-degeneracy conditions. First, both eigenvalues of the differential of $X$ at the node $p$ have to be different. Then, the node, as a critical point of $X$, has two eigenspaces which are tangent to the strong and weak stable (or unstable) manifolds. Even if for smooth systems these invariant manifolds do not need to be preserved by $C^0$-equivalences, in the Filippov Systems setting the strong stable invariant manifold must. As it can be seen in Fig. 7, the strong invariant manifold divides $\Sigma^+$ in two regions. In (20) we show an example where these regions correspond to $\{(x, y) \in \Sigma^+ \colon\ y > 0\}$ and $\{(x, y) \in \Sigma^+ \colon\ y < 0\}$. The points in the first domain belong to an orbit which has the node as an arrival point whereas any point in the second domain belongs to an orbit which has an arrival point in $\Sigma^s$. Therefore, these two open sets must be preserved by topological (and $\Sigma$-)equivalence and therefore its common boundary, which is the strong stable manifold, too.

Moreover, there are infinitely many weak stable manifolds since any other orbit of $X$, besides the strong invariant manifold, tends to the node tangent to the weak eigenspace. Therefore, the second non-degeneracy condition, as in the Boundary–Saddle bifurcation, is that both eigenspaces are transversal to $\Sigma$.

Finally, as in the Boundary–Saddle case, for this singularity it also has to be imposed that the extended sliding vector field, which also has a critical point at $p$ is of the form (19) with $\alpha \neq 0$.

**Remark 4.2.** This last non-degeneracy condition $\alpha \neq 0$ in (19) for the Boundary–Node singularity seems not to be considered in [17]. They assume that if a Filippov vector field $Z = (X, Y)$ is such that $X$ has an attracting node $p = (0, 0) \in \Sigma$ and $Y$ points towards $\Sigma$, then the extended sliding vector field $Z^s$ must have an attractor pseudonode at $p$, namely they consider that the sliding vector field is form (19) with $\alpha < 0$. Nevertheless, the constant $\alpha$ can take either positive or negative sign or be zero, the latter case having more codimension. Indeed, for the Boundary–Node bifurcation satisfying $\alpha > 0$, one can take as a normal form $f(x, y) = x + y$ and

$$Z(x, y) = \begin{cases} X(x, y) = \begin{pmatrix} -4x \\ -y \end{pmatrix} & \text{if } x + y > 0, \\ Y(x, y) = \begin{pmatrix} 2 \\ -1 \end{pmatrix} & \text{if } x + y < 0, \end{cases} \tag{20}$$

where we have chosen the normal form with $\Sigma$ with negative slope, to be allowed to take $X$ in diagonal form. In this case, one can see that $Z^s(x) = 6x + \mathcal{O}(x^2)$, and thus $x = 0$ is repellor. In Fig. 7 we show the generic unfolding of this local bifurcation.

Let us observe that in this unfolding, on the left of the bifurcation value does not exist any critical point of $X$, $Y$ nor $Z^s$ and the only singularity is an invisible Fold–Regular point, whereas on the right of the bifurcation value coexist a node of $X$ with a pseudosaddle of $Z^s$.

#### *4.1.4. Generic Boundary–Focus bifurcation*

As in the Boundary–Saddle and Boundary–Node bifurcations, the singularity $p = (0, 0) \in \Sigma$ belongs to $\partial\Sigma^c \cap \partial\Sigma^s$ or $\partial\Sigma^c \cap \partial\Sigma^e$, and is a critical point of the extended sliding vector field which is of the form (19). So one has to impose again the non-degeneracy condition $\alpha \neq 0$.

Finally, in the case in which $X$ has a repellor focus, $Y$ points towards $\Sigma$ and $\alpha > 0$, there can exist two different behaviors in the unfolding, which are called $BF_1$ and $BF_2$ in [17]. We leave the study of the corresponding codimension-2 local bifurcations emanating from this one as a future work.

### *4.2. Codimension-1 global bifurcations*

As it happens in classical smooth dynamical systems, in generic unfoldings of codimension-2 local bifurcations appear several codimension-1 global bifurcations. Thus, a good understanding of them is necessary.

In [17], the authors classify some codimension-1 global bifurcations, as it is done in classical dynamical systems, involving bifurcations of periodic orbits (which in the present paper are named periodic orbits and cycles) and separatrix connections between a saddle in $\Sigma^+ \cup \Sigma^-$ and a hyperbolic pseudoequilibrium in $\Sigma^s \cup \Sigma^e$, between two hyperbolic pseudoequilibria in $\Sigma^s \cup \Sigma^e$ or between a fold in $\Sigma$ and a saddle in $\Sigma^+ \cup \Sigma^-$ or a hyperbolic pseudoequilibrium in $\Sigma^s \cup \Sigma^e$. Nevertheless, recall that in Filippov Systems there can exist separatrix connections with finite time (for instance between two folds). In fact, all the codimension-1 bifurcations of periodic orbits and cycles can be considered as a particular case of separatrix connections between folds. Therefore, the approach that seems more systematic for these systems (proposed by M.A. Teixeira in [21]) is to study all the cases of connections of separatrices, and from them derive the bifurcation of cycles and periodic orbits as a particular

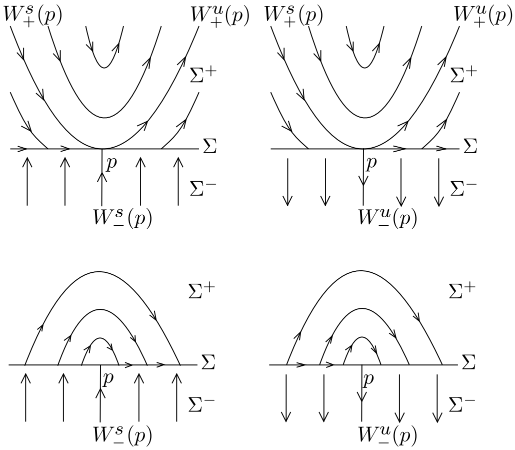


**Fig. 8.** The left and right upper pictures show respectively a sliding visible and an escaping visible folds (see Definition 3.3). The lower ones show sliding invisible (left) and escaping invisible folds (right). In this picture we also show the way of denoting the separatrices. They are denoted by $W^*_\pm(p)$, where $p$ is the fold point, $\pm$ denotes whether they are departing or arriving from $\Sigma^\pm$ and $* = s, u$ denotes whether the separatrix is stable or unstable.

case. With this new approach, we will see in this section that there exist more codimension-1 global bifurcations than the ones established in [17]. In particular, in that paper, the authors did not consider cycles containing sliding and escaping parts, whose existence is shown in this section.

We can classify the codimension-1 global bifurcations given by a separatrix connection, depending on the departing and arrival points. Each of these points, which have to be generic singularities (see Section 3) can be: a Fold–Regular point, a pseudosaddle or a pseudonode in $\Sigma^s \cup \Sigma^e$ or a saddle in $\Sigma^+ \cup \Sigma^-$. Recall that for Filippov Systems the pseudonodes in $\Sigma^s$ ($\Sigma^e$) do have separatrices, which, following our definitions, are the unique regular orbits which arrive to (depart from) them from $\Sigma^+$ and $\Sigma^-$ (see Remark 2.16).

All the separatrix connections involving saddles and pseudoequilibria besides pseudonodes were studied in [17]. In fact, the pseudonode case can be done analogously and we will not give the details here. In [17], the authors also study all the separatrix connections between a Fold–Regular point and any other singularity. However, the separatrix connections between Fold–Regular points are not studied there systematically. Only the cases which lead to the existence of cycles are considered and studied as bifurcations of periodic orbits. So in this paper, we will propose a systematic approach to study separatrix connections between two Fold–Regular points independently whether they lead to the existence of a cycle or not and we will encounter the cases studied in [17] as particular cases. In fact, we will see that the Fold–Fold separatrix connections may lead to bifurcations of periodic orbits or not. Furthermore, this approach seems the best one to generalize to higher dimensional systems in order to study global bifurcations, which up to now have been only studied from other points of view (see for instance [6–8,13,16]).

*4.2.1. Separatrix connections between two Fold–Regular points*

The separatrix connections between two Fold–Regular points can be preliminary classified whether the arrival and departing folds are visible or invisible and escaping or sliding (see Definition 3.3). As it can be seen in Fig. 8, these four types of folds have different number of stable and unstable separatrices. Therefore, one can systematically classify the Fold–Fold separatrix connections considering pairs of stable and unstable separatrices of folds. Thus, these connections can be classified as:

- Homoclinic connections: the departing and arrival point is the same Fold–Regular point. They can be reduced only to four cases: $W^s_+(p) \equiv W^u_+(p)$, both for escaping and sliding visible folds, $W^u_+(p) \equiv W^s_-(p)$, for sliding folds, and $W^u_-(p) \equiv W^s_+(p)$, for escaping folds.

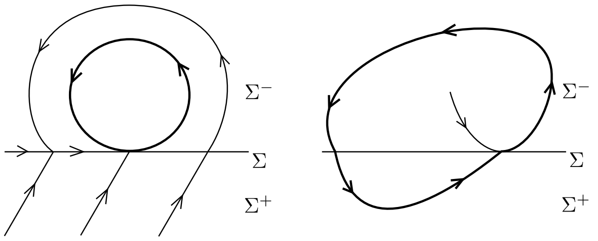


**Fig. 9.** Two examples of homoclinic connections between folds. On the left, the connection is $W_+^s(p) \equiv W_+^u(p)$ where $p$ is a sliding fold whereas on the right the connection is $W_+^u(p) \equiv W_-^s(p)$ where $p$ is also a sliding fold.

- Heteroclinic connections: the arrival and departing points are different Fold–Regular points. There are 16 cases, since there are four possible stable and four possible unstable separatrices (see Fig. 8). Some of them, but not all, may lead to bifurcations of cycles.

We devote the rest of the section to study the cases which lead to more interesting dynamics. The other cases can be studied analogously.

*Homoclinic connections.* As all the homoclinic connections lead to bifurcations of cycles, they are carefully studied in [17] and thus, we just summarize their results.

The case $W_+^s(p) \equiv W_+^u(p)$, both for sliding and escaping folds, was called $TC_1$ and $TC_2$ in [17], and it is also called *grazing-sliding bifurcation* (see [6,7]). An example of this type of connection is shown on the left picture of Fig. 9.

The connections $W_+^u(p) \equiv W_-^s(p)$ for a sliding fold and $W_-^u(p) \equiv W_+^s(p)$ for an escaping fold were called *CC* in [17], and are also sometimes called *crossing-sliding bifurcations* [6,7]. An example of this type of connection is shown on the right picture of Fig. 9.

In all these cases, depending on the attracting or repelling character of the pseudohomoclinic connection two different bifurcations can occur. In one case, a periodic orbit becomes a pseudohomoclinic cycle on the bifurcation value where it hits either $\partial\Sigma^s$ or $\partial\Sigma^e$. In the other case, on one side of the bifurcation value coexist a periodic orbit and a cycle which merge at the bifurcation giving birth to a semistable cycle (the pseudohomoclinic connection), which afterwards disappear. The study of the same bifurcations from a Catastrophe Theory point of view can be seen in [12].

*Heteroclinic connections.* In [17], the authors study two of these cases as bifurcations of periodic orbits. The first case, which they call $SC$ is the connection $W_+^u(p_1) \equiv W_-^s(p_2)$ where $p_1$ and $p_2$ are visible folds of $X$ and $Y$ respectively.

The other case are the connections $W_+^u(p_2) \equiv W_+^s(p_1)$ where $p_1$ is an invisible sliding fold of $Y$ and $p_2$ is a visible sliding fold of $X$, and $W_+^u(p_1) \equiv W_+^s(p_2)$ where $p_1$ and $p_2$ are respectively an invisible escaping fold of $Y$ and visible escaping fold of $X$. These connections can lead to bifurcations of cycles as it can be seen in the upper pictures of Fig. 10 and they are usually called *switching-sliding bifurcation* [6,7] or *buckling bifurcation* [17]. Nevertheless, the same bifurcation can occur in other settings, as it can be seen in the lower pictures of Fig. 10. It is in that sense, that we believe that the separatrix connection approach is the most useful in that cases, since focuses its attention on the part of the phase portrait where the bifurcation occurs, that is, in a neighborhood of the connection.

Finally, we show some cases which do not appear in [17]. The first one corresponds to the case $W_+^u(p_1) \equiv W_+^s(p_2)$ where $p_1$ and $p_2$ are visible sliding folds, which is sometimes interpreted as another type of *grazing-sliding bifurcation*, but which involves two different Fold–Regular points (see the upper pictures of Fig. 11). This case can lead also to a bifurcation of cycles, as it can be seen in the lower pictures of Fig. 11, and in its generic unfolding, the cycle is always persistent in both sides of the bifurcating point and always contains a segment of $\Sigma^s$. Nevertheless, as we show in the upper pictures of Fig. 11, this bifurcation does not automatically imply the existence of a cycle.

The remaining cases, which lacked in [17], are those which involve two Fold–Regular points that are in the boundary of the sliding and the escaping regions. The one which has richer dynamics is

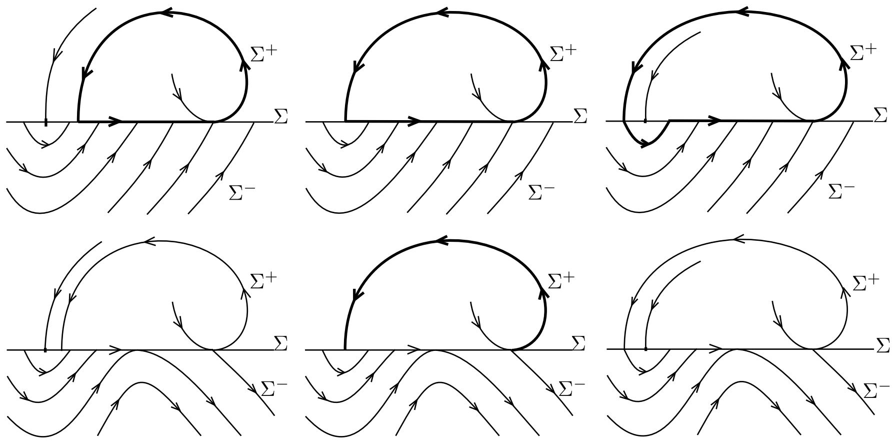


**Fig. 10.** Bifurcation diagram of two different generic unfoldings of the separatrix connection $W^u_+(p_2) \equiv W^s_+(p_1)$ where $p_1$ is an invisible sliding fold of $Y$ and $p_2$ is a visible sliding fold of $X$. In the first case, the separatrix connection leads to a bifurcation of a cycle and is usually called *switching-sliding bifurcation* [6,7] or *buckling bifurcation* [17], whereas in the second one does not exist any cycle.

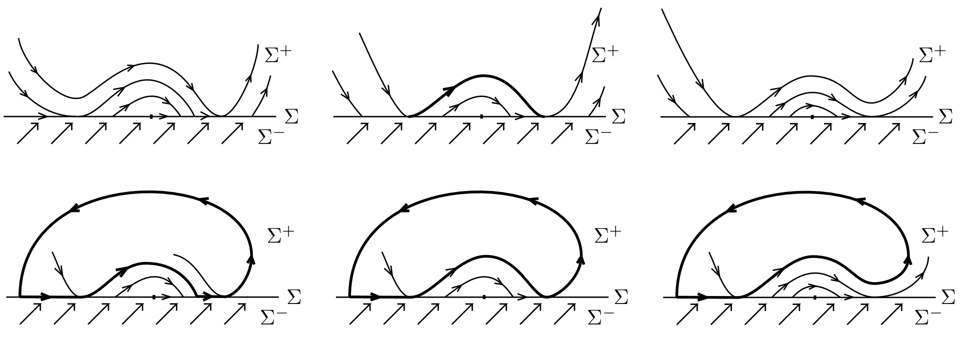


**Fig. 11.** Bifurcation diagram of generic unfoldings of the separatrix connection $W^u_+(p_1) \equiv W^s_+(p_2)$ where $p_1$ and $p_2$ are visible sliding folds. In the lower pictures we show how it can lead, in some cases, to a bifurcation of cycles.

$W^u_+(p_1) \equiv W^s_+(p_2)$ where $p_1$ and $p_2$ are respectively sliding and escaping visible Fold–Regular points. Depending on the behavior of $Y$ nearby $\Sigma$, the Filippov vector field can have interesting dynamics.

The upper part of Fig. 12 illustrates the generic case in which $W^u_-(p_2)$ has an arrival point in $\Sigma^s$. Then, there exists a cycle composed by $W^u_-(p_2)$, a sliding segment and the separatrix connection $W^u_+(p_1) \equiv W^s_+(p_2)$. Moreover, it coexists with a continuum of cycles composed by the separatrix connection, a segment of $\Sigma^e$, a regular orbit in $\Sigma^-$ and a segment of $\Sigma^s$. When we unfold this codimension-1 global bifurcation, on one side (upper left picture of Fig. 12) all these cycles disappear whereas in the other (upper right picture of Fig. 12) only the one composed by $W^u_+(p_1)$ and a sliding segment persists.

The lower part of Fig. 12 illustrates the symmetric case in which $W^s_-(p_1)$ has a departing point in $\Sigma^e$.

**Remark 4.3.** We point out that an analytical approach to study these separatrix connections is to use a Melnikov-like theory (see [18], for a more modern approach for planar vector fields see [11]). As we are dealing with planar autonomous systems, the distance between the perturbed separatrices is given up to first order by a coefficient which is proportional to the perturbation parameter. This coefficient is obtained through a finite time Melnikov computation, since in this case the unperturbed

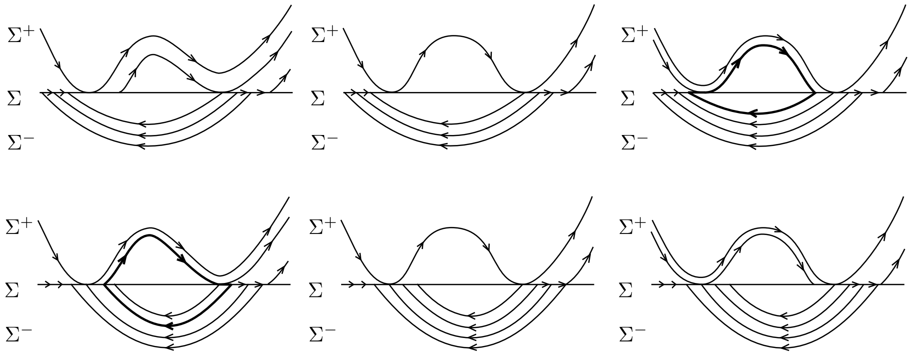


**Fig. 12.** Two different settings in which a codimension-1 global bifurcation given by a separatrix connection between a visible escaping fold and a visible sliding fold lead to a bifurcation of cycles. Let us observe that in both cases in the bifurcating value there exist a continuum of cycles. In the top case, only persist one on the right, which contains a sliding segment, and no one persist on the left, whereas in the bottom case, on the left persist one with escaping segment and on the right all break down.

separatrix connection is continuous but piecewise differentiable. Generically, this coefficient is non-zero and then the connections are destroyed.

## 5. Codimension-2 local bifurcations. Preliminary classification

The full list of different codimension-2 local bifurcations for planar Filippov Systems is considerably large. Therefore, in this section we establish a preliminary classification of them. As we have explained in Section 4.1, to obtain this classification we have to consider the four cases of codimension-1 bifurcations listed in that section and violate one of the non-degeneracy conditions which define them.

We assume that the singularity is located at $p = (0, 0)$. The first set of codimension-2 local bifurcations refers to the singularities related to tangency points:

- One of the vector fields has a fourth order tangency with $\Sigma$ at $p$ whereas the other one is transversal to $\Sigma$.
- One of the vector fields has a cusp or cubic tangency with $\Sigma$ at $p$ whereas the other has a fold or quadratic tangency. We call to this bifurcation *Cusp–Fold* and is carefully studied in Section 12.
- The Filippov vector field has a degenerate Fold–Fold bifurcation since one of the non-degeneracy generic conditions explained in Section 4.1.1 fails. One of these bifurcations will be explained in Section 7.

The second set of codimension-2 local bifurcations refers to the Filippov vector fields $Z = (X, Y)$ such that $X$, $Y$ or $Z^s$ has a critical point at $p \in \Sigma$.

- $X$ (or $Y$) has a non-hyperbolic critical point at $p \in \Sigma$, which is a codimension-1 singularity for $X$ (or $Y$), that is a Saddle–Node or a Hopf singularity, whereas $Y$ (or $X$) is transversal to $\Sigma$. These two bifurcations will be studied in more detail in Sections 13 and 14.
- $p \in \Sigma$ is a hyperbolic critical point of $X$ and a fold of $Y$ (or vice versa). Two of these bifurcations, the Focus–Fold and the Saddle–Fold will be explained respectively in Sections 10 and 11, since they are the cases which present more global codimension-1 bifurcations in their unfoldings.
- $p \in \Sigma$ is a hyperbolic critical point of $X$ whereas $Y$ is transversal to $\Sigma$ but one of the non-degeneracy generic conditions specified in Sections 4.1.2, 4.1.3 and 4.1.4 fails.
- The sliding vector field $Z^s$ has a cusp bifurcation at $p \in \Sigma$ in the sense of Singularity Theory (see [19]), that is $Z^s(p) = (Z^s)'(p) = (Z^s)''(p) = 0$ and $(Z^s)'''(p) \neq 0$.

This pre-classification is complete in the sense that any codimension-2 singularity falls in one of these cases. Moreover, several non-equivalent codimension-2 singularities belong to any of the items of this pre-classification. Some of them do not present more interesting behavior than the behaviors encountered around codimension-1 local bifurcations in [17]. In Sections 6–14, we will study in more detail the cases that present richer behavior, that is more global phenomena and codimension-1 bifurcations around it. In order to have codimension-2 bifurcations one has to impose generic non-degeneracy conditions, as we have done for the codimension-1 ones in Section 4.2. These conditions will be specified for the cases that will be studied in the corresponding sections.

As we have explained in Section 3.1, to simplify the explanation we will mostly work with simple normal forms. Dealing with generic unfoldings instead of normal forms is straightforward in some cases but requires some extra analysis in others, mainly in the cases which involve boundary-equilibria. In these cases one needs to prove that if one takes into account the nonlinear terms of the vector field, the obtained qualitative behavior is equivalent. Being the boundary-equilibrium in $\Sigma$, one cannot use, at least straightforwardly, Hartmann–Grobman Theorem, because it is not guaranteed that $\Sigma$ is preserved by the conjugation provided by this theorem. However, one can deal with the higher order terms using standard tools in dynamical systems analysis to obtain the same bifurcation diagrams. As a consequence, even if we do not prove this fact, all the bifurcation diagrams that we will show are generic and remain the same for any other vector field satisfying the same degeneracy and non-degeneracy conditions.

## 6. Codimension-2 Boundary–Node singularity

As it has been explained in Sections 4.1.2, 4.1.3 and 4.1.4, when one considers a Boundary–Focus, Node or Saddle in $p=(0,0)\in\Sigma$, the sliding vector field which gives the motion in one side of $p$ is of the form $Z^s(x)=\alpha x+\mathcal{O}(x^2)$ (see (19)). Thus, in order to guarantee that the singularity has codimension-1, it has to be imposed $\alpha\neq 0$ in such a way that $\alpha=0$ leads to several codimension-2 singularities. In this section we study one of the cases of codimension-2 Boundary–Node singularity since the others (and also the Boundary–Saddle and Boundary–Focus cases) can be studied analogously, and they do not lead to new interesting dynamics.

We consider a Filippov vector field $Z=(X,Y)$ such that $X$ has an attractor node at $p=(0,0)\in\Sigma$ and $Y$ is transversal to $\Sigma$ and points towards it, in such a way that the corresponding sliding vector field is of the form $Z^s(x)=\beta x^2+\mathcal{O}(x^3)$ with $\beta>0$. We want to point out that the other generic non-degeneracy conditions explained in Section 4.1.3 still have to hold, that is, the eigenvalues of the node have to be different and the weak and strong eigenspaces have to be transversal to $\Sigma$.

To consider a normal form such that the linearization of $X$ at $p$ is diagonal, we have to take $\Sigma$ transversal to the eigenspaces of $X$ at $p$. We choose coordinates such that $\Sigma=\{(x,y)\colon\ x+y=0\}$ and

$$Z(x,y)=\begin{cases} X(x,y)=\left(\begin{smallmatrix}-x+x^2\\ -2y\end{smallmatrix}\right) & \text{if } x+y>0,\\ Y(x,y)=\left(\begin{smallmatrix}-1\\ 2\end{smallmatrix}\right) & \text{if } x+y<0\end{cases}$$

since then, taking $x$ as a local chart of $\Sigma$, the sliding vector field is given by

$$Z^s(x)=\frac{2x^2}{1-x-x^2}=2x^2+\mathcal{O}\bigl(x^3\bigr).$$

The dynamics of $Z$ is illustrated in Fig. 13. Let us observe that it is not possible to take a normal form with $X$ and $\Sigma$ linear to obtain a sliding vector field without linear part and not identically zero. Therefore, to avoid this degeneracy, we consider quadratic terms in $X$. Nevertheless, any non-zero coefficient in front of the quadratic term gives the same qualitative behavior.

A generic unfolding of this singularity can be given by

$$Z_{\varepsilon,\mu}(x,y)=\begin{cases} X_\mu(x,y)=\left(\begin{smallmatrix}-x+x^2+\mu\\ -2y-\mu\end{smallmatrix}\right) & \text{if } x+y>0,\\ Y_\varepsilon(x,y)=\left(\begin{smallmatrix}-1-\varepsilon\\ 2+\varepsilon\end{smallmatrix}\right) & \text{if } x+y<0,\end{cases} \tag{21}$$

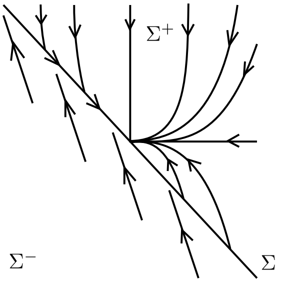


**Fig. 13.** Phase portrait of the degenerate Boundary–Node bifurcation.

in such a way that the node of $X_\mu$ is given by

$$N = \left(\frac{1-\sqrt{1-4\mu}}{2}, \frac{-\mu}{2}\right),$$

which is admissible for $\mu \geqslant 0$ and non-admissible for $\mu < 0$. Moreover, we have chosen the unfolding parameters in such a way that when $N$ is away from $\Sigma$, that is when $\mu \neq 0$, the fold of the vector field $X_\mu$ which appears is located at $F_+ = (0,0)$. The parameter $\varepsilon$ unfolds the other degeneracy, namely, when $\varepsilon \neq 0$, the sliding vector field has a term linear in $x$, since it is given by

$$Z^s_{\varepsilon,\mu}(x) = \frac{\mu + \varepsilon x + (2+\varepsilon)x^2}{1 - x - x^2}.$$

Computing the critical points of $Z^s_{\varepsilon,\mu}$, it is straightforward to see that $Z^s_{\varepsilon,\mu}$ undergoes a Saddle–Node bifurcation provided $\varepsilon^2 - 4\mu(2+\varepsilon) = 0$. Nevertheless, the Saddle–Node point

$$Q = \left(-\frac{\varepsilon}{2(2+\varepsilon)}, \frac{\varepsilon}{2(2+\varepsilon)}\right)$$

only belongs to $\Sigma^s$ provided $\varepsilon > 0$.

First we study the codimension-1 local bifurcations which undergoes the unfolding $Z_{\varepsilon,\mu}$ (see the bifurcation diagram in Fig. 14). The line $\{(\varepsilon,\mu)\colon\ \mu = 0\}$ corresponds to two different kinds of codimension-1 Boundary–Node bifurcations: for $\varepsilon < 0$ is the bifurcation $BN_1$ described in [17] and for $\varepsilon > 0$ is the bifurcation explained in Remark 4.2.

In the curve

$$\eta = \left\{(\varepsilon,\mu)\colon\ \mu = \frac{\varepsilon^2}{4(2+\varepsilon)} \text{ for } \varepsilon > 0\right\}$$

takes place a Saddle–Node bifurcation of the sliding vector field (called *pseudo-Saddle–Node* in [17]). In these two curves occur the only possible local bifurcations of the unfolding, which moreover are the same independently whether we use $\Sigma$ or topological equivalence.

Finally, studying the regions delimited by these curves it can be easily seen that there cannot appear global bifurcations and then, any two vector fields in any of these regions are $\Sigma$-equivalent (and thus topologically equivalent).

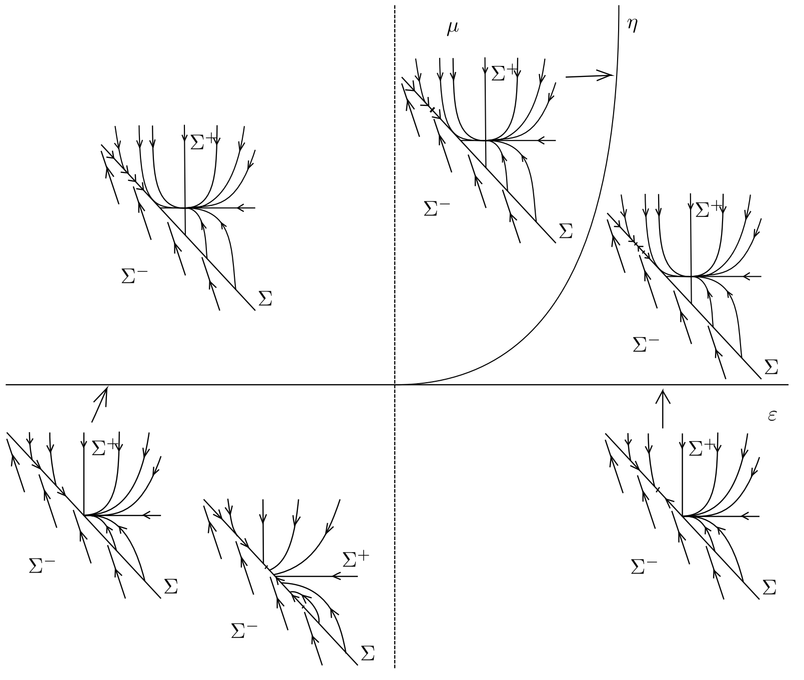


**Fig. 14.** Bifurcation diagram of the generic unfolding of the degenerate Boundary–Node, which is given by (21). Notice that in the curve $\eta$ occurs the Saddle–Node bifurcation of the sliding vector field.

## 7. Codimension-2 invisible Fold–Fold singularity

Let us consider $\Sigma = \{(x, y)\colon\ y = 0\}$ and an invisible Fold–Fold point at $p = (0, 0)$. Then, as we have explained in Section 4.1.1, we can define a return map in $\Pi = \{(x, y) \in \Sigma\colon\ x < 0\}$, which is of the form (18).

Then, for the generic codimension-1 Fold–Fold singularity (called $II_2$ in [17]), one has to impose that $\alpha_X - \alpha_Y \neq 0$ (see (18)). Therefore, taking $\alpha_X - \alpha_Y = 0$ leads to a codimension-2 singularity, whose return map is of the form

$$\phi(x) = x + \beta x^4 + \mathcal{O}\big(x^5\big), \tag{22}$$

where we assume the generic non-degeneracy condition $\beta \neq 0$ ($\beta = 0$ would correspond to a codimension-3 singularity). More concretely, we will focus on the case $\beta < 0$, and then $p$ acts as a repellor focus, and the case $\beta > 0$ can be studied analogously.

We take as a normal form

$$Z(x, y) = \begin{cases} X(x, y) = \begin{pmatrix} 1 \\ -x+x^4 \end{pmatrix} & \text{if } y > 0, \\ Y(x, y) = \begin{pmatrix} -1 \\ -x \end{pmatrix} & \text{if } y < 0 \end{cases}$$

whose associated return map is

$$\phi(x) = x - \frac{2}{5}x^4 + \mathcal{O}\big(x^5\big)$$

and thus, it is of the form (22).

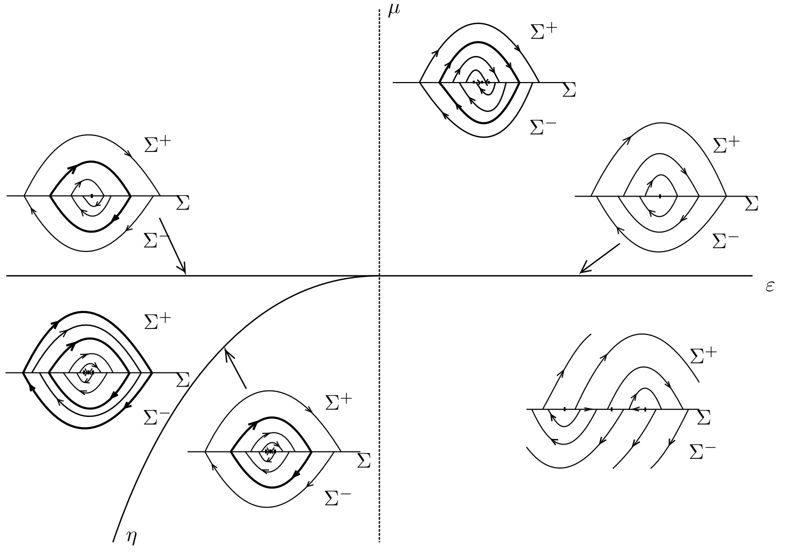


**Fig. 15.** Bifurcation diagram of (23). It remains the same independently whether we use $\Sigma$-equivalences or topological equivalences.

A generic unfolding of this singularity can be given by

$$Z_{\varepsilon,\mu}(x,y) = \begin{cases} X_\varepsilon(x,y) = \binom{1}{-x+\varepsilon x^2+x^4} & \text{if } y > 0, \\ Y_\mu(x,y) = \binom{-1}{-(x-\mu)} & \text{if } y < 0, \end{cases} \tag{23}$$

in such a way that for $\mu \neq 0$ the folds of $X_\varepsilon$ and $Y_\mu$ are $F_+ = (0,0)$ and $F_- = (\mu, 0)$ respectively.

The parameter $\varepsilon$ unfolds the degeneracy of the return map. Indeed, applying Taylor formula to the flow of the smooth vector fields $X_\varepsilon$ and $Y_\mu$ with respect to the initial condition, one can see that, for $\mu = 0$, the return map around the Fold–Fold point $p = (0,0)$ is given by

$$\phi_{\varepsilon,0}(x) = x - \frac{2}{3}\varepsilon x^2 + \frac{4}{9}\varepsilon^2 x^3 - \left(\frac{2}{5} + \frac{16}{27}\varepsilon^3\right)x^4 + \mathcal{O}(x^5). \tag{24}$$

Therefore, $p$ is a generic repellor Fold–Fold for $\varepsilon > 0$ and is a generic attractor Fold–Fold for $\varepsilon < 0$.

Furthermore, for $\mu \neq 0$, it appears a small sliding region between $F_+$ and $F_-$ (for $\mu > 0$) or a small escaping region between $F_-$ and $F_+$ (for $\mu < 0$). In both cases, taking $x$ as a local chart of $\Sigma$, the sliding vector field is given by

$$Z^s_{\varepsilon,\mu}(x) = \frac{\mu - 2x + \varepsilon x^2 + x^4}{\mu - \varepsilon x^2 - x^4}$$

which has a pseudonode $N = (N_x, 0)$ for any $\mu \neq 0$, that satisfies $N_x = \mathcal{O}(\mu)$.

In the unfolding (23) there exist both local and global bifurcations as can be seen in the following proposition (see Fig. 15 for the bifurcation diagram).

**Proposition 7.1.** *For $(\varepsilon, \mu)$ small enough the vector field $Z_{\varepsilon,\mu}$ in* (23) *undergoes the following bifurcations*:

- *A generic attractor Fold–Fold bifurcation* (*see Section* 4.1.1) *in* $\{(\varepsilon,\mu)\colon\ \mu = 0,\ \varepsilon < 0\}$.
- *A generic repellor Fold–Fold bifurcation* (*see Section* 4.1.1) *in* $\{(\varepsilon,\mu)\colon\ \mu = 0,\ \varepsilon > 0\}$.

- *A Saddle–Node bifurcation of periodic orbits in the curve* $\eta$ *(see Fig.* 15*) which is given by*

$$\eta = \left\{(\varepsilon, \mu): \ \mu = -\frac{5}{36}\varepsilon^2 + \mathcal{O}\big(\varepsilon^3\big) \textit{ for } \varepsilon < 0\right\}.$$

**Proof.** We start studying the local bifurcations. Since both folds are given by $F_+ = (0, 0)$ and $F_- = (\mu, 0)$, $Z_{\varepsilon,\mu}$ undergoes a Fold–Fold bifurcation in $\{(\varepsilon, \mu): \ \mu = 0\}$. From the return map (24), one can see that for $\varepsilon < 0$ the Fold–Fold is attracting and for $\varepsilon > 0$ it is repelling. Moreover, from (24) it is straightforward to see that in $\{(\varepsilon, \mu): \ \mu = 0, \ \varepsilon < 0\}$ there exists a repelling periodic orbit, whose intersection points with $\Sigma$ are given by $Q^{\pm} = (Q_x^{\pm}, 0)$ with

$$Q_x^{\pm} = \pm\sqrt{-\frac{5}{3}\varepsilon} + \mathcal{O}(\varepsilon),$$

and which persists for $\mu \neq 0$ and $\varepsilon < 0$.

Therefore, considering also the periodic orbit which appears due to the Fold–Fold generic bifurcation (see Section 4.1.1), we have that close to the curve $\{(\varepsilon, \mu): \ \mu = 0, \ \varepsilon < 0\}$ there exists a periodic orbit for $\mu > 0$ and two periodic orbits for $\mu < 0$ and close to the curve $\{(\varepsilon, \mu): \ \mu = 0, \ \varepsilon > 0\}$ there exists a periodic orbit for $\mu > 0$ and none for $\mu < 0$. These bifurcations are illustrated in Fig. 15.

As a consequence any two vector fields in $\{(\varepsilon, \mu): \ \mu > 0\}$ are $\Sigma$-equivalent (and thus topological equivalent).

In $\{(\varepsilon, \mu): \ \mu < 0\}$, it is clear that a global bifurcation leading to the disappearance of the periodic orbits takes place. In order to detect it, it is enough to point out that in this region these periodic orbits are given by fixed points of the return map $\phi_{\varepsilon,\mu}$ associated to $Z_{\varepsilon,\mu}$. Thus, this bifurcation corresponds to the existence of a double zero of the equation $\phi_{\varepsilon,\mu}(x) = x$. Applying Taylor formula to the flows of the smooth vector fields $X_\varepsilon$ and $Y_\mu$ with respect to the initial conditions, one can see that the return map $\phi_{\varepsilon,\mu}$ is given by

$$\phi_{\varepsilon,\mu}(x) = 2\mu + x - \frac{2}{3}\varepsilon x^2 + \frac{4}{9}\varepsilon^2 x^3 - \left(\frac{2}{5} + \frac{16}{27}\varepsilon^3\right)x^4 + \mathcal{O}\big(x^5\big).$$

Then, the curve $\eta$ in which the Saddle–Node bifurcation of periodic orbits takes place is given by

$$\mu = -\frac{5}{36}\varepsilon^2 + \mathcal{O}\big(\varepsilon^3\big)$$

for $\varepsilon < 0$. $\square$

## 8. Boundary–Saddle with an invariant manifold tangent to $\Sigma$

In order to have a codimension-1 Boundary–Saddle bifurcation, one has to impose that the invariant manifolds of the saddle are transversal to $\Sigma$ and $\alpha \neq 0$ where $\alpha$ is the linear part of the sliding vector field given in (19) (see Section 4.1.2). Therefore, if $\Sigma$ and one of these manifolds are tangent, the singularity has higher codimension. In this section we consider vector fields $Z = (X, Y)$ having the following property: one of the invariant manifold of the saddle $p \in \Sigma$ of $X$ has a quadratic contact with $\Sigma$.

This singularity can present different behaviors depending on:

- Which invariant manifold is tangent (the stable or the unstable one).
- The sign of $Yf(p)$, that is, whether $Y$ points toward $\Sigma$ ($Yf(p) > 0$) or away from $\Sigma$ ($Yf(p) < 0$), recall that $\Sigma$ is defined as $\Sigma = \{(x, y): \ f(x, y) = 0\}$.
- Whether one or three branches of the invariant manifolds are admissible.
- The sign of $\alpha$.

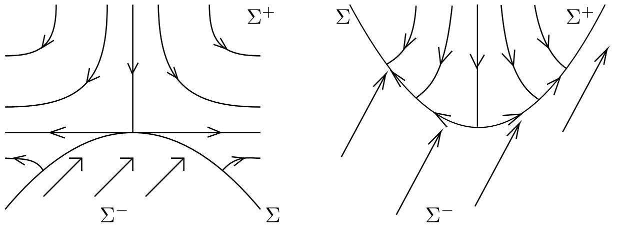


**Fig. 16.** Two kinds of Boundary–Saddle with an invariant manifold tangent to $\Sigma$. On the left the two branches of the unstable invariant manifold and one branch of the stable one are admissible whereas on the right, only one branch of the stable invariant manifold is admissible.

We observe that the number of branches of the invariant manifolds which are admissible depends on the second order terms of the jet of $X$ and $f$ (see Fig. 16). Moreover, we point out that even though in this case $\Sigma^s$ is collapsed to $(0,0)$, we have to consider $Z^s$ as in (19) since the condition $\alpha \neq 0$ is needed to deal with a codimension-2 bifurcation.

In this section, we focus ourselves on the case in which $\Sigma$ is tangent to the unstable invariant manifold, one branch of the stable invariant manifold and the two branches of the unstable invariant manifold are admissible, $Y$ points toward $\Sigma$ (see left picture in Fig. 16) and $\alpha > 0$. In this case, it is straightforward to see that the saddle $p = (0,0) \in \Sigma$ belongs to the boundary of two components of $\Sigma^c$.

To consider a normal form for this singularity, we distort $\Sigma$ in order to be allowed to consider $X$ as a linear vector field in diagonal form. We take coordinates such that $\Sigma = \{(x,y)\colon\ y + x^2 = 0\}$ and the vector field

$$Z(x,y) = \begin{cases} X(x,y) = \begin{pmatrix} 1 & 0 \\ 0 & -1 \end{pmatrix}\begin{pmatrix} x \\ y \end{pmatrix} & \text{if } y + x^2 > 0, \\ Y(x,y) = \begin{pmatrix} 1 \\ 1 \end{pmatrix} & \text{if } y + x^2 < 0 \end{cases}$$

in such a way that $\Sigma$ and $W^u(p)$ are tangent to the $x$-axis at $p = (0,0)$. In order to consider a generic unfolding of this singularity, we again deform $\Sigma$ such that it depends on one parameter:

$$\Sigma \equiv \Sigma_\varepsilon = \bigl\{(x,y)\colon\ f(x,y) = y + \varepsilon x + x^2 = 0\bigr\}$$

and we consider as vector field

$$Z_{\varepsilon,\mu}(x,y) = \begin{cases} X_\mu(x,y) = \begin{pmatrix} 1 & 0 \\ 0 & -1 \end{pmatrix}\begin{pmatrix} x \\ y-\mu \end{pmatrix} & \text{if } y + \varepsilon x + x^2 > 0, \\ Y(x,y) = \begin{pmatrix} 1 \\ 1 \end{pmatrix} & \text{if } y + \varepsilon x + x^2 < 0. \end{cases} \tag{25}$$

Then, the saddle of $X$ is $Q = (0,\mu)$ and therefore it is admissible for $\mu > 0$ and non-admissible for $\mu < 0$.

The tangencies of $X_\mu$ with $\Sigma$ when $\mu \neq 0$ are the solutions of equation $X_\mu f = 0$. This equation reads $3x^2 + 2\varepsilon x + \mu = 0$ whose discriminant is given by $\Delta = 4\varepsilon^2 - 12\mu$. Thus, in the curve $\eta_1 = \{(\varepsilon,\mu)\colon\ \mu = \varepsilon^2/3\}$, $X_\mu$ has a cusp (a cubic tangency, see Definition 2.2) with $\Sigma$. Above this curve does not exist any fold and below it there are two (see Fig. 17) which we call $F_1$ and $F_2$. Therefore, above $\eta_1$, $\Sigma = \Sigma^c$ and below it appears a small sliding region of diameter $\mathcal{O}(\sqrt{\Delta})$ given by

$$\Sigma^s = \left\{(x,y) \in \Sigma\colon\ x \in \left(\frac{-2\varepsilon - \sqrt{4\varepsilon^2 - 12\mu}}{6}, \frac{-2\varepsilon + \sqrt{4\varepsilon^2 - 12\mu}}{6}\right)\right\}.$$

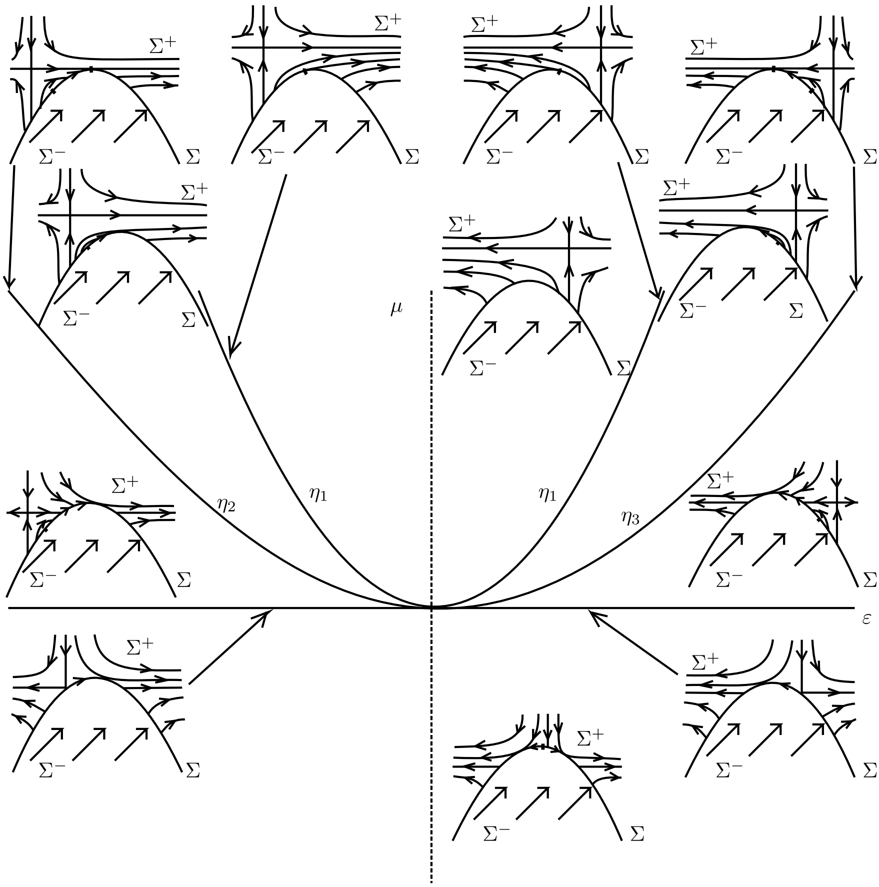


**Fig. 17.** Bifurcation diagram of (25) using $\Sigma$-equivalences.

In $\Sigma^s$, we can compute the sliding vector field taking $x$ as a local chart, which is given by

$$Z^s_{\varepsilon,\mu}(x) = \frac{-\mu + (1-\varepsilon)x - x^2}{1+\varepsilon-\mu+2(1-\varepsilon)x - 3x^2}.$$

Moreover, for $\mu < 0$, it has a pseudosaddle $S = (S_x, S_y) \in \Sigma^s$, with

$$S_x = \frac{1-\varepsilon-\sqrt{(1-\varepsilon)^2 - 4\mu}}{2} \quad \text{and} \quad S_y = -\varepsilon S_x - S_x^2.$$

Next proposition summarizes all the local and global bifurcations which occur nearby the singularity we are considering (see the bifurcation diagram in Fig. 17).

**Proposition 8.1.** *For $(\varepsilon, \mu)$ small enough the vector field $Z_{\varepsilon,\mu}$ in* (25) *undergoes the following bifurcations*:

- *A Boundary–Saddle, called $BS_3$ in* [17], *in* $\{(\varepsilon,\mu)\colon \mu = 0,\ \varepsilon \neq 0\}$.
- *A cusp bifurcation, called $DT_1$ in* [17], *in the curve* $\eta_1 = \{(\varepsilon,\mu)\colon \mu = \varepsilon^2/3\}$.

- *A connection of separatrices between the saddle $Q$ and the fold $F_1$, that is $W^u(Q) \equiv W^s_+(F_1)$, in $\eta_2 = \{(\varepsilon,\mu){:}\ \mu = \varepsilon^2/4,\ \varepsilon < 0\}$.*
- *A connection of separatrices between the saddle $Q$ and the fold $F_2$, that is $W^u(Q) \equiv W^s_+(F_2)$, in $\eta_3 = \{(\varepsilon,\mu){:}\ \mu = \varepsilon^2/4,\ \varepsilon > 0\}$.*

**Proof.** The proof of the existence of the local bifurcations is immediate from the study of tangencies and critical points of $Z_{\varepsilon,\mu}$, which has already been done. In $\{(\varepsilon,\mu){:}\ \mu = 0,\ \varepsilon \neq 0\}$, the saddle $Q$ belongs to $\Sigma$ and thus this line corresponds to the codimension-1 Boundary–Saddle bifurcation called $BS_3$ in [17]. In the curve $\eta_1$ occurs a cusp bifurcation which is called $DT_1$ in [17]. In these two curves in the $(\varepsilon,\mu)$ parameter space occur all the possible codimension-1 local bifurcations, either considering topological equivalence or $\Sigma$-equivalence, which exist in any generic unfolding of the singularity.

Secondly, we study the codimension-1 global bifurcation curves of the unfolding $Z_{\varepsilon,\mu}$. For that purpose, we study the behavior of the vector field in the three regions delimited by the curves above explained.

In $\{(\varepsilon,\mu){:}\ \mu < 0\}$ it can be checked easily that any two vector fields are $\Sigma$-equivalent (and thus topologically equivalent), since for parameters in this region all the vector fields have the same singularities and there is no possibility of connections of separatrices. In the region $\{(\varepsilon,\mu){:}\ 0 < \mu < \varepsilon^2/3\}$, there occurs a global bifurcation given by a separatrix connection between the saddle $Q = (0,\mu)$ and one of the two visible folds, that is $W^u(Q) \equiv W^s_+(F_1)$ and $W^u(Q) \equiv W^s_+(F_2)$ for $\varepsilon > 0$ and for $\varepsilon < 0$ respectively. To compute the curve in the parameter space where these connections take place, we use that the saddle is in diagonal form and that the unstable invariant manifold is just a horizontal line. Then, it is enough to impose that the $y$-coordinates of the saddle and one of the folds coincide to obtain that the connection takes place in $\{(\varepsilon,\mu){:}\ \mu = \varepsilon^2/4\}$.

Finally, above $\eta_1$ does not appear any other global bifurcation, since the only singularity of the vector field $Z_{\varepsilon,\mu}$ is the saddle $Q$ of $X_\mu$ and then, there cannot exist separatrix connections. Therefore any two vector fields belonging to that region are $\Sigma$-equivalent (and thus topologically equivalent). $\square$

The description of the bifurcation diagram is independent whether we use $\Sigma$-equivalence or topological equivalence.

## 9. Non-diagonalizable node in $\Sigma$

In this section we study the Boundary–Node bifurcation in the case in which both eigenvalues coincide and so one of the generic non-degeneracy conditions stated in Section 4.1.3 is violated. Then, to be a codimension-2 local bifurcation, the linear part cannot be diagonalizable.

As it was noticed in [17] (see also [21]), the Boundary–Focus and Boundary–Node are different singularities in planar Filippov Systems, since they cannot be either $\Sigma$-equivalent nor topologically equivalent (see also Sections 4.1.3 and 4.1.4). This fact is genuinely discontinuous since, as it is well known by Hartmann–Grobman Theorem (see [20]), in the smooth case a focus and a node are topologically equivalent (in fact topologically conjugated). Nevertheless, the conjugacy provided by Hartmann–Grobman Theorem cannot be used to construct a homeomorphism as in Proposition 2.22, since it twists the neighborhood of the critical point and therefore, it does not preserve $\Sigma^+$.

Let us consider a Filippov vector field $Z = (X, Y)$ in a neighborhood $U$ of $p \in \Sigma$ such that $Y$ is transversal to $\Sigma$ and $X$ has a node at $p \in \Sigma$ whose Jacobian $DX(p)$ has a Jordan normal form given by

$$\begin{pmatrix} \lambda & 0 \\ 1 & \lambda \end{pmatrix} \tag{26}$$

for certain $\lambda \in \mathbb{R}$, in such a way that the eigenspace associated with the unique eigenvector is transversal to $\Sigma$. Then, $Z$ undergoes a codimension-2 local bifurcation at $p$, independently whether we consider topological equivalences or $\Sigma$-equivalences.

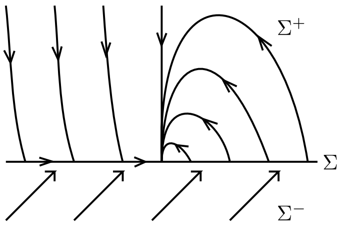


**Fig. 18.** Phase portrait of (27).

We will see that this singularity has a feature not present in any codimension-1 singularity: in its generic (2-parametric) unfolding we will find different codimension-1 bifurcation curves depending whether we use topological equivalence or $\Sigma$-equivalence. In this second case it emerges from the singularity one more curve in the parameter space which corresponds to a codimension-1 global bifurcation.

As said before, this codimension-2 singularity appears when $Y$ is transversal to $\Sigma$ and $X$ has non-diagonalizable linear part with a real non-zero eigenvalue. We only deal with the case of negative eigenvalue ($\lambda < 0$) and $Yf(p) > 0$, since the other ones can be studied in a similar way. In that case, $p \in \partial\Sigma^s \cap \partial\Sigma^c$, and $Z^s(p) = 0$. Therefore, it can be seen as a critical point of the (extended) sliding vector field. In order to have a generic codimension-2 singularity, this critical point has to be hyperbolic. So, as $Z^s(x) = \alpha x + \mathcal{O}(x^2)$ (taking $x$ as a local chart of $\Sigma$ around $p$), $\alpha \neq 0$ must be satisfied. In this section we assume that $\alpha < 0$.

One can choose as a normal form $f(x, y) = y$ and

$$Z(x,y) = \begin{cases} X(x,y) = \begin{pmatrix} -1 & 0 \\ 1 & -1 \end{pmatrix}\begin{pmatrix} x \\ y \end{pmatrix} & \text{if } y > 0, \\ Y(x,y) = \begin{pmatrix} 1 \\ 1 \end{pmatrix} & \text{if } y < 0, \end{cases} \tag{27}$$

which satisfies the explained generic conditions (see Fig. 18).

A generic unfolding of this singularity can be given by

$$Z_{\varepsilon,\mu}(x,y) = \begin{cases} X_{\varepsilon,\mu}(x,y) = \begin{pmatrix} -1 & \varepsilon \\ 1 & -1 \end{pmatrix}\begin{pmatrix} x \\ y-\mu \end{pmatrix} & \text{if } y > 0, \\ Y(x,y) = \begin{pmatrix} 1 \\ 1 \end{pmatrix} & \text{if } y < 0 \end{cases} \tag{28}$$

in such a way that $\mu$ measures the distance of the hyperbolic critical point to $\Sigma$ and $\varepsilon$ the deformation of the eigenvalues.

The hyperbolic critical point $P = (0, \mu) \in \Sigma^+$ is admissible for $\mu > 0$ and non-admissible for $\mu < 0$ (see Fig. 19), and it is a focus for $\varepsilon < 0$ and a node for $\varepsilon > 0$.

Moreover, for any value of the parameters, the point $F = (-\mu, 0) \in \Sigma$ is a visible fold of $X$ for $\mu > 0$ and an invisible fold of $X$ for $\mu < 0$. Furthermore, the sliding vector field is given by

$$Z^s_{\varepsilon,\mu}(x) = \frac{-2x - \mu - \mu\varepsilon}{1 - x - \mu}, \tag{29}$$

which is defined in $\Sigma^s = \{(x, y) \in \Sigma\colon\ x < -\mu\}$. This vector field has a pseudonode

$$N = \left(-\frac{\mu + \mu\varepsilon}{2}, 0\right) \tag{30}$$

provided $\mu < 0$.

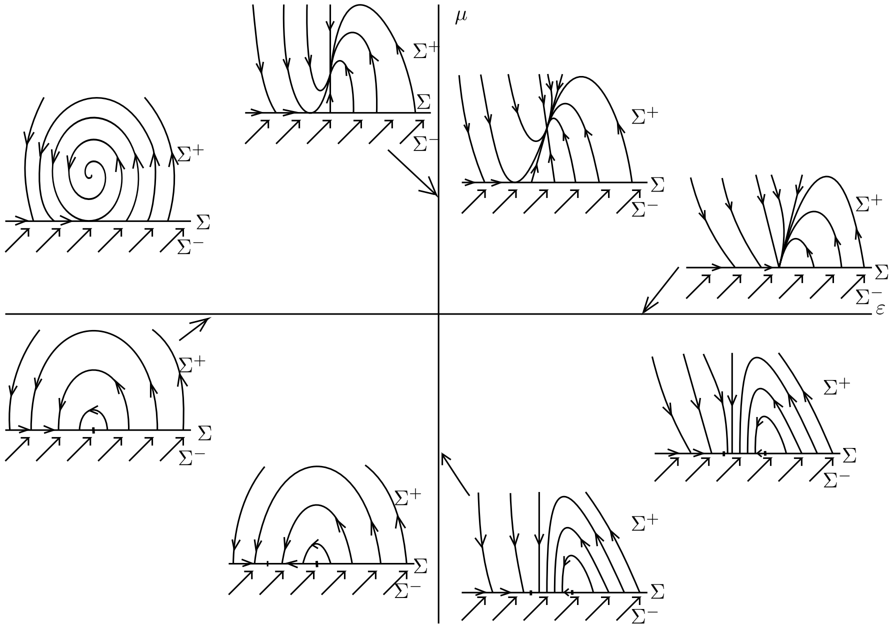


**Fig. 19.** Bifurcation diagram of (28) using $\Sigma$-equivalences. For the bifurcation diagram using topological equivalences, it is enough to remove the bifurcation curve $\varepsilon = 0$.

As already said, the line $\{(\varepsilon, \mu)\colon\ \mu = 0\}$ in the parameter space corresponds to two codimension-1 bifurcation curves (for $\varepsilon > 0$ and $\varepsilon < 0$) in which take place the Boundary–Focus bifurcation $BF_4$ (with reversed time) and Boundary–Node bifurcation $BN_1$, both studied in [17].

We study the possible existence of codimension-1 global bifurcation curves in the unfolding $Z_{\varepsilon,\mu}$. First we consider $\Sigma$-equivalences. One can see that any two vector fields $Z_{\varepsilon,\mu}$ and $Z_{\varepsilon',\mu'}$ are $\Sigma$-equivalent (and thus equivalent) provided $\mu'\mu > 0$ and $\varepsilon'\varepsilon > 0$. One can easily construct a homeomorphism which preserves $\Sigma$ and gives the equivalence.

The line $\{(\varepsilon, \mu)\colon\ \varepsilon = 0,\ \mu > 0\}$ corresponds to the parameter values in which the admissible hyperbolic critical point $P$ changes from a focus to a node. Even if $X_{\varepsilon,\mu}$ and $X_{\varepsilon',\mu'}$ with $\mu > 0$, $\mu' > 0$, $\varepsilon < 0$ and $\varepsilon' > 0$ are locally equivalent in $\Sigma^+$ around the hyperbolic critical point $P$, next proposition will show that $Z_{\varepsilon,\mu}$ and $Z_{\varepsilon',\mu'}$ are not $\Sigma$-equivalent since the homeomorphism which gives the local equivalence in a neighborhood of $P$ in $\Sigma^+$ cannot be extended to a neighborhood intersecting $\Sigma$ and $\Sigma^-$. In fact, next proposition shows that in the line $\{(\varepsilon, \mu)\colon\ \varepsilon = 0,\ \mu > 0\}$ occurs a global bifurcation involving the arrival orbits of $\Sigma^s$.

Finally, we will see that the same happens in the region $\{(\varepsilon, \mu)\colon\ \mu < 0\}$, that is, two vector fields $Z_{\varepsilon,\mu}$ and $Z_{\varepsilon',\mu'}$ with $\mu < 0$, $\mu' < 0$, $\varepsilon < 0$ and $\varepsilon' > 0$, can neither be $\Sigma$-equivalent. Then in the line $\{(\varepsilon, \mu)\colon\ \varepsilon = 0,\ \mu < 0\}$ also occurs a global bifurcation.

**Proposition 9.1.** *The Filippov vector fields $Z_{\varepsilon,\mu}$ and $Z_{\varepsilon',\mu'}$ with $\mu\mu' > 0$, $\varepsilon < 0$ and $\varepsilon' > 0$ are not $\Sigma$-equivalent.*

**Proof.** When $\mu > 0$ and $\mu' > 0$, the corresponding folds $F$ and $F'$ are visible, and then they have three separatrices (see Fig. 19). If we consider the separatrix $W^s_+(F)$, it intersects $\Sigma^c$ whereas $W^s_+(F')$ does not. In fact, the same occurs with all the arrival orbits of points of $\Sigma^s$. Therefore, since both $W^s_+(F)$ and $\Sigma^c$ have to be preserved by $\Sigma$-equivalences, their intersection too, and thus the vector fields $Z_{\varepsilon,\mu}$ and $Z_{\varepsilon',\mu'}$ with $\mu > 0$, $\mu' > 0$, $\varepsilon < 0$ and $\varepsilon' > 0$, cannot be $\Sigma$-equivalent.

For $\mu < 0$ and $\mu' < 0$, it can be seen analogously that $Z_{\varepsilon,\mu}$ and $Z_{\varepsilon',\mu'}$ with $\varepsilon < 0$ and $\varepsilon' > 0$ cannot be equivalent either. In fact, for $Z_{\varepsilon,\mu}$ all the orbits in $\Sigma^+$, which have an arrival point in $\Sigma^s$,

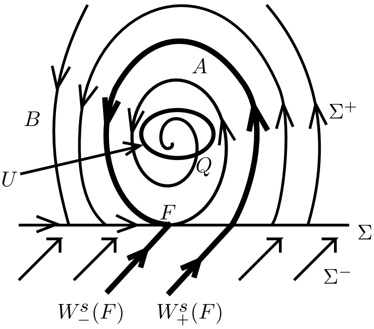


**Fig. 20.** Phase portrait of $Z_{\varepsilon,\mu}$ with $\mu>0$ and $\varepsilon<0$. To define the homeomorphism between $Z_{\varepsilon,\mu}$ and $Z_{\varepsilon',\mu'}$ with $\mu'>0$ and $\varepsilon'>0$ on has to consider the regions $A$ and $B$ delimited by the separatrices $W^s_-(F)\cup W^s_+(F)$.

hit also $\Sigma^c$ in backward time, but for $Z_{\varepsilon',\mu'}$ there exist orbits which arrive to $\Sigma^s$ but remain in $\Sigma^+$ in backward time. Thus, since $\Sigma^c$ and $\Sigma^s$ have to be preserved, the vector fields in the domains $\{(\varepsilon,\mu)\colon\ \varepsilon>0,\ \mu<0\}$ and $\{(\varepsilon,\mu)\colon\ \varepsilon<0,\ \mu<0\}$ cannot be $\Sigma$-equivalent. $\square$

Using $\Sigma$-equivalences one obtains that the unfolding has four different generic behaviors depending on the signs of $\varepsilon$ and $\mu$ and that the codimension-1 bifurcations only occur in $\{(\varepsilon,\mu)\colon\ \mu=0\}$ or $\{(\varepsilon,\mu)\colon\ \varepsilon=0\}$ (see Fig. 19).

If one considers topological equivalences instead of $\Sigma$-equivalences, we will see that the unfolding only presents two generic behaviors, since then the line $\{(\varepsilon,\mu)\colon\ \varepsilon=0\}$ is not a codimension-1 bifurcation curve.

**Proposition 9.2.** *For $\mu$ and $\varepsilon$ small enough, the Filippov vector fields $Z_{\varepsilon,\mu}$ and $Z_{\varepsilon',\mu'}$ with $\mu\mu'>0$ are topologically equivalent.*

**Proof.** We will prove that any two vector fields $Z_{\varepsilon,\mu}$ and $Z_{\varepsilon',\mu'}$ with $\mu\mu'>0$, $\varepsilon<0$ and $\varepsilon'\geqslant 0$ are topologically equivalent. We will construct the homeomorphism $h$ which gives the equivalence piecewise in different regions of the phase space checking *a posteriori* that it is continuous. First we consider neighborhoods $U\subset\Sigma^+$ and $U'\subset\Sigma^+$ of the focus $P=(0,\mu)$ of $Z_{\varepsilon,\mu}$ and the node $P'=(0,\mu')$ of $Z_{\varepsilon',\mu'}$. We choose $U$ and $U'$ such that their boundary intersect the orbits of the corresponding vector fields transversally. These neighborhoods exist since these critical points are hyperbolic (see [20]). Moreover, since the separatrices $W^u_+(F)$ and $W^u_+(F')$ tend to $P$ and $P'$ respectively, there exist points $Q=W^u_+(F)\cap\partial U$ and $Q'=W^u_+(F')\cap\partial U'$. As a first step we use Hartmann–Grobman Theorem to define the homeomorphism $h\colon U\to U'$. The homeomorphism given by this theorem can be chosen in such a way that $h(Q)=Q'$, and therefore $h(W^u_+(F)\cap U)=W^u_+(F')\cap U'$.

In order to extend the homeomorphism $h$ we define regions $A$ and $B$ which are delimited by the separatrices $W^s_-(F)\cup W^s_+(F)$, in such a way that $U\subset A$ (see Fig. 20). In the next step we extend $h$ to the full region $A$. For this purpose we use the flows of both $Z_{\varepsilon,\mu}$ and $Z_{\varepsilon',\mu'}$ reparameterized by the arc-length in order to assure that $h(F)=F'$. With this construction is clear that $h$ is continuous at $\partial U$ and that $h(W^u_+(F))=W^u_+(F')$. Moreover, since $h$ is continuous, it can be extended to $\partial A$, which is made up of $W^s_+(F)$ and $W^s_-(F)$ and thus these separatrices are also preserved.

Finally, in order to extend $h$ to the region $B$ (see Fig. 20), we define it first in $\Sigma^s$. Since it is only one orbit, $h$ can be trivially extended in such a way that $h(F)=F'$. Let us observe that any $R\in\Sigma^s$ reaches $F$, that is, exists $t_R>0$ such that $\varphi_{Z^s_{\varepsilon,\mu}}(t,R)\to F$ as $t\to t_R$. For the other points in $B$, we define $h$ using the flows $Z_{\varepsilon,\mu}$ and $Z_{\varepsilon',\mu'}$ and reparameterizing again by the arc-length to assure that $h$ is continuous in $\partial B$ since in these points the definition has to coincide with the one established in $\partial A$.

For $\mu<0$, the construction of the homeomorphism is simpler. In order to construct $h$ we start by defining it on $\Sigma^s$. By Hartmann–Grobman Theorem, we can define an orientation preserving homeo-

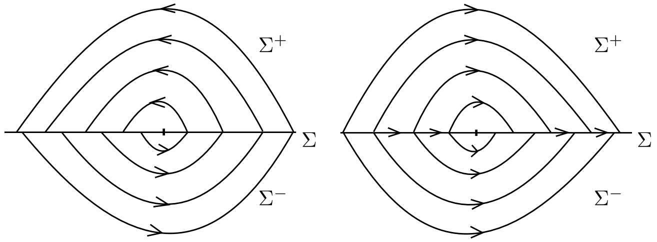


**Fig. 21.** Two kinds of Focus–Fold singularities. In both, the focus is repelling and the fold is invisible. In the left one $p \in \partial\Sigma^c$, whereas in the right one $p \in \partial\Sigma^e \cap \partial\Sigma^s$.

morphism $h : \overline{\Sigma^s} \to \overline{\Sigma'^s}$ such that $h(N) = N'$ and $h(F) = F'$, where $N$ is the pseudonode of $Z^s_{\varepsilon,\mu}$ given in (30) and $N'$ is the corresponding one for $Z^s_{\varepsilon',\mu'}$ and $F$ and $F'$ are the folds. As the orbit of any point of $\Sigma^+ \cup \Sigma^-$ has an arrival point in $\Sigma^s$, $h$ can be extended through the flow to them as it has been done for the points in the region $B$ in the case $\mu > 0$ (see Fig. 20). Let us observe that with this construction $h(W^s_-(F)) = W^s_-(F')$, $h(W^s_-(P)) = W^s_-(P')$ and $h(W^s_+(P)) = W^s_+(P')$. $\square$

## 10. Focus–Fold singularity

A Filippov vector field $Z = (X, Y)$ has a Focus–Fold singularity when $X$ has a hyperbolic focus at $p \in \Sigma$ and $Y$ has a fold at the same point. This singularity presents a particular interest since in some of its generic unfoldings can appear several global bifurcations as existence of separatrix connections and bifurcations of cycles, which were explained in [17] and have been reviewed in Section 4.2. Of course, this singularity can present different behavior depending whether the focus is attracting or repelling, the fold is visible or invisible and whether $p$ belongs to the boundary of two components of $\Sigma^c$ or between $\Sigma^s$ and $\Sigma^e$ (see Fig. 21).

In this section we study the case in which $p$ is a repelling focus of $X$ and an invisible fold of $Y$ such that $p \in \partial\Sigma^c$, since this case gives rise to more global phenomena around the singularity.

We choose as a normal form $f(x, y) = y$ and

$$Z(x,y) = \begin{cases} X(x,y) = \begin{pmatrix} 1 & -1 \\ 1 & 1 \end{pmatrix}\begin{pmatrix} x \\ y \end{pmatrix} & \text{if } y > 0, \\ Y(x,y) = \begin{pmatrix} 1 \\ x \end{pmatrix} & \text{if } y < 0. \end{cases}$$

As in the Fold–Fold singularity (see Section 4.1.1), both vector fields have associated involutions $\phi_X$ and $\phi_Y$, which are defined in a neighborhood of $\Sigma$ around $p$. Taking $x$ as a local chart in $\Sigma$, it can be easily seen that the return map $\phi = \phi_X \circ \phi_Y$ is of the form $\phi(x) = \alpha x + \mathcal{O}(x^2)$ with $\alpha > 1$, and thus $p$ behaves as a repelling focus for $Z$.

A generic unfolding of this singularity can be given by

$$Z_{\varepsilon,\mu}(x,y) = \begin{cases} X_\mu(x,y) = \begin{pmatrix} 1 & -1 \\ 1 & 1 \end{pmatrix}\begin{pmatrix} x+\mu \\ y-\mu \end{pmatrix} & \text{if } y > 0, \\ Y_\varepsilon(x,y) = \begin{pmatrix} 1 \\ x-\varepsilon \end{pmatrix} & \text{if } y < 0, \end{cases} \tag{31}$$

in such a way that $\mu$ controls the distance of the focus $P = (-\mu, \mu)$ to $\Sigma$. Then, $P$ is admissible for $\mu > 0$ and non-admissible for $\mu < 0$. Moreover, we have chosen $X_\mu$ in such a way that the fold which appears when the focus $P$ is away from $\Sigma$ is given by $F_+ = (0, 0)$. In this way, $\varepsilon$ measures the distance between the fold $F_- = (\varepsilon, 0)$ of $Y_\varepsilon$ and the fold $F_+ = (0, 0)$ of $X_\mu$.

It can be checked that for $\varepsilon > 0$,

$$\Sigma = \overline{\Sigma^e} \cup \overline{\Sigma^c} \quad \text{with } \Sigma^e = \{(x,0)\colon x \in (0,\varepsilon)\} \text{ and } \Sigma^c = \{(x,0)\colon x < 0\} \cup \{(x,0)\colon x > \varepsilon\},$$

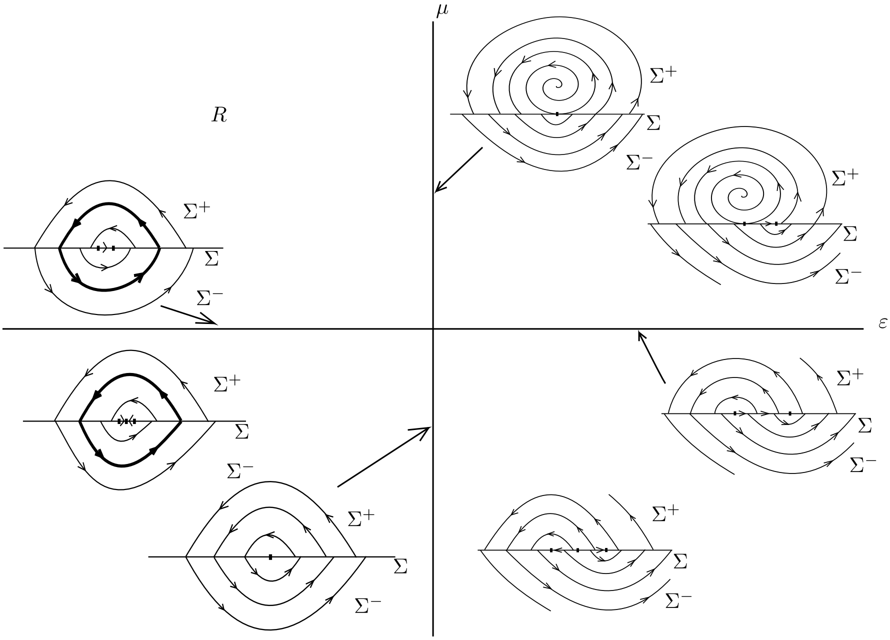


**Fig. 22.** Bifurcation diagram of (31) using either topological or $\Sigma$-equivalences. The behavior in the region $R$ can be seen in Fig. 23.

and for $\varepsilon < 0$,

$$\Sigma = \overline{\Sigma^s} \cup \overline{\Sigma^c} \quad \text{with } \Sigma^s = \{(x,0)\colon\ x \in (\varepsilon, 0)\} \text{ and } \Sigma^c = \{(x,0)\colon\ x < \varepsilon\} \cup \{(x,0)\colon\ x > 0\}.$$

In both $\Sigma^s$ and $\Sigma^e$, the sliding vector field is given by

$$Z^s_{\varepsilon,\mu}(x) = \frac{2\mu\varepsilon + (1 - 2\mu + \varepsilon)x + x^2}{\varepsilon}$$

and it can be seen that for $\mu < 0$, it has a pseudonode $N$ which is attracting for $\varepsilon > 0$ and repelling for $\varepsilon < 0$.

First we study the existence of local bifurcations in this unfolding (see Fig. 22). The line $\{(\varepsilon,\mu)\colon\ \mu = 0\}$ in the parameter space corresponds to two different codimension-1 Boundary–Focus bifurcations, for $\varepsilon > 0$ and $\varepsilon < 0$, since the focus $P = (0,0)$ belongs to $\Sigma$. For $\varepsilon > 0$, $P \in \partial\Sigma^e$ and then occurs the Boundary–Focus bifurcation $BF_3$ explained in [17], whereas for $\varepsilon < 0$ the Boundary–Focus bifurcation $BF_4$ in [17] takes place, since $P \in \partial\Sigma^s$. Moreover, in the transition from $\varepsilon < 0$ to $\varepsilon > 0$ it occurs a non-smooth Hopf-like bifurcation since it gives rise to the birth of a periodic orbit. We give the name Hopf-like bifurcation to this phenomenon since, as in the smooth case, $P$ changes from unstable (for $\varepsilon > 0$) to stable (for $\varepsilon < 0$) due to the appearance of escaping and sliding region for $\varepsilon > 0$ and $\varepsilon < 0$ respectively.

The line $\{(\varepsilon,\mu)\colon\ \varepsilon = 0\}$ also corresponds to two codimension-1 local bifurcations, since in this line both folds $F_+$ and $F_-$ coincide at $(0,0)$, being both invisible for $\mu < 0$ and being $F_+$ visible and $F_-$ invisible for $\mu > 0$. Therefore, for $\mu > 0$ and $\mu < 0$ occur respectively bifurcations $VI_1$ and $II_2$, which are explained in [17] (see also Section 4.1.1). This last one gives birth to a periodic orbit for $\varepsilon < 0$. Let us observe that as $\mu$ goes to zero, we obtain the codimension-2 bifurcation, in which the Fold–Fold singularity becomes a Focus–Fold at the same time of the birth of a periodic orbit.

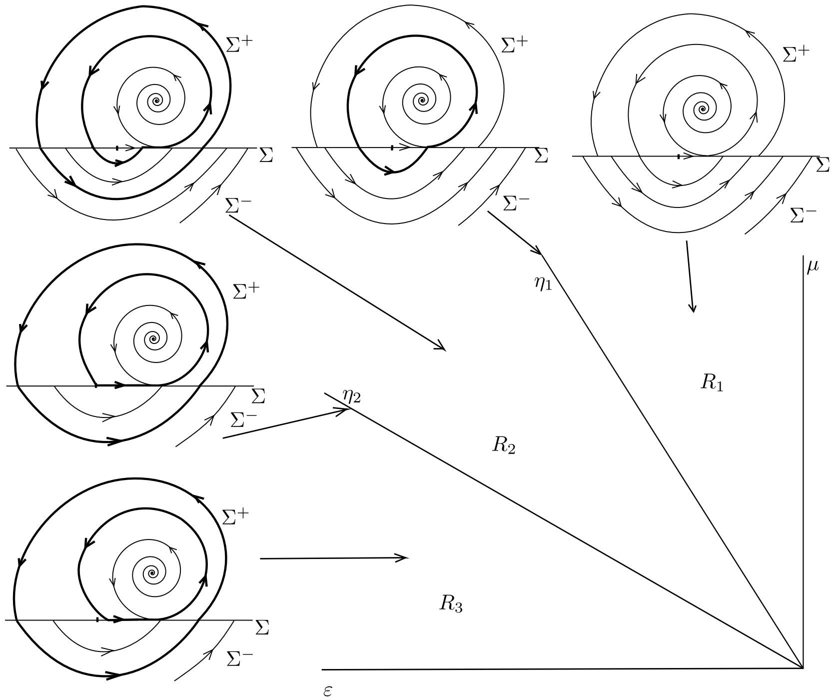


**Fig. 23.** Bifurcation diagram of (31) for parameters belonging to $R = \{(\varepsilon, \mu)\colon\ \varepsilon < 0,\ \mu > 0\}$. The bifurcations undergone in this region of the parameter space remain the same either using $\Sigma$-equivalences or topological equivalences.

In these two lines in the $(\varepsilon, \mu)$ parameter space take place all the possible codimension-1 local bifurcations, either considering topological or $\Sigma$-equivalence, which exist in any generic unfolding of the singularity.

We study the possible existence of codimension-1 global bifurcation curves of the unfolding $Z_{\varepsilon,\mu}$. For that purpose, we study the behavior of the vector field in the four quadrants considering the signs of $\mu$ and $\varepsilon$. In the quadrants $\{(\varepsilon, \mu)\colon\ \mu > 0,\ \varepsilon > 0\}$, $\{(\varepsilon, \mu)\colon\ \mu < 0,\ \varepsilon > 0\}$ and $\{(\varepsilon, \mu)\colon\ \mu < 0,\ \varepsilon < 0\}$, one can see that any two vector fields with parameters belonging to the same quadrant are $\Sigma$-equivalent (and thus topologically equivalent).

Next proposition shows that in the region $R = \{(\varepsilon, \mu)\colon\ \mu > 0,\ \varepsilon < 0\}$ the systems present a richer dynamics.

**Proposition 10.1.** *There exist two curves $\eta_1$ and $\eta_2$ in $R = \{(\varepsilon, \mu)\colon\ \mu > 0,\ \varepsilon < 0\}$ where the Filippov vector field $Z_{\varepsilon,\mu}$ in* (31)*, undergoes codimension*-1 *global bifurcations characterized by*:

- *If $(\varepsilon, \mu) \in \eta_1$, then there exists a homoclinic connection of the fold $F_+$, $W^u_+(F_+) \equiv W^s_-(F_+)$, which is semistable and gives rise to a bifurcation of cycles called $CC_2$ in* [17].
- *If $(\varepsilon, \mu) \in \eta_2$, then there exists a heteroclinic connection between the folds $F_+$ and $F_-$, $W^u_+(F_+) \equiv W^s_+(F_-)$, which gives rise to a bifurcation of cycles called* buckling bifurcation *in* [17] *and* switching-sliding *in* [4,14].

**Proof.** In $R$ there exist a visible fold $F_+$ and an invisible fold $F_-$ which have respectively three and one separatrices. We will see that the bifurcations that appear in this region correspond to two different separatrix connections, which give rise to cycles (see Section 4.2).

We describe the different behaviors changing parameters in anticlockwise sense in $R$. We consider regions $R_1$, $R_2$ and $R_3$ as can be seen in Fig. 23.

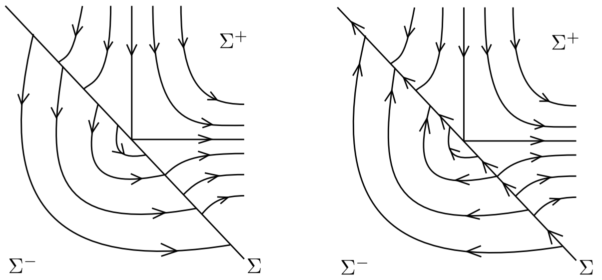


**Fig. 24.** Two kinds of Saddle–Fold singularities. In the first case, $p \in \partial\Sigma^c$ and in the second one $p \in \partial\Sigma^s \cap \partial\Sigma^e$.

In the vertical line we have a Fold–Fold bifurcation (see Fig. 22) in such a way that in $R_1$ it appears a small sliding region between $F_-$ and $F_+$.

The first bifurcation to occur (in the curve $\eta_1$) is the connection between $W^u_+(F_+)$ and $W^s_-(F_+)$ (a pseudohomoclinic orbit), which gives rise to a cycle. To see that this cycle is semistable, we recall that for $(\varepsilon,\mu)=(0,0)$ the Focus–Fold behaves as a repelling focus and the same happens for $(\varepsilon,\mu)$ small enough. Nevertheless, all the points in the interior of the cycle tend to $\Sigma^s$ in finite time and so are globally attracted by the fold $F_+$. Therefore, the cycle is attracting from inside and repelling from outside. This bifurcation, called $CC_2$ in [17], is described in that paper (see also Section 4.2). In $R_1$ there is no cycle whereas when we cross $\eta_1$, it appears a repellor periodic orbit and an attracting cycle, which is composed by a sliding segment, $W^u_+(F_+)$ and $F_+$. Both the cycle and the periodic orbit are persistent in all the region $R_2$.

In $\eta_2$ it occurs another separatrix connection: $W^u_+(F_+) \equiv W^s_+(F_-)$ (a heteroclinic orbit). This bifurcation is called *buckling bifurcation* in [17] (and *switching-sliding* in [4,14]) and in both $R_2$ and $R_3$ the attracting cycle is persistent. Moreover in $R_3$, it does not intersect $\Sigma^-$. The repelling periodic orbit does not undergo any change and it persists also in $R_3$. Finally, in $R_3$, the attracting cycle shrinks when the parameters tend to $\{(\varepsilon,\mu)\colon\ \mu=0\}$ and it merges with the focus $P$ as it tends to $\Sigma$, whereas the repellor periodic orbit becomes the periodic orbit which also exists for $\mu=0$ and $\varepsilon<0$. $\square$

Let us observe that the description of the bifurcation diagram coincides either considering topological equivalence or $\Sigma$-equivalence.

## 11. Saddle–Fold singularity

One of the local bifurcations which present an unfolding with a considerably rich behavior, that is with several global phenomena, is the Saddle–Fold bifurcation. In this case the unfolding of the codimension-2 singularity has infinitely many codimension-1 bifurcation curves which accumulate. This singularity occurs when the vector field $X$ has a saddle at a point $p \in \Sigma$ and the vector field $Y$ has a fold or quadratic tangency with $\Sigma$ at the same point. In order to have a generic codimension-2 singularity one has to impose non-degeneracy conditions: the eigenspaces of the saddle have to be transversal to $\Sigma$ and the modulus of the eigenvalues of the saddle have to be different. The reason why this last condition is needed will be clear later when we unfold the singularity. Of course, this singularity can present different behavior depending on which eigenvalue has bigger modulus and depending whether $p$ belongs to the boundary of two components of $\Sigma^c$ or to the boundary between $\Sigma^s$ and $\Sigma^e$ (see Fig. 24).

In this section we study the case in which the positive eigenvalue has bigger modulus than the negative one and $p \in \partial\Sigma^c$, which is shown in the left picture of Fig. 24. The other ones can be studied analogously.

For this case, we can choose $\Sigma=\{(x,y)\colon\ f(x,y)=x+y=0\}$ to be allowed to take the normal form with the saddle with diagonal linear part. So, we can take

$$Z(x,y)=\begin{cases} X(x,y)=\begin{pmatrix} \lambda_1 x \\ -\lambda_2 y\end{pmatrix} & \text{if } x+y>0,\\ Y(x,y)=\begin{pmatrix} 1+x-y \\ -1+x-y\end{pmatrix} & \text{if } x+y<0\end{cases}$$

with $\lambda_1 > \lambda_2$. In fact, the higher order terms in $X$ will not play any role in the discussion of the bifurcation diagram.

We have taken $Y$ in such form since then, taking $x$ as a local chart for $\Sigma$, the involution associated to the fold is given simply by $\phi_Y(x) = -x$, which makes the explanation clearer. For the normal form we could have taken (for instance) $\lambda_1 = 2$ and $\lambda_2 = 1$, that would make the computations simpler. Nevertheless, for this singularity we will keep the constants $\lambda_1$ and $\lambda_2$ in order to make clear why the condition $\lambda_1 \neq \lambda_2$ is needed to have a codimension-2 singularity.

A generic unfolding of this singularity is given by

$$Z_{\varepsilon,\mu}(x,y)=\begin{cases} X_\mu(x,y)=\begin{pmatrix} \lambda_1 x-\mu \\ -\lambda_2 y+\mu\end{pmatrix} & \text{if } x+y>0,\\ Y_\varepsilon(x,y)=\begin{pmatrix} 1+x-y-\varepsilon \\ -1+x-y-\varepsilon\end{pmatrix} & \text{if } x+y<0\end{cases} \tag{32}$$

in such a way that the saddle is given by $S = (\mu/\lambda_1, \mu/\lambda_2)$ and therefore it is admissible for $\mu > 0$ and non-admissible for $\mu < 0$. Moreover, when $\mu \neq 0$, the vector field $X_\mu$ has a fold located at $F_+ = (0,0)$. The fold of $Y_\varepsilon$ is given by $F_- = (\varepsilon/2, -\varepsilon/2)$ in such a way that the parameter $\varepsilon$ unfolds the other degeneracy: for $\mu \neq 0$, the two folds $F_+$ and $F_-$ are different provided $\varepsilon \neq 0$.

The different singularities and regions present in $\Sigma$ for $Z_{\varepsilon,\mu}$ in (32) are summarized in the following proposition, whose proof is straightforward and is omitted.

**Proposition 11.1.** *For $(\varepsilon, \mu)$ small enough, the Filippov vector field $Z_{\varepsilon,\mu}$ in (32) satisfies:*

- *For $\varepsilon \neq 0$, $F_- = (\varepsilon/2, -\varepsilon/2)$ is a fold of $Y_\varepsilon$ and $F_+ = (0,0)$ is a fold of $X_\mu$.*
- *$\Sigma$ is divided as:*
  - *For $\varepsilon > 0$: $\Sigma^e = \{(x,y) \in \Sigma\colon\ 0 < x < \varepsilon/2\}$ and $\Sigma^c = \Sigma \setminus \overline{\Sigma^e}$.*
  - *For $\varepsilon = 0$: $\Sigma^c = \Sigma \setminus \{(0,0)\}$.*
  - *For $\varepsilon < 0$: $\Sigma^s = \{(x,y) \in \Sigma\colon\ \varepsilon/2 < x < 0\}$ and $\Sigma^c = \Sigma \setminus \overline{\Sigma^s}$.*
- *The sliding vector field $Z^s_{\varepsilon,\mu}$ defined in $\Sigma^e$ for $\varepsilon > 0$ and in $\Sigma^s$ for $\varepsilon < 0$, has a pseudonode $P$, which is repelling for $\varepsilon > 0$ and attracting for $\varepsilon < 0$.*

### *11.1. Codimension-1 local bifurcations of the unfolding*

First we study the existence of local bifurcations in the unfolding (see Fig. 25). The line $\{(\varepsilon,\mu)\colon\ \mu = 0\}$ in the parameter space corresponds to two different codimension-1 Boundary–Saddle bifurcations, for $\varepsilon > 0$ and $\varepsilon < 0$, since the saddle $S = (0,0)$ belongs to $\Sigma$ (see Section 4.1.2). In the case $\varepsilon > 0$, $p \in \partial\Sigma^e$ and then occurs the bifurcation $BS_2$ explained in [17], whereas in $\varepsilon < 0$, since $p \in \partial\Sigma^s$, reversing time it takes place the bifurcation $BS_2$ in [17].

The line $\{(\varepsilon,\mu)\colon\ \varepsilon = 0\}$ also corresponds to two codimension-1 local bifurcations, since in this line both folds $F_+$ and $F_-$ coincide in $(0,0)$. Moreover, $F_+$ is invisible for $\mu > 0$ and invisible for $\mu < 0$. Therefore, for $\mu > 0$ and $\mu < 0$ occur respectively bifurcations $VI_1$ and $II_2$ explained in [17] (see also Section 4.1.1).

The first one, as it was seen in that paper, gives birth to a periodic orbit on one side of the bifurcation parameter. To know on which side of the bifurcation point appears this periodic orbit, one has to study whether the return map associated to the Fold–Fold (see Section 4.1.1) is contracting or expanding. For this purpose, we have to compute the expansion of this return map. Straightforward computations give that, taking $x$ as a local chart for $\Sigma$, the return map for $x < 0$ is given by

$$\phi(x) = x - \frac{2}{3\mu}(\lambda_1 - \lambda_2)x^2 + \mathcal{O}\big(x^3\big).$$

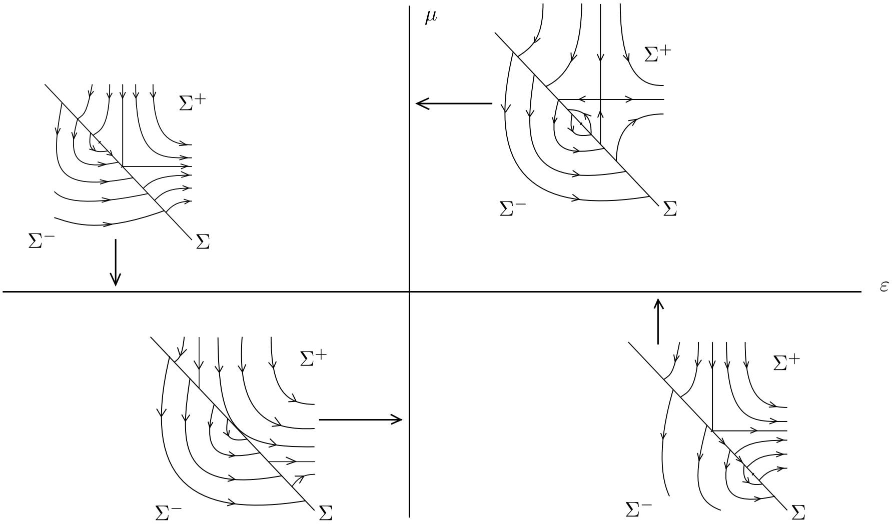


**Fig. 25.** Codimension-1 local bifurcations which appear in a generic unfolding of the Saddle–Fold singularity.

Therefore, since in the generic case we have $\lambda_1 \neq \lambda_2$, the return map is attracting provided $\lambda_1 < \lambda_2$ and repelling provided $\lambda_1 > \lambda_2$. For the case $\lambda_1 = \lambda_2$, which would have more codimension, we would need to study the higher order terms of $\phi$ to detect the local behavior around the singularity. In the case we are studying, in which $\lambda_1 > \lambda_2$, the singularity acts as a repellor focus, and therefore the periodic orbit appears for $\varepsilon < 0$.

In these two lines in the $(\varepsilon, \mu)$ parameter space occur all the possible codimension-1 local bifurcations, either considering topological equivalence or $\Sigma$-equivalence, which exist in any generic unfolding of the singularity we are considering.

### 11.2. Codimension-1 global bifurcations of the unfolding

Next step is to study the possible existence of codimension-1 global bifurcation curves in the unfolding $Z_{\varepsilon,\mu}$. We start with the region of the parameter space with $\mu < 0$. In that region, it is straightforward to see that in the quadrants $\{(\varepsilon, \mu)\colon\ \mu < 0,\ \varepsilon > 0\}$ and $\{(\varepsilon, \mu)\colon\ \mu < 0,\ \varepsilon < 0\}$ any two vector fields with parameters belonging to the same quadrant are $\Sigma$-equivalent, and thus topologically equivalent (see Fig. 26).

The region $\{(\varepsilon, \mu)\colon\ \mu > 0\}$ has richer behavior since it presents infinitely many curves where global bifurcations occur. We study it in three steps. First, recall that in the vertical axis $\{(\varepsilon, \mu)\colon\ \varepsilon = 0, \mu > 0\}$ occurs a Fold–Fold bifurcation which gives birth to a periodic orbit for $\varepsilon < 0$. This periodic orbit is repellor and is persistent in all the region $R_2$ of the parameter space (see Fig. 27), and it breaks down when it hits the stable and unstable invariant manifolds of the saddle $S$ becoming a homoclinic orbit. Using that the involution associated to the fold of $Y_\varepsilon$ is $\phi_{Y_\varepsilon}(x) = -x + \varepsilon$, it is straightforward to see that this global bifurcation occurs in the curve

$$\nu = \left\{(\varepsilon, \mu)\colon\ \mu = -\frac{\lambda_1\lambda_2}{\lambda_1 - \lambda_2}\varepsilon\right\} \tag{33}$$

(see Fig. 27). As a second step, we study the possible global bifurcations in $R_1$ (see Fig. 27). Recall that for parameters in $R_1$ the saddle $S$ is admissible and that in $\Sigma$ we have a small segment of $\Sigma^e$ and three singularities which, from left to right, are $F_-$, the pseudonode $P$ and $F_+$.

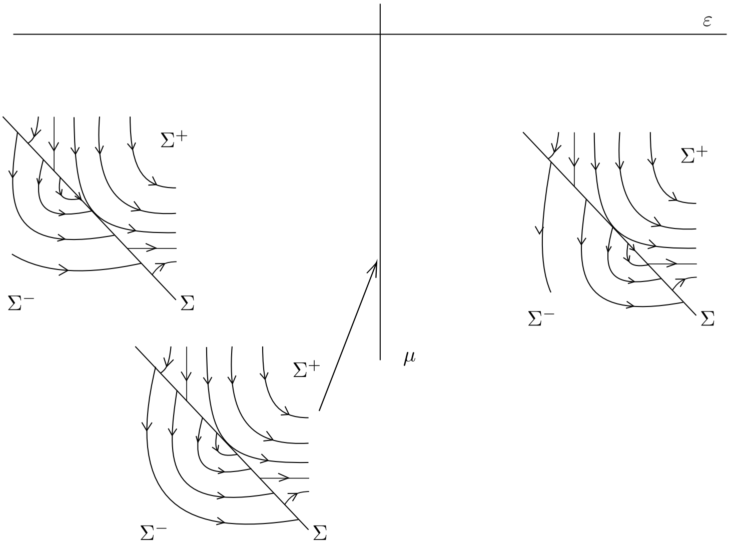


**Fig. 26.** Different dynamics around the Saddle–Fold local bifurcation given by (32) for $\mu < 0$. Recall that for this range of parameters, the saddle is non-admissible.

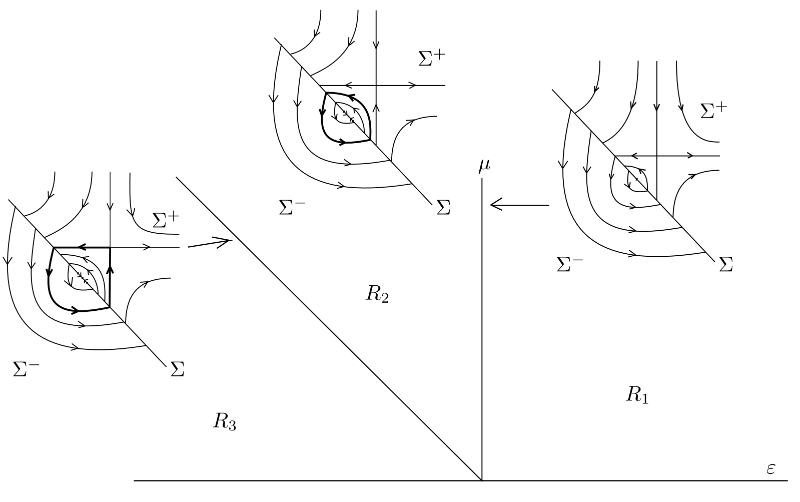


**Fig. 27.** Different dynamics around the Saddle–Fold local bifurcation given by (32) for $\mu > 0$. Recall that, for this range of parameters, the saddle is admissible. In the curve $\nu$ it appears a homoclinic connection which is a global codimension-1 bifurcation.

**Proposition 11.2.** *Let us consider $(\varepsilon, \mu) \in R_1$ small enough. Then, there exists a family of curves $\{\eta_n\}_{n \geqslant 1}$ in the parameter space emanating from $(0, 0)$ which accumulate to the vertical axis. Moreover, in these curves take place the following separatrix connections*:

- *If $n = 4k + 1$ with $k \geqslant 0$: $W^s(S) \equiv W^u_+(F_-)$.*
- *If $n = 4k + 2$ with $k \geqslant 0$: $W^s(S) \equiv W^u_-(P)$.*
- *If $n = 4k + 3$ with $k \geqslant 0$: $W^s(S) \equiv W^u_-(F_+)$.*
- *If $n = 4k + 4$ with $k \geqslant 0$: $W^s(S) \equiv W^u_+(P)$.*

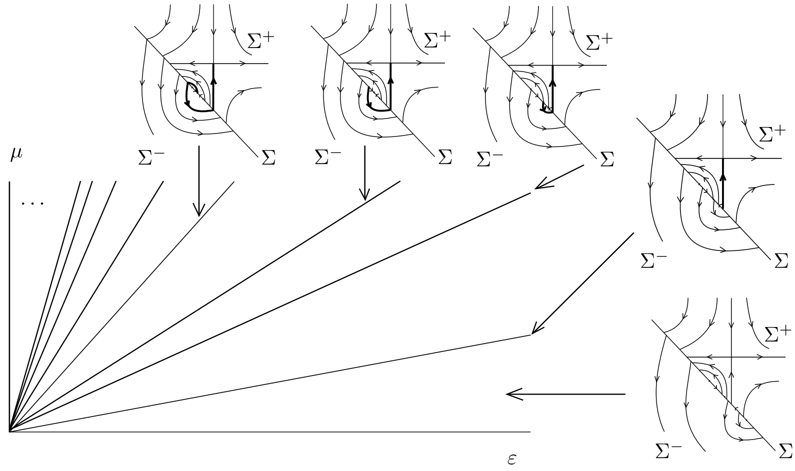


**Fig. 28.** Different dynamics in region $R_1$ (see Fig. 27). In this region there exist infinitely many codimension-1 bifurcations curves $\{\eta_n\}_{n\geqslant 1}$ which accumulate to the vertical axis $\{(\varepsilon,\mu)\colon\ \varepsilon=0\}$.

**Proof.** We describe the different behaviors anticlockwise. In the horizontal line of the parameter space (for $\varepsilon>0$), the saddle $S$ belongs to $\Sigma$ and it is on the left of the fold $F_-$, in such a way that between these two points there exists a small escaping region. Moving the parameters anticlockwise, the saddle becomes admissible in such a way that the departing point of $W^s(S)$ belongs to $\Sigma^e$ (see Fig. 28). Recall that $Z^s_{\varepsilon,\mu}$ has a pseudonode $P$ which can be seen that is located on the left of the departing point of the unstable manifold. As the parameters change, the folds $F_+$ and $F_-$ become closer and therefore $\Sigma^e$ shrinks. The first bifurcation to occur, in $\eta_1$, is a separatrix connection between the saddle $S$ and $F_-$, that is $W^s(S)\equiv W^u_+(F_-)$. After this curve, $W^s(S)$ crosses $\Sigma^c$ and then hits $\Sigma^e$ from $\Sigma^-$. Thus, the next bifurcations to occur, in $\eta_2$ is a separatrix connection between the saddle $S$ and the pseudonode $P$: $W^s(S)\equiv W^u_-(P)$, and in the following curve $\eta_3$ a separatrix connection between the saddle and $F_+$: $W^s(S)\equiv W^u_-(F_+)$. After this bifurcation, $W^s(S)$ crosses twice $\Sigma^c$. Therefore, varying the parameters we encounter two more consecutive curves $\eta_4$ and $\eta_5$ that correspond respectively $W^s(S)\equiv W^u_+(P)$ and $W^s(S)\equiv W^u_+(F_-)$. This procedure can be repeated iteratively in such a way that we obtain a sequence of curves which correspond to global bifurcations given by separatrix connections which make more and more turns around the folds as we change the parameters: $W^s(S)\equiv W^u_+(F_-)$, $W^s(S)\equiv W^u_-(P)$, $W^s(S)\equiv W^u_-(F_+)$, $W^s(S)\equiv W^u_+(P)$, $W^s(S)\equiv W^u_+(F_-)$, .... These infinitely many curves accumulate to the vertical axis where both folds collapse to a single point and therefore $\Sigma^e$ disappears. $\square$

Finally, we study the global bifurcations in the region $R_3$. In this region we find a similar structure as the one in the region $R_1$, but in this case the connections are between the unstable manifold of the saddle and the unstable pseudoseparatrices of $F_+$, $P$ and $F_-$ (see Fig. 29). The other main difference with respect to the region $R_1$ is that the bifurcation curves do not accumulate to the vertical axis when both folds coincide in the same point and the sliding region collapses but they accumulate to the curve $\nu$, in (33), in which exists the homoclinic orbit of the saddle, that we have found before.

## 12. Fold–Cusp singularity

In this section we unfold the Fold–Cusp singularity. This singularity occurs when at the same point $p\in\Sigma=\{(x,y)\colon\ f(x,y)=0\}$ the vector field $X$ has a cubic tangency or cusp ($Xf(p)=0$ and $X^2f(p)=0$) whereas $Y$ has a quadratic tangency or fold ($Yf(p)=0$). The most important feature of

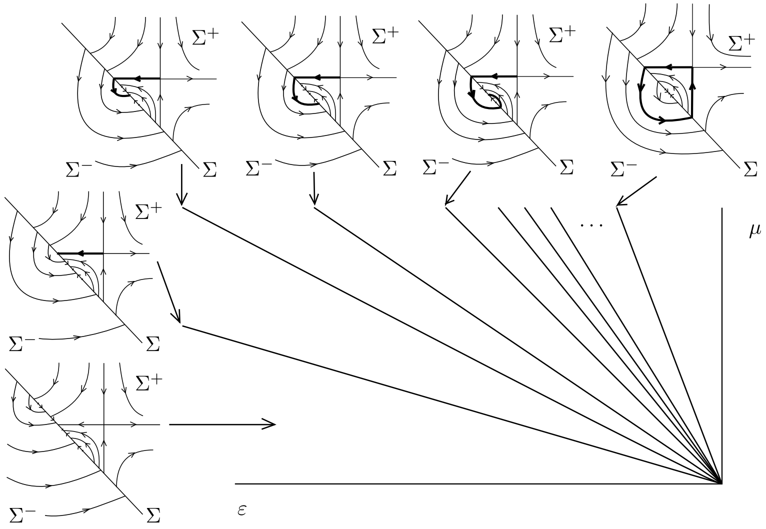


**Fig. 29.** Different dynamics in the region $R_3$ (see Fig. 27). In this region there exists infinitely many codimension-1 bifurcations curves which accumulate to the curve $\nu$.

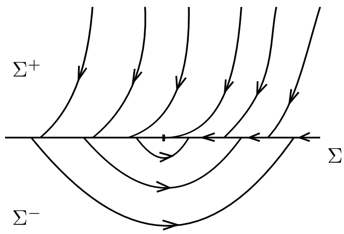


**Fig. 30.** The Cusp–Fold singularity satisfying $X^3 f(p) < 0$ and $Y^2 f(p) > 0$.

this singularity, as it happened in the Saddle–Fold singularity studied in Section 11, is that its generic unfolding presents infinitely many codimension-1 global bifurcation branches related to separatrix connections and bifurcations of periodic orbits and cycles. In order to have a generic codimension-2 singularity, one has to impose the non-degeneracy conditions $X^3 f(p) \neq 0$ and $Y^2 f(p) \neq 0$. Depending on the sign of these two constants and depending whether $X(p)$ and $Y(p)$, which are parallel, point towards the same or opposite direction, the singularity presents different behavior. In this section we focus our attention on the case $X^3 f(p) < 0$, $Y^2 f(p) > 0$ (invisible tangency) and $X(p)$ and $Y(p)$ pointing oppositely (see Fig. 30). All the other cases can be studied analogously. In this case we take $f(x, y) = y,\ p = (0, 0)$ and

$$Z(x, y) = \begin{cases} X(x, y) = \begin{pmatrix} -1 \\ -x^2 \end{pmatrix} & \text{if } y > 0, \\ Y(x, y) = \begin{pmatrix} 1 \\ x \end{pmatrix} & \text{if } y < 0, \end{cases}$$

whose phase portrait can be seen in Fig. 30. We have chosen $Y$ in such form since then the involution associated to the fold is given in its normal form by $\phi_Y(x) = -x$. It is straightforward to see that for $Z$, $\Sigma^c = \{(x, y) \in \Sigma\colon\ x < 0\}$ and $\Sigma^s = \{(x, y) \in \Sigma\colon\ x > 0\}$. In $\Sigma^s$ we can define the sliding vector field $Z^s$ which satisfies $Z^s(0) < 0$.

A generic unfolding of this singularity can be given by

$$Z_{\varepsilon,\mu}(x,y)=\begin{cases} X_\varepsilon(x,y)=\binom{-1}{-x^2+\varepsilon} & \text{if } y>0,\\ Y_\mu(x,y)=\binom{1}{x-\mu} & \text{if } y<0, \end{cases} \tag{34}$$

in such a way that $\varepsilon$ unfolds the cusp singularity, as it is done in [17], where the cusp singularity is called double tangency. The fold of $Y_\mu$ is given by $F_-=(\mu,0)$ and therefore, when $\varepsilon=0$, $\mu$ gives the distance between the cusp and the fold $F_-$.

When $\varepsilon\neq 0$ the cusp point disappears in such a way that $X_\varepsilon$ is transversal to $\Sigma$ for $\varepsilon<0$ and for $\varepsilon>0$ an invisible fold $F_+^1=(-\sqrt{\varepsilon},0)$ and a visible one $F_+^2=(\sqrt{\varepsilon},0)$ appear. Next proposition, whose proof is straightforward, shows how the regions $\Sigma^e$, $\Sigma^c$ and $\Sigma^s$ for $Z_{\varepsilon,\mu}$ change drastically depending on the values of the parameters $\mu$ and $\varepsilon$.

**Proposition 12.1.** *For $\mu$ and $\varepsilon$ small enough, the Filippov vector field in* (34) *satisfies the following statements*:

- *For $\varepsilon<0$, it has the fold $F_-=(\mu,0)$ and for $\varepsilon>0$ it has the folds $F_-=(\mu,0)$, $F_+^1=(-\sqrt{\varepsilon},0)$ and $F_+^2=(\sqrt{\varepsilon},0)$.*
- *The escaping and the sliding regions are given by*:
  - *In $R_1=\{(\varepsilon,\mu)\colon\ \varepsilon<0\}$, then $\Sigma^s=\{(x,y)\in\Sigma\colon\ x>\mu\}$ and $\Sigma^e$ does not exist.*
  - *In $R_2=\{(\varepsilon,\mu)\colon\ \varepsilon>0,\ \mu>\sqrt{\varepsilon}\}$, then $\Sigma^s=\{(x,y)\in\Sigma\colon\ x>\mu\}$ and $\Sigma^e=\{(x,y)\in\Sigma\colon\ -\sqrt{\varepsilon}<x<\sqrt{\varepsilon}\}$.*
  - *In $R_3=\{(\varepsilon,\mu)\colon\ \varepsilon<0,\ \sqrt{\varepsilon}<\mu<\sqrt{\varepsilon}\}$, then $\Sigma^s=\{(x,y)\in\Sigma\colon\ x>\sqrt{\varepsilon}\}$ and $\Sigma^e=\{(x,y)\in\Sigma\colon -\sqrt{\varepsilon}<x<\mu\}$.*
  - *In $R_4=\{(\varepsilon,\mu)\colon\ \varepsilon<0,\ \mu<-\sqrt{\varepsilon}\}$, then $\Sigma^s=\{(x,y)\in\Sigma\colon\ \mu<x<-\sqrt{\varepsilon}\}\cup\{(x,y)\in\Sigma\colon\ x>\varepsilon\}$ and $\Sigma^e$ does not exist.*
- *For any $(\varepsilon,\mu)\in R_1\cup R_2\cup R_3\cup R_4$, the sliding vector field defined in $\Sigma^s\cup\Sigma^e$, is given by*

$$Z^s_{\varepsilon,\mu}(x)=\frac{-x+x^2+\mu-\varepsilon}{x^2+x-\mu-\varepsilon} \tag{35}$$

  *and it has a critical point given by*

$$P=\left(\frac{1-\sqrt{1-4(\mu-\varepsilon)}}{2},0\right). \tag{36}$$

- *If $(\varepsilon,\mu)\in R_1\cup R_2\cup R_4$, $P\in\Sigma^s$ and it is an attractor pseudonode. Otherwise, if $(\varepsilon,\mu)\in R_3$, $P\in\Sigma^e$ and it is a repellor pseudonode.*
- *Therefore the singularities in $\Sigma$ are ordered as*:
  - *if $(\varepsilon,\mu)\in R_1$: $F_-<_\Sigma P$,*
  - *if $(\varepsilon,\mu)\in R_2$: $F_+^1<_\Sigma F_+^2<_\Sigma F_-<_\Sigma P$,*
  - *if $(\varepsilon,\mu)\in R_3$: $F_+^1<_\Sigma P<_\Sigma F_-<_\Sigma F_+^2$,*
  - *if $(\varepsilon,\mu)\in R_4$: $F_-<_\Sigma P<_\Sigma F_+^1<_\Sigma F_+^2$,*

  *where $<_\Sigma$ is the order in $\Sigma$ induced by the first coordinate.*

### *12.1. Codimension-1 local bifurcations of the unfolding*

First, we study the existence of codimension-1 local bifurcations (see Fig. 31). All the local bifurcations of the unfolding take place in the boundaries between the regions $R_i$ defined in Proposition 12.1.

The line $\{(\varepsilon,\mu)\colon\ \varepsilon=0\}$ in the parameter space corresponds to two different cusp bifurcations. For $\mu>0$, the cusp point belongs to $\overline{\Sigma^c}$ and then in this curve takes place the bifurcation $DT_1$ in [17] whereas for $\mu<0$ it belongs to $\overline{\Sigma^s}$ and then in this curve takes place the bifurcation $DT_2$ in [17].

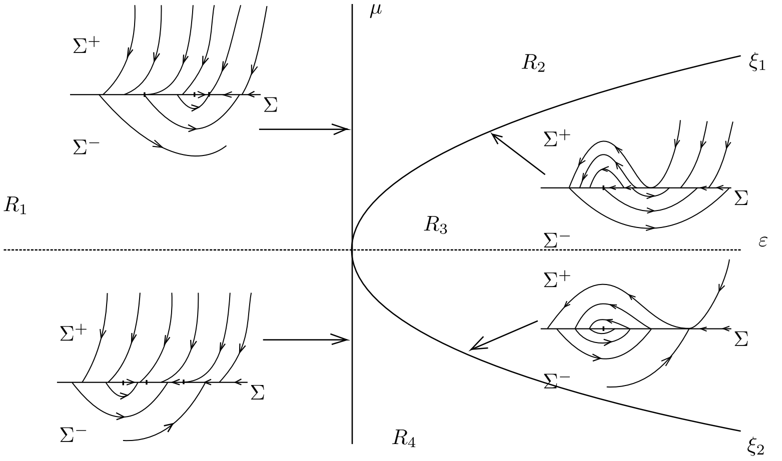


**Fig. 31.** Codimension-1 local bifurcations which appear in the unfolding of the Cusp–Fold singularity given by (34).

Furthermore, for either $\mu > 0$ or $\mu < 0$, the pseudonode $P$ of $Z^s$ in (36) which existed in $R_1$, $R_2$, $R_3$ and $R_4$, also exists and lies on the left of the cusp for $\mu < 0$.

In the curves

$$\xi_1 = \left\{(\varepsilon, \mu)\colon\ \mu = \sqrt{\varepsilon},\ \varepsilon > 0\right\} \quad \text{and} \quad \xi_2 = \left\{(\varepsilon, \mu)\colon\ \mu = -\sqrt{\varepsilon},\ \varepsilon > 0\right\} \tag{37}$$

take place the Fold–Fold bifurcations $VI_2$ and $II_2$ studied in [17], since in the first curve we have $F_- = F_+^2$ and in the second one $F_- = F_+^1$.

In $\xi_1$, the two folds $F_-$ and $F_+^2$ merge with the pseudonode $P$ in $(0, \mu)$. Furthermore, in $\xi_1$ the extended sliding vector field $Z^s_{\varepsilon,\mu}$ in (35) has a removable singularity in this point. In fact, it is equivalent to

$$Z^s_{\varepsilon,\sqrt{\varepsilon}}(x) = \frac{-1 + \sqrt{\varepsilon} - x}{1 + \sqrt{\varepsilon} + x}$$

which is regular at the Fold–Fold point.

Moreover, in $\xi_1$, there exist infinitely many cycles which are given by a segment of $\Sigma^s$, the Fold–Fold point, a segment of $\Sigma^e$ and a regular orbit. There exists also another cycle $\Gamma_{\varepsilon,\mu}$, which is given by a segment of $\Sigma^s$, the Fold–Fold point and its unique unstable separatrix. This last one, is the only one which persists for parameters below this curve as an attractor cycle coexisting with the repellor node $P$. For parameters above the curve, all the cycles break down and then the pseudonode $P$ becomes a global attractor.

Finally, we analyze the Fold–Fold bifurcation $F_- = F_+^1$ that takes place in $\xi_2$. Since both $F_-$ and $F_+^1$ are invisible folds, we can consider the return map to study the dynamics around it (see Section 4.1.1).

As a first step, we consider the involutions associated to both folds. It is straightforward to see that the one associated to $F_-$ is given by

$$\phi_{Y_\mu}(x) = -x + 2\mu. \tag{38}$$

The involution associated to the fold $F_+^1$ of $X_\varepsilon$ is well defined between the fold $F_+^2$ and the point

$$Q = (-2\sqrt{\varepsilon}, 0) \tag{39}$$

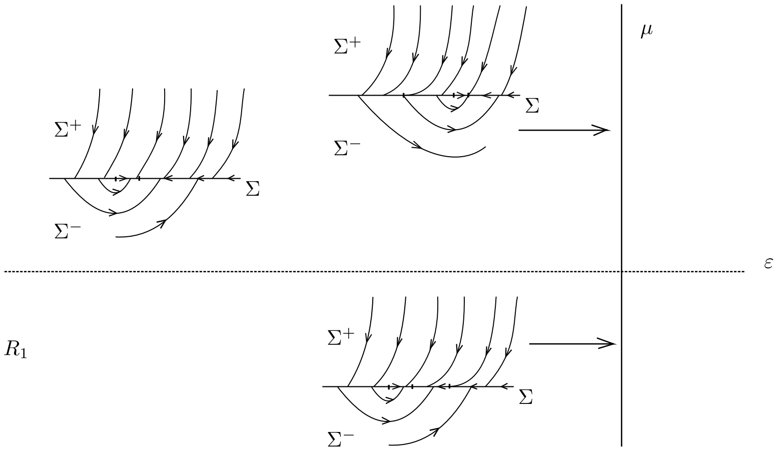


**Fig. 32.** Different dynamics of the unfolding (34) for parameters $(\varepsilon, \mu) \in R_1$ defined in Proposition 12.1. In that region does not take place any codimension-1 global bifurcation.

which is the arrival of $W_+^u(F_+^2)$ in $\Sigma^c$. This involution $\phi_{X_\varepsilon}$ can be also computed explicitly integrating the differential equation and it is given by

$$\phi_{X_\varepsilon}(x) = x - \frac{3x + \sqrt{12\varepsilon - 3x^2}}{2} = -\sqrt{\varepsilon} - (x + \sqrt{\varepsilon}) + \frac{1}{3\sqrt{\varepsilon}}(x + \sqrt{\varepsilon})^2 + \mathcal{O}_3(x + \sqrt{\varepsilon}) \tag{40}$$

and therefore, since $\mu = -\sqrt{\varepsilon}$ in $\xi_2$, it can be seen that for $x < -\sqrt{\varepsilon}$,

$$\phi_{\varepsilon, -\sqrt{\varepsilon}}(x) = \phi_{X_\varepsilon} \circ \phi_{Y_{-\sqrt{\varepsilon}}}(x) = -\sqrt{\varepsilon} + (x + \sqrt{\varepsilon}) + \frac{1}{3\sqrt{\varepsilon}}(x + \sqrt{\varepsilon})^2 + \mathcal{O}_3(x + \sqrt{\varepsilon})$$

and thus it is contracting. This fact combined with the appearance of a small escaping segment for parameters in $R_3$, as it was seen in Section 4.1.1, implies that, coexisting with the repellor pseudonode $P \in \Sigma^e$ (see Proposition 12.1), appears a small attractor periodic orbit. In the region $R_4$ only appears a small sliding segment which contains the pseudonode $P$, that is a global attractor.

As we will see in Section 12.2, when the parameters move in $R_3$, this periodic orbit undergoes a crossing-sliding bifurcation and becomes the cycle $\Gamma_{\varepsilon,\mu}$ born in $\xi_1$. For this reason, we will also denote this periodic orbit by $\Gamma_{\varepsilon,\mu}$.

In these curves in the $(\varepsilon, \mu)$ parameter space occur all the possible codimension-1 local bifurcations, either considering topological equivalence or $\Sigma$-equivalence, which exist in any generic unfolding of the singularity we are considering.

### *12.2. Codimension-1 global bifurcations of the unfolding*

Next step is to study the possible existence of codimension-1 global bifurcation curves in the unfolding $Z_{\varepsilon,\mu}$. We study them in the four regions defined in Proposition 12.1 (see also Fig. 31).

We start in the region $R_1$. In that region, all the Filippov vector fields have a visible Fold–Regular point which divides $\Sigma$ in $\Sigma^c$ and $\Sigma^s$. Moreover, in $\Sigma^s$ all the Filippov vector fields have a pseudonode. Therefore, any two vector fields with parameters belonging to $R_1$ are $\Sigma$-equivalent, and thus topologically equivalent (see Fig. 32). The construction of the homeomorphism follows the same lines as the construction explained in Section 9.

To describe the dynamics in $R_2$ we move the parameters clockwise. Recall that, by Proposition 12.1, the four singularities in $\Sigma$ are ordered as $F_+^1 <_\Sigma F_+^2 <_\Sigma F_- <_\Sigma P$, where $<_\Sigma$ is the order in $\Sigma$ induced by the first coordinate (see Fig. 33). When the parameters cross the vertical line, the folds

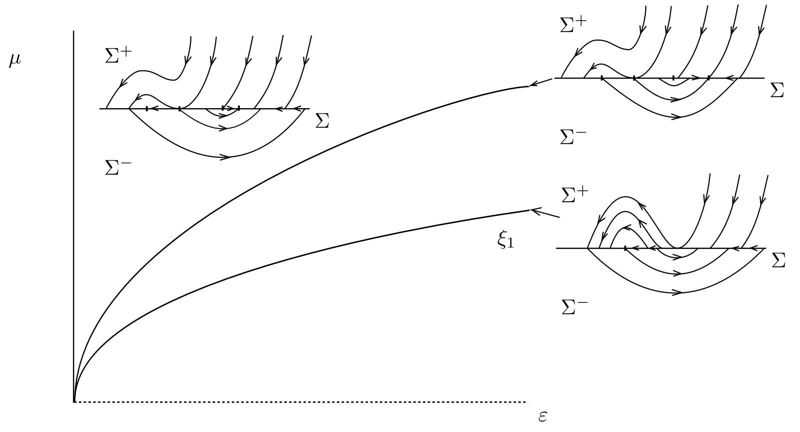


**Fig. 33.** Different dynamics of the unfolding (34) for parameters $(\varepsilon, \mu) \in R_2$ defined in Proposition 12.1. In that region only takes place a codimension-1 global bifurcation given by a separatrix connection.

$F_+^1 = (-\sqrt{\varepsilon}, 0)$ and $F_+^2 = (\sqrt{\varepsilon}, 0)$ and a small escaping region between them appear (see Proposition 12.1). Moreover, $W_-^u(F_+^2)$ has an arrival point in $\Sigma^s$ which lies on the right of the pseudonode $P$.

When we move the parameters clockwise, this arrival point moves to the left until, in a codimension-1 bifurcation curve, it coincides with $P$ giving birth to a separatrix connection between $F_+^2$ and $P$ given by $W_-^u(F_+^2) \equiv W_-^s(P)$. The bifurcation curve is given by the equation $\phi_{Y_\mu}(F_+^2) = P$ where $\phi_{Y_\mu}$ is the involution given in (38). Expanding asymptotically, one obtains that this curve is given by

$$\mu = \sqrt{\varepsilon} + 8\varepsilon + \mathcal{O}\big(\varepsilon^{3/2}\big)$$

for $\varepsilon > 0$. This global bifurcation is the only one in $R_2$. Below this curve, in $R_2$, the arrival points of the unstable separatrices $W_+^u(F_+^2)$ and $W_-^u(F_+^1)$ lie always on the right of $P$, so no other separatrix connections are possible in this region. Finally, the folds $F_+^2$ and $F_-$ become closer until they collide in $\xi_1$ (see (37)).

Before studying $R_3$, we consider $R_4$ since it is simpler. In the region $R_4$ we will see that all the codimension-1 global bifurcations are related to separatrix connections. As it happened in the Saddle–Fold bifurcation explained in Section 11, we will obtain an infinite sequence of codimension-1 global bifurcation curves associated to separatrix connections which accumulate to the Fold–Fold bifurcation curve $\xi_2$ (see Fig. 34).

**Proposition 12.2.** *Let us consider $(\varepsilon, \mu) \in R_4$ small enough. Then, there exists a family of curves $\{\eta_n\}_{n \geqslant 1}$ in the parameter space emanating from $(0, 0)$, which accumulate to $\xi_2$ (see (37)). Moreover, in these curves take place the following separatrix connections:*

- *If $n = 4k + 1$ with $k \geqslant 0$: $W_+^u(F_+^2) \equiv W_+^s(P)$.*
- *If $n = 4k + 2$ with $k \geqslant 0$: $W_+^u(F_+^2) \equiv W_+^s(F_-)$.*
- *If $n = 4k + 3$ with $k \geqslant 0$: $W_+^u(F_+^2) \equiv W_-^s(P)$.*
- *If $n = 4k + 4$ with $k \geqslant 0$: $W_+^u(F_+^2) = W_-^s(F_+^1)$.*

*In addition, the separatrix connections intersect $\Sigma$ $2k + 2$ times if $n = 4k + 1, 4k + 2$ or $2k + 3$ times if $n = 4k + 3, 4k + 4$.*

**Proof.** In order to analyze $\{\eta_n\}$, we describe the different dynamics anticlockwise in $R_4$. Recall that in the vertical axis $\varepsilon = 0$ there exists a cusp bifurcation which gives birth to the folds $F_+^1 = (-\sqrt{\varepsilon}, 0)$ and

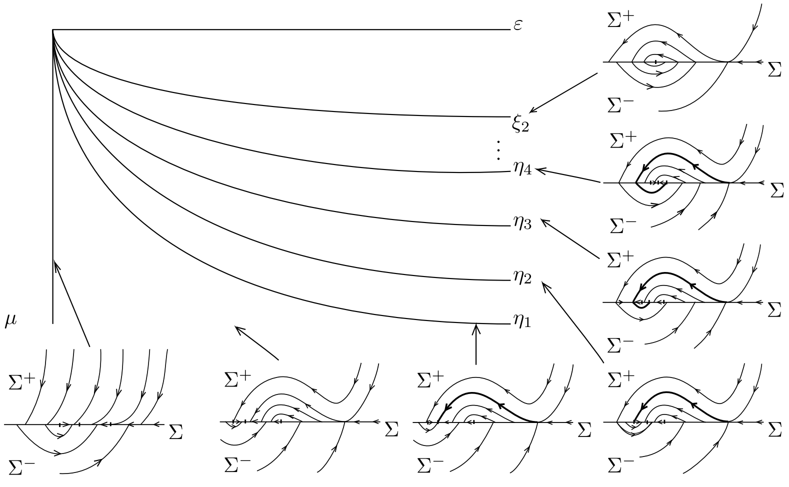


**Fig. 34.** Different dynamics of the unfolding (34) for parameters $(\varepsilon, \mu) \in R_4$ defined in Proposition 12.1. In that region, as is stated in Proposition 12.2, take place an infinite number of codimension-1 global bifurcations in the curves $\{\eta_n\}_{n\geqslant 1}$ given by separatrix connections.

$F_+^2 = (\sqrt{\varepsilon}, 0)$ for $\varepsilon > 0$ (see Fig. 34). Therefore, for parameters belonging to $R_4$, the four singularities which exist in $\Sigma$ are ordered as $F_- <_\Sigma P <_\Sigma F_+^1 <_\Sigma F_+^2$, where $<_\Sigma$ is the order in $\Sigma$ induced by the first coordinate (see Proposition 12.1). Recall, moreover, that the point $Q$ which is the arrival point of $W_+^u(F_+^2)$ in $\Sigma$ is given by (39) and therefore after crossing $\{\varepsilon = 0\}$ satisfies $P <_\Sigma Q <_\Sigma F_+^1$. Then, the first bifurcation to occur is a separatrix connection between $F_+^2$ and $P$ given by $W_+^u(F_+^2) \equiv W_+^s(P)$ in $\eta_1$ whose equation is given by $P = Q$.

Then, as the parameters change the fold $F_-$ become closer to $F_+^1$, in such a way that takes place a connection $W_+^u(F_+^2) \equiv W_+^s(F_-)$ in $\eta_2$, whose equation is given by $Q = F_-$. Then, $W_+^u(F_+^2)$ hits $\Sigma^c$, namely $Q \in \Sigma^c$, and then it arrives to $\Sigma^s$ through $\Sigma^-$, in such a way that the next global bifurcation is given by the connection $W_+^u(F_+^2) \equiv W_-^s(P)$ in $\eta_3$, whose equation is given by $\phi_{Y_\mu}(Q) = P$.

The last possible separatrix connection is when $W_+^u(F_+^2) = W_-^s(F_+^1)$, which takes place in $\eta_4$, whose equation is given by $\phi_{Y_\mu}(Q) = F_+^1$.

As the parameters change anticlockwise, we encounter the sequence of global bifurcations given by separatrix connections which make more and more turns around $\Sigma^s$ that accumulate to $\xi_2$ where $F_-$, $F_+^1$ and $P$ collapse and one of the components of $\Sigma^s$ disappear. $\square$

The existence of global bifurcations for parameters in the region $R_3$, is summarized in next proposition.

**Proposition 12.3.** *Let us consider $(\varepsilon, \mu) \in R_3$ small enough. Then*:

- *There exists a curve $\nu_\infty$ arising from $(0, 0)$, in which takes place a codimension-1 global bifurcation since the periodic orbit $\Gamma_{\varepsilon,\mu}$ becomes the pseudohomoclinic connection $W_+^u(F_+^2) \equiv W_-^u(F_+^2)$.*
- *There exists a sequence of curves $\{\nu_n\}$ in the parameter space arising from $(0, 0)$, which accumulate to $\nu_\infty$. Moreover, in these curves take place the following separatrix connections*:
  - *If $n = 4k + 1$ with $\geqslant 0$: $W_-^s(F_+^2) \equiv W_-^u(P)$.*
  - *If $n = 4k + 2$ with $\geqslant 0$: $W_-^s(F_+^2) \equiv W_-^u(F_+^1)$.*
  - *If $n = 4k + 3$ with $\geqslant 0$: $W_-^s(F_+^2) \equiv W_+^u(P)$.*
  - *If $n = 4k + 4$ with $\geqslant 0$: $W_-^s(F_+^2) \equiv W_+^u(F_-)$.*

  *In addition, the separatrix connections intersect $\Sigma$ $2k + 2$ times if $n = 4k + 1, 4k + 2$ or $2k + 3$ times if $n = 4k + 3, 4k + 4$.*

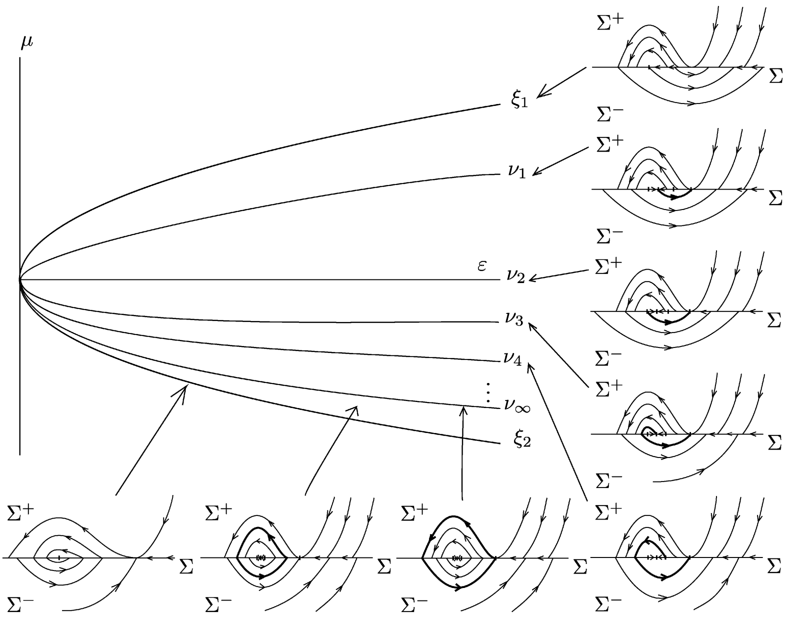


**Fig. 35.** Different dynamics of the unfolding (34) for parameters $(\varepsilon,\mu) \in R_3$ defined in Proposition 12.1. In that region, as is stated in Proposition 12.3, take place an infinite number of codimension-1 global bifurcations in the curves $\{\nu_n\}_{n\geqslant 1}$ given by separatrix connections.

**Proof.** First, we consider parameters close to the curve $\xi_2$ and we vary them anticlockwise. Recall that, as we have explained in Proposition 12.1, when the parameters cross $\xi_2$, it appears a small escaping region which contains $P$, in such a way that the singularities in $\Sigma$ are ordered as $F_+^1 <_\Sigma P <_\Sigma F_- <_\Sigma F_+^2$, where $<_\Sigma$ is the order in $\Sigma$ induced by the first coordinate. Moreover, it also appears the periodic orbit $\Gamma_{\varepsilon,\mu}$ (see Section 4.1). Considering the involutions (38) and (40), one can compute the intersecting points between $\Gamma_{\varepsilon,\mu}$ and $\Sigma^c$ which are given by $\Gamma^\pm_{\varepsilon,\mu} = (x_\pm, 0)$ with

$$x_\pm = \mu \pm \sqrt{3\left(\varepsilon - \mu^2\right)}.$$

Let us observe, that they satisfy $\Gamma^-_{\varepsilon,\mu} <_\Sigma F_+^1 <_\Sigma P <_\Sigma F_- <_\Sigma \Gamma^+_{\varepsilon,\mu}$. Furthermore, as the parameters change anticlockwise, the periodic orbit becomes bigger until it hits $F_+^2$, giving rise to a pseudo-homoclinic connection $W_+^u(F_+^2) \equiv W_-^u(F_+^2)$ in such a way that the periodic orbit becomes a cycle. This bifurcation is usually called crossing-sliding bifurcation (see Section 4.2), and takes place in the curve $\nu_\infty$ where holds $F_+^2 = \Gamma^+_{\varepsilon,\mu}$, namely $x_+ = \sqrt{\varepsilon}$. It can be seen that $\nu_\infty = \{(\varepsilon,\mu)\colon\ \mu = -\sqrt{\varepsilon}/2\}$.

We study the rest of the region $R_3$ changing the parameters clockwise from $\xi_1$. As we have explained in Section 12.1, below the curve $\xi_1$ only persists the attractor cycle $\Gamma_{\varepsilon,\mu}$ which is given by a sliding segment, the fold $F_+^2$ and its unique unstable separatrix $W_+^u(F_+^2)$. An easy computation shows that $\Gamma_{\varepsilon,\mu}$ exists until the parameters reach the crossing-sliding bifurcation curves $\nu_\infty$ (see Fig. 35), when it becomes a pseudohomoclinic connection to $F_+^2$ and afterwards a periodic orbit which does not hit $\Sigma^s$.

Since in the region $R_3$ the four singularities in $\Sigma$ are ordered as $F_+^1 <_\Sigma P <_\Sigma F_- <_\Sigma F_+^2$, for parameters below $\xi_1$ all the unstable separatrices of $F_+^1$, $P$ and $F_-$ have an arrival point in $\Sigma^s$. The first bifurcation to occur is a separatrix connection $W_-^u(P) \equiv W_-^s(F_+^2)$ in the curve $\nu_1$ given by $\phi_{Y_\mu}(P) = F_+^2$. Therefore, it can be seen that $\nu_1$ has the following asymptotic expansion

$$\mu = \sqrt{\varepsilon} - 2\varepsilon^{3/2} + \mathcal{O}\left(\varepsilon^2\right).$$

After that, we encounter the connection $W_-^u(F_+^1) \equiv W_-^s(F_+^2)$ in the curve $\nu_2$ given by $\phi_{Y_\mu}(F_+^1) = F_+^2$, and therefore $\nu_2 = \{(\varepsilon, \mu)\colon\ \mu = 0,\ \varepsilon > 0\}$. Now, the point $\phi_{Y_\mu}(F_+^2)$ lies in $\Sigma^c$, and therefore the next bifurcation occurs when $\phi_{\varepsilon,\mu}(F_+^2) = \phi_{X_\varepsilon} \circ \phi_{Y_\mu}(F_+^2) = P$. In this curve $\nu_3$ takes place $W_-^s(F_+^2) \equiv W_+^u(P)$, and has asymptotic expansion

$$\mu = -\frac{2}{7}\sqrt{\varepsilon} + \frac{75}{343}\varepsilon + \mathcal{O}\big(\varepsilon^{3/2}\big).$$

The last possible separatrix connection is $W_-^s(F_+^2) \equiv W_+^u(F_-)$. It takes place in $\nu_4$ and happens when $\phi_{\varepsilon,\mu}(F_+^2) = \phi_{X_\varepsilon} \circ \phi_{Y_\mu}(F_+^2) = F_-$. Using this equation, one can obtain the following asymptotic expansion for $\nu_4$

$$\mu = -\frac{2}{7}\sqrt{\varepsilon} + \mathcal{O}\big(\varepsilon^{3/2}\big).$$

Changing the parameters clockwise, there exist, as it happened in the region $R_4$ an infinite sequence of codimension-1 global bifurcations curves given by separatrix connections between $W_-^s(F_+^2)$ and consecutively $W_-^u(P)$, $W_-^u(F_+^1)$, $W_+^u(P)$ and $W_+^u(F_-)$, which accumulate to the crossing-sliding curve $\nu_\infty$. $\square$

The description of the unfolding is exactly the same either we consider topological equivalence or $\Sigma$-equivalence.

## 13. Boundary–Saddle–Node singularity

A Filippov vector field $Z = (X, Y)$ has a Boundary–Saddle–Node local bifurcation when $X$ has a Saddle–Node singularity at $p \in \Sigma$ whereas $Y$ is transversal to $\Sigma = \{(x, y)\colon\ f(x, y) = 0\}$ at that point. In order to have a generic codimension-2 singularity one has to impose non-degeneracy conditions. First of all, the eigenspaces of $DX(p)$ have to be transversal to $\Sigma$. In this way, the stable or unstable invariant manifold and the center invariant manifolds of $p$ as a critical point of $X$ are transversal to $\Sigma$. Moreover, as $p \in \partial\Sigma^e \cap \partial\Sigma^c$ or $p \in \partial\Sigma^s \cap \partial\Sigma^c$ (depending on the sign of $Yf(p)$, that is whether $Y$ points towards $\Sigma$ or away from $\Sigma$), there exists a sliding vector field defined on one side of $p$. Taking $x$ as a local chart of $\Sigma$, it is of the form

$$Z^s(x) = \alpha x + \mathcal{O}\big(x^2\big).$$

Therefore, as it happened in the Boundary–Saddle, Boundary–Node and Boundary–Focus bifurcations explained in Sections 4.1.3, 4.1.2 and 4.1.4 respectively, one has to impose that $\alpha \neq 0$. In the Saddle–Node case, this condition is equivalent to impose that $Y(p)$ and the eigenspace associated to the non-zero eigenvalue of the Saddle–Node are not collinear.

Of course this singularity can present different behaviors depending on several factors. First of all, it depends whether $p \in \partial\Sigma^e \cap \partial\Sigma^c$ or $p \in \partial\Sigma^s \cap \partial\Sigma^c$ and also on the sign of $\alpha$ and the sign of the non-zero eigenvalue of the Saddle–Node. Finally, we can obtain different behaviors depending on which branch of the eigenspace of the 0 eigenvalue is the admissible one (see Fig. 36).

In this section, we focus our attention on the case $p \in \partial\Sigma^s \cap \partial\Sigma^c$, such that the non-zero eigenvalue of the Saddle–Node is negative, $\alpha < 0$ and that the admissible part of the eigenspace of the 0 eigenvalue is the unstable one. All the other cases present similar behavior and can be studied analogously.

As a normal form we take $p = (0, 0)$, $\Sigma = \{(x, y)\colon\ f(x, y) = x + y = 0\}$ and

$$Z(x,y) = \begin{cases} X(x,y) = \begin{pmatrix} x^2 \\ -y \end{pmatrix} & \text{if } x + y > 0, \\ Y(x,y) = \begin{pmatrix} 1 \\ 1 \end{pmatrix} & \text{if } x + y < 0, \end{cases}$$

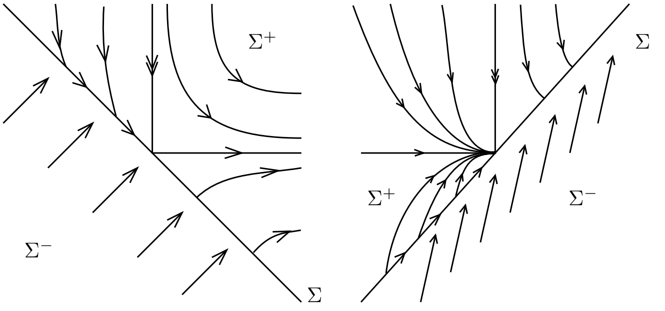


**Fig. 36.** Two kinds of Boundary–Saddle–Node singularities in which $Y$ points towards $\Sigma$ and $\alpha < 0$. These two kinds depend on which branch of the eigenspace of 0 eigenvalue, and then on which branch of the center manifolds, is admissible. On the left picture it is admissible the unstable branch of the center manifolds whereas on the right one, it is admissible the stable branch of the center manifolds.

whose phase portrait can be seen in the left picture of Fig. 36. We make this choice because it satisfies the non-degeneracy condition about the transversality of the eigenspaces of $DX(p)$ with $\Sigma$ and keeps $DX(p)$ in diagonal form.

It is straightforward to see that for $Z$, $\Sigma^s = \{(x, y) \in \Sigma\colon\ x < 0\}$ and $\Sigma^c = \{(x, y) \in \Sigma\colon\ x > 0\}$. In $\Sigma^s$ we can define the sliding vector field $Z^s$ which satisfies $Z_s'(0) < 0$.

A generic unfolding of this singularity can be given by

$$Z_{\varepsilon,\mu}(x, y) = \begin{cases} X_{\varepsilon,\mu}(x, y) = \binom{x^2+\varepsilon}{-y+\mu} & \text{if } x + y > 0, \\ Y(x, y) = \binom{1}{1} & \text{if } x + y < 0, \end{cases} \tag{41}$$

in such a way that $\varepsilon$ unfolds the Saddle–Node bifurcation of $X$. When $\varepsilon = 0$ the Saddle–Node point is given by $Q = (0, \mu)$, and then is admissible for $\mu > 0$ and non-admissible for $\mu < 0$.

For $\varepsilon > 0$, $X_{\varepsilon,\mu}$ does not have critical point whereas for $\varepsilon < 0$ it has a node $N = (-\sqrt{-\varepsilon}, \mu)$ and a saddle $S = (\sqrt{-\varepsilon}, \mu)$. However, $N$ and $S$ are only admissible provided $\mu > \sqrt{-\varepsilon}$ and $\mu > -\sqrt{-\varepsilon}$ respectively.

Moreover, when $\mu \neq 0$ it appears a fold of $X$ in $\Sigma$,

$$F = \left(\frac{-1 + \sqrt{1 - 4(\varepsilon + \mu)}}{2}, \frac{1 - \sqrt{1 - 4(\varepsilon + \mu)}}{2}\right)$$

which is always the boundary between $\Sigma^s$ and $\Sigma^c$. In $\Sigma^s$, taking $x$ as a local chart, the sliding vector field is given by

$$Z^s_{\varepsilon,\mu}(x) = \frac{\varepsilon + \mu - x + x^2}{2 - \mu - \varepsilon - x - x^2},$$

which has a pseudonode

$$P = \left(\frac{-1 + \sqrt{1 - 8(\mu + 2\varepsilon)}}{4}, \frac{1 - \sqrt{1 - 8(\mu + 2\varepsilon)}}{4}\right),$$

that is visible provided $\varepsilon < 0$ and $-\sqrt{-\varepsilon} < \mu < \sqrt{-\varepsilon}$.

In the unfolding of the Boundary–Saddle–Node bifurcation only appear codimension-1 local bifurcations as it is shown in next proposition (see also Fig. 37).

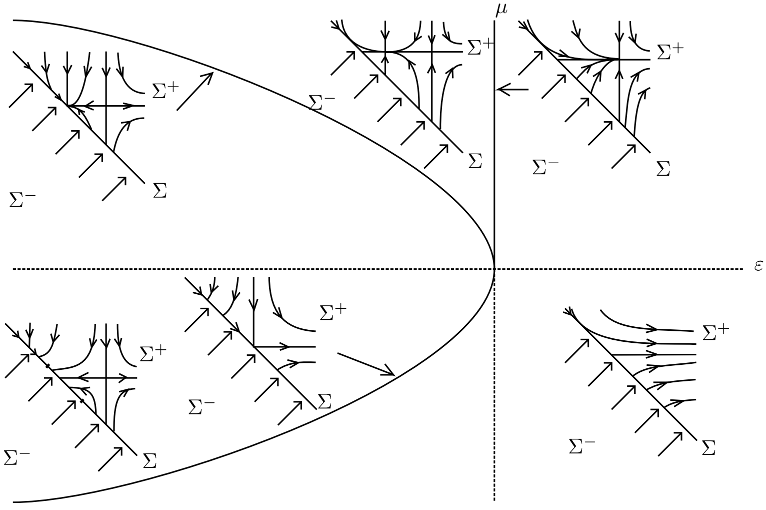


**Fig. 37.** Different dynamics of the unfolding (41).

**Proposition 13.1.** *For $(\varepsilon, \mu)$ small enough the vector field $Z_{\varepsilon,\mu}$ in* (41) *undergoes the following local bifurcations*:

- *A smooth Saddle–Node bifurcation in $\Sigma^+$ in the line* $\{(\varepsilon, \mu)\colon\ \varepsilon = 0,\ \mu > 0\}$.
- *A Boundary–Node bifurcation, called $BN_2$ in* [17], *in* $\{(\varepsilon, \mu)\colon\ \mu = \sqrt{-\varepsilon},\ \varepsilon < 0\}$.
- *A Boundary–Saddle bifurcation, called $BS_1$ in* [17], *in* $\{(\varepsilon, \mu)\colon\ \mu = -\sqrt{-\varepsilon},\ \varepsilon < 0\}$.

The bifurcations stated in this proposition, whose proof is straightforward, are the only possible local bifurcations of the unfolding. Moreover, they are the same independently whether we use $\Sigma$-equivalence or topologically equivalence.

Finally, studying the regions delimited by these curves it can be easily seen that any two vector fields in any of these regions are $\Sigma$-equivalent (and thus topologically equivalent). Therefore, there cannot appear global bifurcations for $(\varepsilon, \mu)$ small enough.

## 14. Boundary–Hopf singularity

A Filippov vector field $Z = (X, Y)$ has a Boundary–Hopf singularity when $X$ has a Hopf singularity at $p \in \Sigma$ whereas $Y$ is transversal to $\Sigma$ at that point. In order to have a generic codimension-2 singularity one has to impose an additional generic non-degeneracy condition. Since $p \in \partial\Sigma^c \cap \partial\Sigma^s$ or $p \in \partial\Sigma^c \cap \partial\Sigma^e$, there exists a sliding vector field $Z^s$ which is defined on one side of $p$. Taking $x$ as a local chart of $\Sigma$, $Z^s$ is of the form

$$Z^s(x) = \alpha x + \mathcal{O}(x^2).$$

Therefore, one has to impose $\alpha \neq 0$.

Of course, this singularity can present different behaviors depending whether $p \in \partial\Sigma^c \cap \partial\Sigma^s$ or $p \in \partial\Sigma^c \cap \partial\Sigma^e$ (namely, $Y$ points towards $\Sigma$ or away from $\Sigma$), whether the Hopf bifurcation is supercritical or subcritical and on the sign of $\alpha$.

In this section, taking $p \in \partial\Sigma^c \cap \partial\Sigma^s$ and $\alpha < 0$, we will study both the supercritical and subcritical cases. All the other cases present similar behavior and can be studied analogously. In this case, we take $p = (0, 0)$, $\Sigma = \{(x, y)\colon\ f(x, y) = y = 0\}$ and

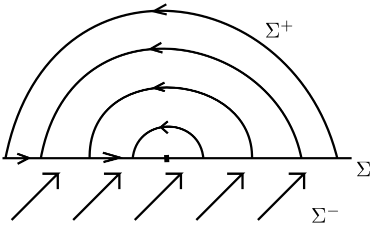


**Fig. 38.** Phase portrait of the Boundary–Hopf singularity in (42) in which $p \in \partial\Sigma^c \cap \partial\Sigma^s$. In the supercritical ($\sigma = -1$) and subcritical ($\sigma = 1$) cases the phase portraits are topologically equivalent.

$$Z^\sigma(x, y) = \begin{cases} X^\sigma(x, y) = \begin{pmatrix} -y+\sigma x(x^2+y^2) \\ x+\sigma y(x^2+y^2) \end{pmatrix} & \text{if } y > 0, \\ Y(x, y) = \begin{pmatrix} 1 \\ 1 \end{pmatrix} & \text{if } y < 0, \end{cases} \tag{42}$$

where $\sigma = -1, +1$ corresponds to the supercritical and subcritical cases. The phase portraits of both $Z^\sigma$ are topologically equivalent and can be seen in Fig. 38. It is straightforward to see that for both $Z^\sigma$, $\Sigma^c = \{(x, y) \in \Sigma\colon\ x > 0\}$, $\Sigma^s = \{(x, y) \in \Sigma\colon\ x < 0\}$ and the sliding vector field $Z^{\sigma,s}$ satisfies $(Z^{\sigma,s})'(0) < 0$.

A generic unfolding of these singularities can be given by

$$Z^\sigma_{\varepsilon,\mu}(x, y) = \begin{cases} X^\sigma_{\varepsilon,\mu}(x, y) = \begin{pmatrix} \varepsilon x-(y-\mu)+\sigma x(x^2+(y-\mu)^2) \\ x+\varepsilon(y-\mu)+\sigma(y-\mu)(x^2+(y-\mu)^2) \end{pmatrix} & \text{if } y > 0, \\ Y(x, y) = \begin{pmatrix} 1 \\ 1 \end{pmatrix} & \text{if } y < 0, \end{cases} \tag{43}$$

in such a way that $\varepsilon$ unfolds the Hopf bifurcation. $X^\sigma_{\varepsilon,\mu}$ has a critical point $P = (0, \mu)$ which is admissible for $\mu > 0$ and non-admissible for $\mu < 0$. Therefore, $\mu$ moves $P$ transversally to $\Sigma$.

When $\mu \neq 0$, it appears a fold $F = (F_x, 0)$ which is visible for $\mu > 0$ and invisible for $\mu < 0$ and satisfies

$$F_x = \frac{1 - \sqrt{1 - 4\sigma\mu(\mu\varepsilon + \sigma\mu^3)}}{2\sigma\mu}. \tag{44}$$

In $\Sigma^s$, taking $x < F_x$ as a local chart, the sliding vector field is given by

$$Z^{\sigma,s}_{\varepsilon,\mu}(x) = \frac{\mu + \mu\varepsilon + \sigma\mu^3 + (-1 + \varepsilon + \sigma\mu^2)x + \sigma\mu x^2 + \sigma x^3}{1 + \mu\varepsilon + \sigma\mu^3 - x + \sigma\mu x^2}$$

and has a pseudonode $N = (N_x, 0)$ which satisfies $N_x = \mu + o(\mu, \varepsilon)$ and exists provided $\mu < 0$ for both $\sigma = \pm 1$, since $F_x < N_x$ for $\mu < 0$.

In the unfolding of $Z^\sigma_{\varepsilon,\mu}$ in (43) there exist both local and global bifurcations as can be seen in the following proposition.

**Proposition 14.1.** *For $(\varepsilon, \mu)$ small enough the vector field $Z^\sigma_{\varepsilon,\mu}$ in (43) undergoes the following bifurcations*:

- *A Boundary–Focus bifurcation, called $BF_3$ in* [17], *in* $\{(\varepsilon, \mu)\colon\ \mu = 0,\ \varepsilon > 0\}$.
- *A Boundary–Focus bifurcation, which corresponds to $BF_4$ in* [17] *with reversed time, in* $\{(\varepsilon, \mu)\colon\ \mu = 0,\ \varepsilon < 0\}$.
- *A smooth Hopf bifurcation in* $\{(\varepsilon, \mu)\colon\ \varepsilon = 0,\ \mu > 0\}$.

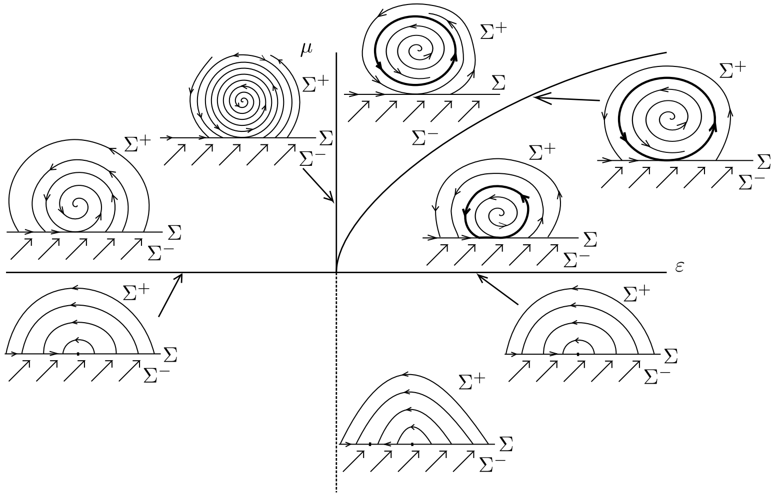


**Fig. 39.** Different dynamics of the unfolding (43) with $\sigma = -1$.

- *For $\sigma = -1$ (supercritical case) in $\{(\varepsilon, \mu)\colon\ \mu = \sqrt{\varepsilon},\ \varepsilon > 0\}$ takes place a separatrix connection $W^u_+(F) = W^s_+(F)$, which is in fact a grazing-sliding bifurcation (called $TC_1$ in [17]).*
- *For $\sigma = +1$ (subcritical case) in $\{(\varepsilon, \mu)\colon\ \mu = \sqrt{-\varepsilon},\ \varepsilon < 0\}$ takes place a separatrix connection $W^u_+(F) = W^s_+(F)$, which is in fact a grazing-sliding bifurcation (called $TC_2$ in [17]).*

**Proof.** The local bifurcations for both the supercritical and subcritical cases are the same. $X^\sigma_{\varepsilon,\mu}$ has a critical point $P = (0, \mu)$ which is a hyperbolic focus provided $\varepsilon \neq 0$. Moreover, it is attractor for $\varepsilon < 0$ and repellor for $\varepsilon > 0$. Therefore, since for $\mu = 0$, $P \in \Sigma$, in $\{(\varepsilon, \mu)\colon\ \mu = 0,\ \varepsilon > 0\}$ and $\{(\varepsilon, \mu)\colon\ \mu = 0,\ \varepsilon < 0\}$ takes place respectively $BF_3$ and $BF_4$ with time reversed.

When $\varepsilon = 0$ the critical point $P$ looses its hyperbolicity and undergoes a Hopf bifurcation, which is visible provided $\mu > 0$. Therefore in the supercritical case it appears a periodic orbit in $\Sigma^+$ for $\varepsilon > 0$ and in the subcritical for $\varepsilon < 0$.

In these three curves occur all the possible local bifurcations of $Z^\sigma_{\varepsilon,\mu}$. Regarding the global bifurcations, the unfolding of the supercritical and subcritical cases differ.

We first consider the supercritical case (see Fig. 39). It can be easily seen that any two vector fields in the regions $\{(\varepsilon, \mu)\colon\ \mu < 0\}$ are $\Sigma$-equivalent (and thus topologically equivalent), and the same happens in $\{(\varepsilon, \mu)\colon\ \varepsilon < 0,\ \mu > 0\}$. In $\{(\varepsilon, \mu)\colon\ \varepsilon > 0,\ \mu > 0\}$ appears a global bifurcation. We describe the dynamics clockwise. In the vertical axis the Hopf bifurcation takes place, and thus for $\varepsilon > 0$ it appears a small attractor periodic orbit which coexists with the repellor focus. For the normal form in (43), this periodic orbit is given $x^2 + (y - \mu)^2 = \varepsilon$ and therefore, as we change the parameters clockwise, it increases until it hits $\Sigma$ tangentially at $\mu = \sqrt{\varepsilon}$ at the fold $F$ in (44) leading to the separatrix connection $W^u_+(F) = W^s_+(F)$. Therefore, in this curve takes place a so-called grazing bifurcation ($TC_1$ in [17]). If we continue changing the parameters, the periodic orbit becomes a cycle which has a small sliding segment. Finally this cycle shrinks until it disappears in the Boundary–Focus bifurcation ($BF_3$ in [17]) which takes place in $\{(\varepsilon, \mu)\colon\ \mu = 0,\ \varepsilon > 0\}$.

Finally, we describe the global bifurcations of the subcritical case (see Fig. 40). It can be easily seen that any two vector fields in the region $\{(\varepsilon, \mu)\colon\ \mu < 0\}$ and also in $\{(\varepsilon, \mu)\colon\ \varepsilon < 0,\ \mu > 0\}$ are $\Sigma$-equivalent (and thus topologically equivalent). In this last region, it exists an attractor cycle which appears due to the Boundary–Focus bifurcation ($BF_3$ in [17]) in $\{(\varepsilon, \mu)\colon\ \mu = 0,\ \varepsilon > 0\}$, which coexists with the repellor focus $P$.

In $\{(\varepsilon, \mu)\colon\ \varepsilon > 0,\ \mu > 0\}$ appears a global bifurcation. We describe the dynamics anticlockwise. In the vertical axis the Hopf bifurcation of $P$ takes place, and thus for $\varepsilon < 0$ it appears a small repellor periodic orbit which coexists with the attractor focus $P$ and the cycle. As we change the parameters,

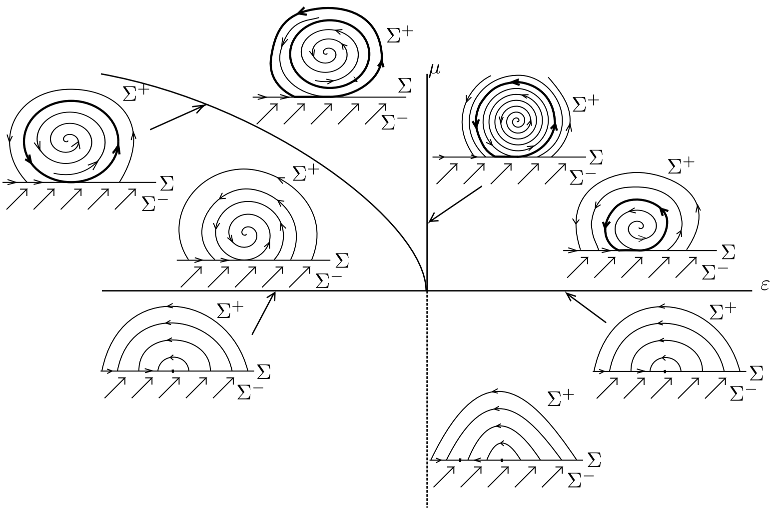


**Fig. 40.** Different dynamics of the unfolding (43) with $\sigma = 1$.

the periodic orbit becomes bigger and closer to the cycle. Reasoning as in the supercritical case, it can be seen that the cycle and the periodic orbit merge at the same time as they graze tangentially $\Sigma$ in $\mu = \sqrt{-\varepsilon}$. Therefore, in this curve takes place a grazing bifurcation called $TC_2$ in [17]. If we cross this curve, the periodic orbit and the cycle disappear in such a way that the attractor focus becomes a global attractor, which approaches $\Sigma$ until it hits it in $\{(\varepsilon, \mu)\colon\ \mu = 0,\ \varepsilon < 0\}$ in the Boundary–Focus bifurcation. $\square$

## Acknowledgments

The authors want to thank E. Ponce and also the referee for his help to improve the final version of the manuscript.

M. Guardia and T.M. Seara have been partially supported by the Spanish MCyT/FEDER grant MTM2009-06973 and the Catalan SGR grant 2009SGR859 and M.A. Teixeira by FAPESP-Brazil grant 2007/06896-05. In addition, the research of M. Guardia has been supported by the Spanish PhD grant FPU AP2005-1314.

## References

[1] V.I. Arnol′d, Ordinary Differential Equations, The MIT Press, Cambridge, MA, London, 1973, translated from Russian and edited by Richard A. Silverman.

[2] N.N. Bautin, E.A. Leontovich, Metody i priemy kachestvennogo issledovaniya dinamicheskikh sistem na ploskosti, Spravochnaya Matematicheskaya Biblioteka (Mathematical Reference Library), Nauka, Moscow, 1976.

[3] Mireille E. Broucke, Charles C. Pugh, Slobodan N. Simić, Structural stability of piecewise smooth systems, in: The Geometry of Differential Equations and Dynamical Systems, Comput. Appl. Math. 20 (1–2) (2001) 51–89.

[4] Mario di Bernardo, Chris J. Budd, Alan R. Champneys, Piotr Kowalczyk, Arne B. Nordmark, Gerard Olivar Tost, Petri T. Piiroinen, Bifurcations in nonsmooth dynamical systems, SIAM Rev. 50 (4) (2008) 629–701.

[5] M. di Bernardo, C.J. Budd, A.R. Champneys, P. Kowalczyk, Piecewise-Smooth Dynamical Systems: Theory and Applications, Appl. Math. Sci., vol. 163, Springer-Verlag London Ltd., London, 2008.

[6] M. di Bernardo, M.I. Feigin, S.J. Hogan, M.E. Homer, Local analysis of $C$-bifurcations in $n$-dimensional piecewise-smooth dynamical systems, Chaos Solitons Fractals 10 (11) (1999) 1881–1908.

[7] M. di Bernardo, Piotr Kowalczyk, A. Nordmark, Bifurcations of dynamical systems with sliding: derivation of normal-form mappings, Phys. D 170 (3–4) (2002) 175–205.

[8] M. di Bernardo, P. Kowalczyk, A. Nordmark, Sliding bifurcations: a novel mechanism for the sudden onset of chaos in dry friction oscillators, Internat. J. Bifur. Chaos Appl. Sci. Engrg. 13 (10) (2003) 2935–2948.

[9] Mario di Bernardo, Daniel J. Pagano, Enrique Ponce, Nonhyperbolic boundary equilibrium bifurcations in planar Filippov systems: a case study approach, Internat. J. Bifur. Chaos Appl. Sci. Engrg. 18 (5) (2008) 1377–1392.

[10] A.F. Filippov, Differential Equations with Discontinuous Right-Hand Sides, Math. Appl. (Sov. Ser.), vol. 18, Kluwer Academic Publishers Group, Dordrecht, 1988.
[11] J. Guckenheimer, P. Holmes, Nonlinear Oscillations, Dynamical Systems, and Bifurcations of Vector Fields, Springer-Verlag, 1983.
[12] M.R. Jeffrey, S.J. Hogan, The geometry of generic sliding bifurcations, SIAM Rev. (2011), in press.
[13] P. Kowalczyk, M. di Bernardo, Two-parameter degenerate sliding bifurcations in Filippov systems, Phys. D 204 (3–4) (2005) 204–229.
[14] P. Kowalczyk, M. di Bernardo, A.R. Champneys, S.J. Hogan, M. Homer, P.T. Piiroinen, Yu.A. Kuznetsov, A. Nordmark, Two-parameter discontinuity-induced bifurcations of limit cycles: classification and open problems, Internat. J. Bifur. Chaos Appl. Sci. Engrg. 16 (3) (2006) 601–629.
[15] V.S. Kozlova, Roughness of a discontinuous system, Vestnik Moskov. Univ. Ser. I Mat. Mekh. 5 (1984) 16–20.
[16] P. Kowalczyk, P.T. Piiroinen, Two-parameter sliding bifurcations of periodic solutions in a dry-friction oscillator, Phys. D 237 (8) (2008) 1053–1073.
[17] Yu.A. Kuznetsov, S. Rinaldi, A. Gragnani, One-parameter bifurcations in planar Filippov systems, Internat. J. Bifur. Chaos Appl. Sci. Engrg. 13 (8) (2003) 2157–2188.
[18] V.K. Mel′nikov, On the stability of a center for time-periodic perturbations, Tr. Mosk. Mat. Obs. 12 (1963) 3–52.
[19] J. Sotomayor, Generic one-parameter families of vector fields on two-dimensional manifolds, Inst. Hautes Études Sci. Publ. Math. 43 (1974) 5–46.
[20] J. Sotomayor, Liç oes de equaç oes diferenciais ordinárias, Projeto Euclides (Euclid Project), vol. 11, Instituto de Matemática Pura e Aplicada, Rio de Janeiro, 1979.
[21] Marco Antonio Teixeira, Generic bifurcation in manifolds with boundary, J. Differential Equations 25 (1) (1977) 65–89.
[22] Marco Antonio Teixeira, Generic bifurcation of certain singularities, Boll. Un. Mat. Ital. B (5) 16 (1) (1979) 238–254.
[23] Marco Antonio Teixeira, Generic singularities of discontinuous vector fields, An. Acad. Brasil. Ciênc. 53 (2) (1981).
[24] Marco Antonio Teixeira, Stability conditions for discontinuous vector fields, J. Differential Equations 88 (1) (1990).
[25] Marco Antonio Teixeira, Generic bifurcation of sliding vector fields, J. Math. Anal. Appl. 176 (2) (1993).
[26] Marco Antonio Teixeira, On attractivity of discontinuous systems, Dynam. Systems Appl. 5 (1) (1996).
[27] Marco Antonio Teixeira, Codimension two singularities of sliding vector fields, Bull. Belg. Math. Soc. Simon Stevin 6 (3) (1999).
[28] Marco Antonio Teixeira, Perturbation theory for non-smooth systems, in: Robert Meyers (Ed.), Encyclopedia of Complexity and Systems Science, Springer, 2009, pp. 6697–6719.